NTEC
Nottingham Transportation Engineering Centre

The University of Nottingham
UNITED KINGDOM · CHINA · MALAYSIA

EFFECT OF HEATING ENERGY, STEEL FIBRES, BITUMEN TYPES AND AGEING ON THE SELF-HEALING PHENOMENA IN HOT MIX ASPHALT

By

Harith K K Ajam

B.Sc. Civil Eng., M.Sc. Highways and Airports Eng.

Thesis submitted to the University of Nottingham for the degree of Doctor of Philosophy

January 2019

Abstract

Hot mix asphalt is one of the most common types of pavement surface materials used in the world. The combined effects of traffic loading and the environment will cause every flexible pavement, no matter how well-designed/constructed to deteriorate over time. Once a crack is open in the pavement, and because of bitumen viscoelastic properties, it starts healing and, if it has enough rest time, it can even close completely. Furthermore, asphalt self-healing is a viscosity related phenomenon that accelerates by reducing the viscosity of bitumen as it increases the capillarity flow through the cracks. One method to achieve this is by exposing the pavement to heat energy, which also produces a thermal expansion that contributes to the circulation of the bitumen through cracks.

In this research, three aspects were investigated. Firstly, asphalt self-healing has been induced in cracked asphalt beams with different air voids contents (dense, semi-dense and porous) by exposing them for various times under infrared radiation and induction heating. Infrared heating has been used to simulate solar radiation. The results show that both methods reach similar and satisfactory healing ratios at around 90%. However, induction heating is more energy efficient because the effect is concentrated on the binder, instead of heating the whole mix. This can be translated into much shorter heating times to reach the same healing level. An optimum healing energy was found, after which higher amounts of infrared radiation damage the properties of the healed material. Moreover, it has been observed that dense mixtures obtained better healing with low energy but the maximum healing ratios obtained by them were lower than those obtained by semi-

dense and porous mixtures by about 12 to 15% respectively. A new healing model was proposed involving not only surface tension, hydrostatic forces and energy dissipation but also other factors, such as differential temperature between aggregates and binder and thermal expansion.

Secondly, improper disposal of metal waste in landfills is one of the primary means by which metals, mainly produced in different industrial sectors, reach the soil and ground water. These can migrate to surrounding ecosystems and bio-magnify in plants and animals endangering the human food chain. At the same time, the addition of metal particles in asphalt mixes produces a series of beneficial effects, such as enhancing their mechanical performance, durability and electrical conductivity making possible applications, such as ice/snow melting and crack healing by electromagnetic induction. Research was undertaken to assess and compare the use of two different types of waste metal fibres (recovered from old tyres and shavings from the machining industry) and two other types of commercial particles (steel wool and steel grit) regarding their effect on volumetric, mechanical and healing properties of asphalt mixes. General results showed that all fibres improve the mix properties with similar healing, mechanical and leaching properties, and with a proper design, the improvement in such properties by using waste metals is comparable to that obtained by using commercial particles. It was also found that fibres from old tyres are especially suitable for low structural layers (base and sub-base), while the use of metal shavings is particularly recommended in superficial courses.

Finally, the effect of bitumen was studied in two forms: aged and virgin. Over the service life of asphalt roads, different factors produce, in the bitumen, a hardening process known as “ageing”. Also, the addition of recycled, aged material (i.e. RAP) to new mixes modifies the viscosity of the mix. The research studied how these two actions affect the capacity for healing, by electromagnetic induction, of asphalt mixes. Mixes subjected to different ageing processes or containing different amounts of RAP were tested. Results show that both ageing and RAP content contribute to increasing binder stiffness and air voids content in the mix. Therefore, the healing process becomes less effective and energy efficient. For the worst ageing and RAP stage, still more than 20% healing occurred.

On the other hand, the influence of virgin bitumen properties on the induction healing capacity of asphalt mixtures was studied. The main conclusion that can be extracted is that, for the range of bitumens commonly used, the fact of changing the type of bitumen does not significantly affect the healing capacity of the resulting asphalt mix.

List of Publications

Published:

AJAM, H., LASTRA-GONZALEZ, P., GOMEZ-MEIJIDE, B. & GARCÍA, Á. 2016. Self-Healing of Dense Asphalt Concrete by Two Different Approaches: Electromagnetic Induction and Infrared Radiation. In: CHABOT, A., BUTTLAR, G. W., DAVE, V. E., PETIT, C. & TEBALDI, G. (eds.) 8th RILEM International Conference on Mechanisms of Cracking and Debonding in Pavements. Dordrecht: Springer Netherlands.

GOMEZ-MEIJIDE, B., AJAM, H., LASTRA-GONZALEZ, P. & GARCIA, A. 2016. Effect of air voids content on asphalt self-healing via induction and infrared heating. Construction and Building Materials, 126, 957-966.

AJAM, H., LASTRA-GONZÁLEZ, P., GÓMEZ-MEIJIDE, B., AIREY, G. & GARCIA, A. 2017. Self-Healing of Dense Asphalt Concrete by Two Different Approaches: Electromagnetic Induction and Infrared Radiation. Journal of Testing and Evaluation, 45, 1933-1940.

GOMEZ-MEIJIDE, B., AJAM, H., GARCIA, A. & AL, H. 2017. Effect of waste metallic particles on asphalt induction heating. The 10th International Conference on the Bearing Capacity of Roads, Railways and Airfields (BCRRA 2017). Athens, Greece.

Gomez-Meijide, B., Salih, S., Ajam, H. & Garcia, A. 2018. Effect of binder thermal expansion on healing performance of asphalt mixtures. ISAP.

AJAM, H., GOMEZ-MEIJIDE, B., ARTAMENDI, I. & GARCIA, A. 2018. Mechanical and healing properties of asphalt mixes reinforced with different types of waste and commercial metal particles. Journal of Cleaner Production, 192, 138-150.

GOMEZ-MEIJIDE, B., AJAM, H., LASTRA-GONZÁLEZ, P. & GARCIA, A. 2018. Effect of ageing and RAP content on the induction healing properties of asphalt mixtures. Construction and Building Materials, 179, 468-476.

GOMEZ-MEIJIDE, B., AJAM, H., GARCIA, A. AND VANSTEENKISTE, S., 2018. Effect of bitumen properties in the induction healing capacity of asphalt mixes. Construction and Building Materials, 190, pp.131-139.

Acknowledgments

In the name of Allah, the Most Gracious and the Most Merciful. I would like to express my sincere gratitude to my supervisors Prof. Dr. Gordon Airey, Dr. Alvaro Garcia and Dr. Breixo Gomez-Meijide for providing me the opportunity to do this research with valuable guidance, interest and encouragement over the years. In addition, I appreciate the valuable advices, kindness and encouragement from Dr. Nick Thom, my internal assessor, through my first and second year report.

Sincere appreciation is due to the Ministry of Higher Education and Scientific Research in Iraq, the University of Babylon for providing a scholarship to conduct this PhD study.

Appreciation is due University of Nottingham for providing facilities and support to this project. My gratitude must be conveyed to the technical laboratory staff: Mr. Richard Blackmore, Mr. Martyn Barrett, Mr. Lawrence Pont, Mr. Jonathan Watson, Mr. Matthew Thomas, Mr. Antony Beska and Miss. Laura Weatherby at Nottingham Transportation Engineering Centre (NTEC) for all their valuable assistance regarding laboratory experimental works. My appreciation needs to be expressed to a long list of colleagues for their time in discussion and their supporting. Moreover, I would like to thank the following people who helped me by different means: Mr. Christopher Fox for his help with the first CT-scan images and Dr. Sturrock Craig (School of Biosciences) for his help with the remaining CT-scan images. Mr. Max Mason for his help on optical microscopy and thermal expansion tests. Vikki Archibald, Jacob Uguna and David Mee for the valuable assistance during the leaching test.

Special thanks is given to my lovely wife, Maryam Baiee who always gives encouragement, support and advice that made my education possible and will never be forgotten and my little princes, Ibrahim, Jafar and Adam. Lastly, I would like to thank all members in my family and friends. Their love, encouragement, expectation and sacrifice are the origin of my inspiration.

Dedication

To My Family with Love and

Respect

Declaration

This research described in this thesis was conducted at the Civil Engineering Department, the University of Nottingham between October 2014 and January 2019. I declare that the work is my own and has not been submitted for a degree at another university.

Harith Khaleel Kadhim Ajam

The University of Nottingham

Table of Content

List of Figures

List of Tables

List of Abbreviations and Notations

ν	Poisson ratio
τ	Heating energy
ρ	Density
τ_c	Cooling energy
τ_h	Heating energy
2-way ANOVA	2-way analysis of variance
AC	Alternating Current
BOS	Basic oxygen steelmaking
BRRC	Belgian Road Research Centre
BS	British Standard
CI	Index of Colloidal Stability
CT-Scan	X-Ray Computed Tomography
DBM	Dense Bitumen Macadam
E*	Complex modulus (Tensile)
EAF	Electric arc furnaces
EN	European Standard
$F_b(\tau)$	Ultimate force for breaking samples measured by 3-point bending test after healing
F_i	Initial ultimate force for breaking samples measured by 3-point bending test
g	Gravity
G*	Complex modulus (Shear)
GEL	Gelatinous
G_{mb}	Bulk specific gravity
G_{mm}	Maximum specific gravity
G_{sa}	Bulk specific gravity of aggregate
G_{ss}	Bulk specific gravity of steel
HMA	Hot Mix Asphalt
ITS	Indirect Tensile Strength
ITS_{dry}	Indirect Tensile Strength of dry samples
ITSR	Indirect Tensile Strength Ratio (Water damage)
ITS_{wet}	Indirect Tensile Strength of conditioned samples in water
k	Heat transfer coefficient
kc	Heat transfer coefficient (cooling)
kh	Heat transfer coefficient (heating)
P_a	Aggregate percent by total weight of asphalt mix
PAV	Pressure Ageing Vessel
PAV	Oxidative pressure ageing vessel
P_s	Steel percent by total weight of asphalt mix
PTV	Pendulum Test Value
RAP	Reclaimed Asphalt Pavement
RCAT	Rotating cylinder ageing test
RILEM	The international union of laboratories and experts in construction materials, systems and structures
RTFOT	Rolling thin film oven test

$S(\tau)$	Healing Ratio
SARA	Saturates, Asphaltencs, Resins and Aromatic
S_m	Stiffness Modulus
SMA	Stone Matrix Asphalt
SOL	Solution
T	Temperature
t	Time
T_{air}	Ambient temperature
t_c	Cooling time
TFOT	Thin film oven test
t_{heat}	Heating time
TSCS	Thin surface course systems
T_{ss}	Steady state temperature
V_a	Air voids content
VFA	Voids filled with asphalt
VMA	Voids in mineral aggregate
η^*	Complex viscosity

Chapter 1: **Introduction**

1.1 Overview and Problem Statement

Highway networks are the most used among all modes of transportation. Therefore, and because of overloading from commercial vehicles and climatic changes, highway pavements suffer from one or more types of distress, which may progress to failure. The providing of suitable and preventive maintenance will eliminate the deterioration of pavements. Highway pavement maintenance activities aim to preserve pavement conditions, strengthen pavement structures, and extend the service life of pavements (Fwa et al., 1990).

Hot mix asphalt is one of the most common types of pavement surface material used across the world. The combined effects of traffic loading and the environment will cause every flexible pavement, no matter how well-designed/constructed to deteriorate over time. It is common knowledge that once a crack is open in the pavement, because of bitumen viscoelastic properties, it starts healing and, if it has enough rest time, it can even close completely. Furthermore, the healing process can be accelerated by exposing the pavement to heat energy, which will minimize the failure progress, which in turn mean that thinner pavements, with longer lifetimes, could be built. On the other hand, in hot countries (like Iraq, Spain and others) this phenomenon doesn’t work even after a long rest time and the cracks reappear.

1.2 Aims and Objectives

In this research, the aims and objectives are divided into different categories.

Firstly, study the self-healing phenomenon in asphalt mixes and the effect of heating time, heating rate and heating temperature for different air voids mixes. The optimum heating time and heating temperature will be evaluated to find out why in hot countries this phenomenon doesn't work. This process will be performed by using infrared lights as a heating source to mimic the environmental heating (sun heat) and compare the results with the induction heating technique.

Secondly, compare the healing efficiency and changes in the mechanical properties of hot mix asphalt containing four different steel fibres. These fibres are mainly by-products and waste materials to minimize the production cost. At the same time, this would also help to reduce the amount of heavy waste disposed in landfills.

Finally, evaluate the effect of bitumen on the healing abilities of the asphalt mix. Aged hot mix asphalt (HMA) with different ageing stages, different reclaimed asphalt pavement (RAP) content and five virgin bitumens will be used to investigate their effect on mix self-repair.

1.3 Research Methodology and Thesis Structure

To achieve the above aim and objectives, the following methodology consisting of ten tasks was adopted:

1.3.1 Task 1: Review of Literature

Chapter 2 reviews literature regarding asphalt materials, particularly bitumen and its mechanical properties. Bitumen ageing is an important factor in asphalt pavement distress and will be investigated here. Self-healing attempts to reverse failure mechanisms of asphalt; hence these failure mechanisms will be explored for better understanding. Moreover, the review introduces the self-healing phenomenon in asphalt and describes the concept of novel techniques focussing on induction heating, which is the main healing technique used through the study.

1.3.2 Task 2: Materials Characterization, Mixture Design and Manufacturing

Chapter 3 characterizes the main material properties and mix design concepts used throughout the experimental work and the outlines the procedures implemented to obtain the results.

1.3.3 Task 3: Induction Heating vs Infrared Heating

This task compares the self-healing efficiency of two heating methods induction and infrared heating, investigating the air void percentage, heating time, and heating rate effect on the self-healing. These aspects are covered in Chapter 4.

1.3.4 Task 4: Steel Fibre Type Effect on Self-Healing

In this task, the mechanical properties and the heating potential of different recycled metal products and by-products as conductive particles in

the hot asphalt mix are evaluated, to find suitable and cheap alternatives for the conductive particles to minimize the mix production cost without compromising its properties. This task is presented in Chapter 5.

1.3.5 Task 5: Ageing and RAP Effect on Self-Healing

This task investigates mixtures representing a broad range of different age levels and degrees of RAP (reclaimed asphalt pavement) on induction healing. Therefore, mechanical, rheological and thermal analysis were evaluated. The results are included as Chapter 7.

1.3.6 Task 6: Bitumen Source and Grade Effect on Self-Healing

To understand how self-healing is affected by the source and type of bitumen, different grades and sources binder added to mixtures were investigated. The rheology and mechanical properties were tested. Furthermore, chemical analyses were conducted through SARA test (saturates, asphaltenes, resins and aromatics). This is reported in Chapter 6.

1.3.7 Task 7: Overall Conclusions and Recommendations

Here a combined discussion of all the experimental phases and a synthesis of the testing results is performed to provide a comprehensive picture of the whole project. Then, overall conclusions and practical implications of the study are presented. This task is the focus of Chapters 8.

Chapter 2: **Literature Review**

2.1 Overview

The self-healing phenomenon of bituminous materials has been known about for over four decades; but it was only recently that engineers have begun to explore methods of accelerating this natural healing in asphalt pavements. Self-healing has the potential to extend the service life of pavements, significantly reducing maintenance costs, creating a sustainable means of road engineering. To be able to understand self-healing in asphalt pavements it is important to consider and explore all the factors that contribute to it.

This chapter therefore reviews literature in order to provide a suitable background into the subject of self-healing in asphalt pavements before then introducing novel self-healing techniques. This chapter will then explore literature regarding the physics of induction heating and its use in asphalt pavements, on which part of the research will focus.

2.2 Asphalt Pavement Structure

Asphalt pavements are a combination of aggregate and bituminous material constructed in various thicknesses and types (Martin and Wallace, 1958). Although asphalt is mainly used for paving roads, it can also be used for various other purposes. The versatility of asphalt makes it such a widely used material. Among others, it can be found in the following sectors: Transportation (roads, railway beds, airport runways, taxiways), Recreation (playgrounds, bicycle paths, running tracks, tennis courts), Agriculture (barn

floors, greenhouse floors), Industrial (ports, landfill caps, work sites) and Building construction (floorings) (Thom, 2014, Mallick and El-Korchi, 2013).

Aggregates used for asphalt mixtures could be crushed rock, sand, gravel or slags. In order to bind the aggregates into a cohesive mixture a binder is used. Most commonly, bitumen is used as a binder. An average asphalt pavement consists of the road structure above the formation level which includes unbound and bituminous-bound materials. This gives the pavement the ability to distribute the loads of the traffic before it arrives at the formation level. Asphalt pavements are known as flexible pavements, which are normally constituted of several distinct layers overlying the subgrade. The lowest of these layers is the sub-base above which are laid the base and the surfacing layers (Yoder and Witczak, 1975); the surface layers consist of a wearing course and a binder course. Pavement design considers the nature of the subgrade and the volume and constitution of the traffic. A desirable pavement transmits traffic stresses through each layer and to the soil beneath without compromise to the structural integrity of the road. The wearing course plays little structural role but provides a safe contact with vehicle tyres and has a waterproofing function protecting underlying material, although porous asphalts are an exception to this. It must also be durable to resist deterioration from environmental factors. The binder course and the road base must have the ability to spread the wheel load so that underlying layers are not overstressed (Hunter, 1994); they must be high in stiffness, crack resistant and deformation resistant. The subgrade beneath these layers consists of granular materials and soils; if the subgrade

is weak it will be necessary to have a capping layer over it such as a hydraulically bound material (Thom, 2014). Figure 2-1 illustrates the different layers of asphalt pavements.

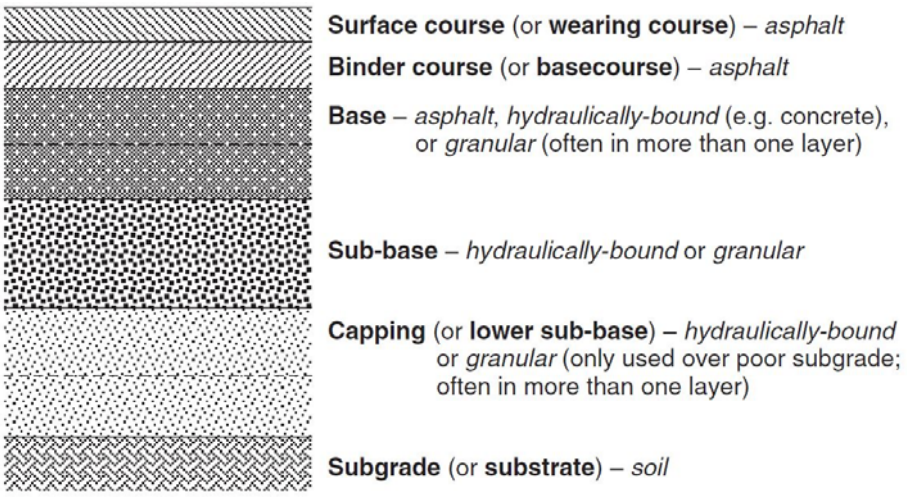

Figure 2-1 Typical asphalt pavement layers
(Thom, 2014)

Flexible pavement design uses the principle of load spread; load of any magnitude may be dissipated by carrying it deep into the ground through successive layers of granular material (Martin and Wallace, 1958). The intensity of the load diminishes as it is transferred through the soil by spreading over an increasingly large area; this enables materials with less stiffness to be employed as depth increases, minimising material costs. Figure 2-2 demonstrates the stress distribution through the layers; the level of stress induced in overlying layers is dependent on the elastic stiffness of layers beneath. Hunter outlined that the interaction between the elastic stiffness of the base, the shear stress in the foundation and the tensile stress in the road base are essential to pavement design (Hunter, 1994). It is correct to say that with stiffer materials employed in the upper layers there will be a noticeable reduction of subgrade stress and deflection. However

Yoder makes a clear point: although materials with a higher modulus reduce the risks associated with a subgrade mode of distress, such as shear, the presence of this layer increases the tensile stress in the bottom of this layer as well as increasing horizontal shearing stress. Hence during design it is required to ensure both the shearing resistance and the flexural resistance of this stiff layer are great enough to sustain these higher stress conditions (Yoder and Witczak, 1975).

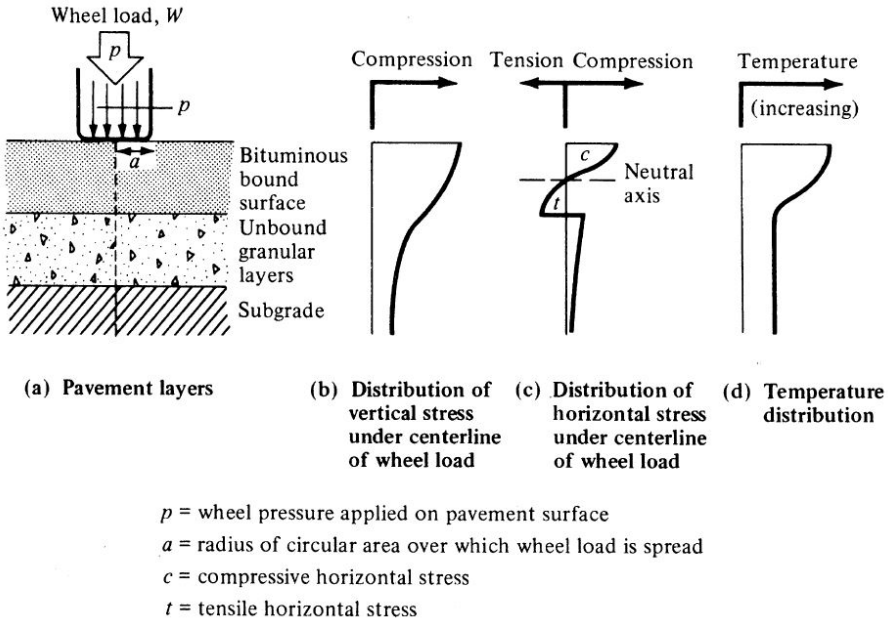

Figure 2-2 Stress distribution through asphaltic layers
(Garber and Hoel, 2014)

2.3 Classification of Asphalt Mixtures

To offer the best performance under different conditions, there are a wide range of asphalt mixes possible. For example, to fulfil the roads need to withstand high traffic and environmentally induced stresses; the respective mix used should have sufficient stiffness and resistance to

deformation, yet have acceptable flexural strength to resist cracking. Besides, desirable functional characteristics such as skid resistance, noise reduction, durability and drainage are often required. This section covers three of the more common types of hot mix asphalt. Other flexible pavements such as bituminous surface treatments (BSTs) are considered by most agencies to be a form of maintenance. HMA mix types differ from each other mainly in maximum aggregate size, aggregate gradation and asphalt binder content/type (Pavement_Intractive, 2010, Yoder and Witczak, 1975, Highways_England, 2008a, Highways_England, 2008b, EAPA, 2007). The three most common types of HMA are:

2.3.1 Dense-Graded HMA

A dense-graded mix is a well-graded HMA mixture intended for general use. When properly designed and constructed, a dense-graded mix is relatively impermeable. Dense-graded mixes are generally referred to by their nominal maximum aggregate size. They can further be classified as either fine-graded or coarse-graded. Fine-graded mixes have more fine and sand sized particles than coarse-graded mixes, see Figure 2-3. Dense graded HMA contains all sizes of aggregate particles. There are enough fine particles to effectively separate many of the coarse particles. Therefore, stress transmission through the HMA structure relies on both the coarse and fine particles. Voids in mineral aggregate are generally between 11 and 17%, air voids are generally near 4% and bitumen content can range between 4.5 and 6% (Highways_England, 2008b, Pavement_Intractive, 2010).

Figure 2-3 Dense-graded HMA
(Pavement_Intractive, 2010)

2.3.2 Gap-Graded HMA

Gap-graded HMA (or Stone matrix asphalt (SMA)) is designed to maximize deformation (rutting) resistance and durability by using a structural basis of stone-on-stone contact. Because the aggregates are all in contact, rut resistance relies on aggregate properties rather than asphalt binder properties. Since aggregates do not deform as much as asphalt binder under load, this stone-on-stone contact greatly reduces rutting. SMA is generally more expensive than a typical dense-graded HMA (by 20-25 percent) because it requires more durable aggregates, higher binder content and, typically, a modified asphalt binder and fibres. In the right situations it should be cost-effective because of its increased rut resistance and improved durability. SMA was originally developed in Europe to resist rutting and studded tire wear, see Figure 2-4. Gap graded HMA contains few mid-sized particles. Stress transmission goes through coarse particles; fines generally fill in space between the coarse particles giving the HMA more resistance to deformation. VMA (17%+) is higher than for dense graded HMA but the

bitumen content (6%+) is also higher, which results in about the same volume of air voids (4%) (Highways_England, 2008b, Pavement_Intractive, 2010).

Figure 2-4 Gap-graded HMA
(Pavement_Intractive, 2010)

2.3.3 Open-Graded HMA

An open-graded HMA mixture is designed to be water permeable (dense-graded and SMA mixes usually are not permeable). These mixes use only crushed stone (or gravel) and a small percentage of manufactured sands. Open-graded mixes are typically used as wearing courses or underlying drainage layers because of the special advantages offered by their porosity, see Figure 2-5. Open graded HMA contains few fine aggregate particles. This creates large air voids between the coarse and medium-sized particles. These air voids, often between 15 and 20% of the total volume, make the HMA water permeable. VMA is generally between 20 and 25%, while the bitumen content can range between 3.5 and 6% (Highways_England, 2008b, Pavement_Intractive, 2010, EAPA, 1998).

Figure 2-5 Open-graded HMA
(Pavement_Intractive, 2010)

2.4 The Mechanics of Asphalt Materials

Asphalt is a complex, unique material due to its composition, its manufacturing process, its use environment and its performance or failure modes. Asphalt typically comprises a bituminous binder, graded aggregate and air voids. The properties of the material depend on the type and grade of the binder and type and gradation of aggregate. Other constituents may include additives such as fillers, rubbers and plastics often used to enhance the properties of the asphalt mix; Isacsson and Lu talk in detail about bitumen additives and their effects on functional properties of the pavement, presenting new test methods (Isacsson and Lu, 1995).

2.4.1 An Introduction to Bitumen

Bitumen is a complex, viscoelastic material manufactured from crude oil through a series of distillation processes undertaken during the refining of petroleum. Different petroleum sources and refining procedures

will end up with binders of different molecular structure and compositions (Wang, 2012). This complexity results in a wide range of physical properties that can be measured in UK through a combination of empirical and rheological testing; these properties however must meet the specification requirements outlined by the British Standard BS EN12591:2009 (BSI, 2009a). As previously mentioned flexible pavements work by spreading loads from bitumen-bound layers to underlying unbound material to prevent overstressing, also providing stiffness and bearing capacity. The mechanical properties of asphalt are highly dependent on the properties of the binder; hence it is important to be able to understand and measure the rheological and mechanical properties of bitumen (Domone and Illston, 2010).

2.4.2 Bitumen Constitution

Rheology is the study of flow and deformation of matter; changes in the constitution and/or structure of a material will result in a change of rheology. Therefore, it is important to understand how the constitution and structure of bitumen interact to influence its rheology. Bitumen is a complex mixture of molecules, predominantly hydrocarbons with a small amount of heterocyclic species and functional groups containing sulphur, nitrogen and oxygen atoms as well as traces of metals like nickel and magnesium (Traxler, 1936).

Bitumen composition varies depending on the source of crude oil and its manufacturing process; chemists have simplified the chemical composition of bitumen into more homogenous fractions based on solvent extraction, absorption, chromatography and molecular distillation (Zakar,

1971). Bitumen can be separated into two chemical groups: asphaltenes and maltenes; maltenes can be further separated into saturates, aromatics and resins. Asphaltenes affect the rheological properties of bitumen; increasing the asphaltene content produces harder, more viscous bitumen (Read and Whiteoak, 2003) with a higher glass transition (typically asphalt binders range from -40^{o}C to 0^{o}C) (Read and Whiteoak, 2003). Resins are dispersing agents or peptisers for asphaltenes; their proportion to asphaltenes governs the structural character of the bitumen, the solution (SOL) or gelatinous (GEL) type character of the bitumen. The addition of resins hardens the bitumen (Read and Whiteoak, 2003).

Aromatics are the main dispersers for the peptised asphaltenes. Saturates are non-polar viscous oils; increasing the saturate content softens the bitumen. The structure of bitumen is regarded as a colloidal system with high molecular weight asphaltene micelles dispersed or dissolved in a lower molecular weight oily medium (Read and Whiteoak, 2003). The index of colloidal stability (CI) is the ratio of asphaltenes and saturates to resins and aromatics, it is used to describe the stability of the colloidal structure; the greater the CI value the more the bitumen is considered as GEL type bitumen, the lower the CI value the more stable the colloidal structure (Domone and Illston, 2010). The physical and mechanical properties of bitumen are defined by its constitution and structure.

2.4.3 The Mechanical Properties of Bitumen

Bitumen has two important rheological properties, being thermoplastic and viscoelastic. Having thermoplastic properties the viscosity of the material reduces when heated and increases when cooled;

showing a glass like behaviour at low temperatures (<0°C) and fluid like behaviour at high temperatures (>60°C) (Domone and Illston, 2010), this process is reversible. At intermediate temperatures (0-60°C) bitumen has visco-elastic properties, so when a force is applied to the material its structure will distort as well as flow. Viscous flow is irrecoverable, whereas elastic behaviour, like distortion, is recoverable. The relative proportions of viscous and elastic response exhibited by bitumen when a force is applied depend on its constitution, the loading rate and temperature (Hunter, 1994). A material responds to stress by movement; recoverable movement is recorded as strain, irrecoverable movement is recorded as the rate of strain. Viscosity is the measure of the resistance to flow of a liquid and is defined by the ratio of shearing stress to the corresponding rate of shearing strain. The stiffness modulus is the parameter for solids defined as the ratio of applied stress to the corresponding strain.

The physical behaviour of bitumen is complex. Airey discusses the different empirical tests used to describe the physical properties of bitumen in a simplified manner, including the two consistency tests required by the European standard EN12591: 2009 (BSI, 2009a) (Domone and Illston, 2010).

2.4.4 The Ageing of Bitumen

The properties of bitumen, like many other organic materials, are altered in the presence of oxygen, ultraviolet radiation and changes in temperature. These external influences on the material can cause changes in its chemical composition affecting its rheological and mechanical

properties. This process is known as ageing and can cause bitumen to harden, reducing its viscosity and increasing its stiffness. Ageing can be seen as an improvement to structural performance; for example the hardening, also known as curing, of bitumen over time will result in a 200% increase in elastic stiffness of dense bitumen macadam (DBM) in the first few years of service (Nunn et al., 1997).

Ageing can also be detrimental, reducing pavement flexibility hence reducing the strain level to failure and its stress relaxation behaviour, heightening sensitivity to fretting and cracking (Hagos, 2008). Traxler (1963) has tabulated the variety of factors that can cause ageing, stating the most important as oxidation, volatilisation, steric or physical factors and exudation of oils. Bitumen over time oxidises if it is in contact with atmospheric oxygen, the more permeable the pavement structure the more susceptible it is to this process; oxidation is known as long-term ageing. Polar molecules within bitumen combine with oxygen, which can associate into micelles of higher micellar weight increasing the viscosity of bitumen (Read and Whiteoak, 2003). During asphalt production, transportation and laying (short-term ageing) bitumen loses considerable mass due to loss of volatiles; high temperature will result in a volatile loss and will change the nature of the oxygen reaction with the bitumen components (Domone and Illston, 2010); however Hagos (2008) reports that loss of volatiles over the pavements life is insignificant. Long-term ageing is difficult to examine because of the difficulty of simulating in-situ conditions; laboratory methods such as the pressure-ageing vessel (PAV) are not considered

entirely accurate and require revising into a more complex model (Read and Whiteoak, 2003, Hagos, 2008, Domone and Illston, 2010).

2.4.5 Bitumen Adhesion or Aggregate Bonding

Bitumen's adhesive properties are fundamental to asphalt pavements, binding aggregate particles together. There are many factors that can affect bitumen-aggregate adhesion, but most of these factors can be controlled during production; one of the main factors is mineralogical composition. It is the physico-chemical properties of the aggregate that can affect bitumen adhesion such as its chemical composition, shape/size/texture, structure and residual valency (Read and Whiteoak, 2003). The type of aggregate can affect adhesion based on its affinity for bitumen; siliceous aggregates for example tend to cause adhesive failures due to their high silicon oxide content, which makes coating them with bitumen difficult. Difficulty in coating the aggregate is also because aggregates tend to be hydrophilic and oleophobic, favouring water instead of the bitumen; this can be demonstrated by the residual valency or the surface charge of an aggregate. Unbalanced surface charges of an aggregate possess a surface energy that can attract liquids of opposite polarity, creating an adhesive bond between them. With multiple liquids, the one that can best satisfy the energy requirement will adhere better. The phenomenon of stripping is when water can better satisfy the surface energy requirement of the aggregate, leading to a separation of bitumen (Read and Whiteoak, 2003, Domone and Illston, 2010). The physiomechanical absorption properties of bitumen are another important factor of bitumen-aggregate adhesion. The absorption of bitumen depends on the petrographic

characteristics of the aggregate. Domone and Illston (2010) state that a fine microstructure of pores, voids and microcracks will increase the surface available to the bitumen by a considerable amount, though a general assumption is that with rougher surfaces there is a better adhesion. For good adhesion there must also be a balance between the wettability of the aggregate (i.e. a smooth surface), which allows the bitumen to coat the aggregate, and a rough surface texture that grips the binder once wetted.

The modes of failure, for example ravelling see Figure 2-6, in asphalt pavements are adhesive or cohesive (Hagos, 2008). Adhesive failure is predominantly a result of damage caused by the effects of water; cohesive failure is caused when the stress levels in the binder exceed its strength. The effect of water can instigate cohesive failure by 'softening' the binder, reducing its structural integrity and strength. Alternatively, as the material ages and hardens the binder, it may better resist the effects of water on its adhesive strength; however the chances of cracking are greater. Kanitpong and Bahia (2003) investigated this damaging effect of water with regard to the cohesive and adhesive properties of binders. They found that water damage in binders could be seen as stripping (adhesive failure) or the reduced resistance to traffic induced stresses (cohesive failure). There are a number of mechanisms that cause a loss of adhesion and hence de-bonding of bitumen and aggregate, most of which involve the action of water. Read and Whiteoak (2003) go into detail about each of the following mechanisms: displacement-relating to the thermodynamic equilibrium of aggregate/ bitumen/ water, detachment, film rupture, blistering and pitting, spontaneous emulsification, hydraulic scouring and pore pressure.

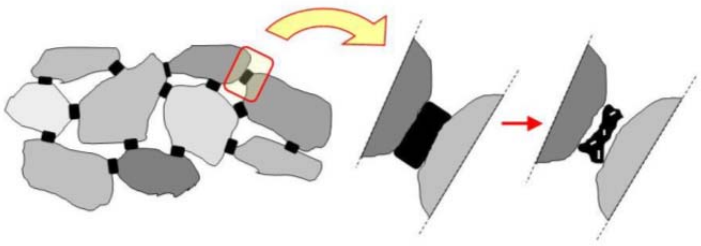

Figure 2-6 The mechanism of ravelling
(Hagos, 2008)

When it comes to improving the adhesion of bitumen and aggregate there are several options. Hydrated Lime is a proven additive to asphalt pavements, reversing ageing and increasing fatigue resistance; The Asphalt Task Force explore the benefits of using lime in pavement in detail (European_Lime_Association, 2010). Hydrated Lime is used to increase adhesion in two ways: ketones present in the lime attach themselves to the aggregate preventing the effects stripping and calcium ions present in the lime create a hydrophobic surface repelling water (Read and Whiteoak, 2003). Alternative methods might be to modify the viscosity of bitumen through the use of rejuvenators, better wetting of the aggregate and the use of fatty amines that can create strong ionically bonded crosslinks between the bitumen and aggregate.

2.4.6 The Stiffness of Asphalt Mixes

Asphalt as a combined material of an aggregate and bitumen must provide a suitable surface for vehicle contact and also protect underlying materials from both environmental conditions and vehicle loading. To be able to resist loading the asphalt must have a sufficient stiffness modulus. Stiffness is the resistance to deformation under applied stress conditions. As

asphalt mixture is a visco-elastic material, the stiffness of asphalt mixture normally includes elastic and viscous components. The proportions of each component rely primarily on the temperature and the loading time. Under low temperature and short loading time, the asphalt mixture will behave elastically. On the contrary, the relation between stress and strain will be more viscous under high temperature and long loading time (Read and Whiteoak, 2003). The stiffness of asphalt mixes is highly important in determining how well a pavement performs and analysing the pavements response to traffic loading. Furthermore, the stiffness of asphalt will increase as the bitumen ages and its viscosity increases.

2.4.7 Failure Mechanisms through Permanent Deformation

Permanent deformation or rutting is due to traffic loading displacing asphalt away from the wheel paths; the result is a series of depressions and humps along the sides of the wheel paths. Permanent deformation can only occur if the aggregate skeleton deforms; therefore properties that result in low plastic strain, for example increased aggregate content and particle to particle contact, are favourable to resist permanent deformation.

During low temperatures, plastic strain in aggregate particles is slight because the bitumen binder inhibits it, removing stress away from the particle contacts. With increasing temperatures, stress at particle to particle contact increases to a point which can induce particle slipping and hence permanent deformation in terms of the aggregate skeleton. A low air void content can cause extra compressive stresses in the binder, which means there is less normal stress at particle contacts increasing the chance of particle slip (Thom, 2014).

2.4.8 Failure Mechanisms through Fatigue and Fracture

Asphalt contains an aggregate skeleton, a bitumen binder and a percentage of air voids; under strain, the aggregate skeleton deforms via two mechanisms outlined by Thom (2014): compression at particle contacts and inter-particle slip (combined with rotation and separation). If there is no inter-particle slip then the stiffness of the material is assumed as that of the aggregate used (with the addition of the contact law and the effects of the binder). Under traffic loading, strain imposed on the mortar (fine aggregate/sand/filler-bitumen) may cause inter-particle slip to occur. Thom (2014) illustrates this slip at particles contacts in Figure 2-7 and Figure 2-8. As the contact between aggregate particles is approached strain in the mortar increases to a point where it is infinite; infinite strain can only be described as fracture (Thom, 2014), which will lead to particle slip and separation to occur. Fractures can propagate until they reach a region where strain is sufficiently low, causing gradual weakening of the structure. Fatigue is the propagation and enlargement of these fracture zones at particle contacts controlled by strain within the mixture. Little et al. (1997) state that fatigue is a two-stage process: (a) microcrack growth and healing and (b) macrocrack growth and healing. Where, the propagation of micro cracks may lead to larger and more serious macro cracks.

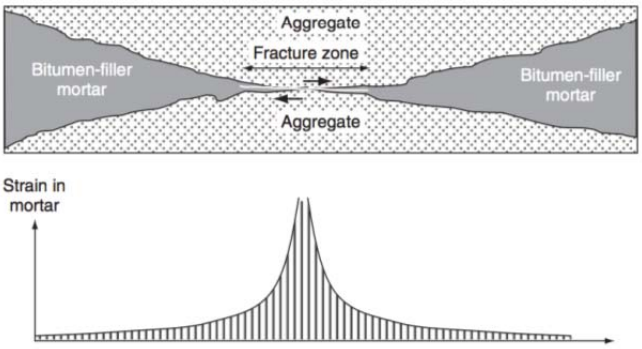

Figure 2-7 Stress distribution in fraction zone
(Thom, 2014)

Figure 2-8 Development of cracks in asphalt mastic
(Asphalt_Research_Consortium, 2011)

Fracture mechanics depend on temperature and rest periods between loads, the critical situation being when there is a low temperature and short rest periods. Rest periods, the time between consecutive wheel load applications, are important to allow fracture zones to heal and stresses/strains to relax due to viscous flow of the bitumen (Osman, 2004). With low temperature bitumen has an increased stiffness restricting inter-particle movement; with a greater stiffness there is increased stress that passes through the binder increasing the chances of its fracture. With high temperatures there is far less stress in the binder and the phenomenon of healing may occur, where the bitumen becomes less viscous and flows into any fractures. Thom (2014) suggests there is “a state of dynamic flux”,

where with low temperatures there is a high stiffness and increased damage, and with high temperatures there is a low stiffness but also healing.

There is little research into the combined effects of both temperature and cyclic loading; Osman (2004) makes a simple analysis that, “a more elevated temperature, like a longer rest period, increases the healing capacity of the bitumen”; however temperature and rest periods are independent, where there is a high temperature there could be short rest periods. It is particularly hard to model rest periods when considering the effects of self-healing because they are entirely dependent on the road and its traffic volume at different times (Read, 1996).

2.5 Self-Healing Materials

The self-healing concept is developed from biological and natural phenomena, which help organisms to recover, repair cracks and to extend the life span. Similarly, ideas are explored by material scientists to develop many kinds of novel self-healing materials. Table 2-1 lists novel self-healing mechanisms used in advanced composite structures from mimicking nature (Trask et al., 2007). There are mainly two types of novel self-healing material systems, namely liquid based and solid based self-healing systems (Qiu, 2012).

The concept of self-healing materials is not new; the Romans used lime in their mortars over 2000 years ago, lime dissolves in rainwater and can seep into cracks filling them when the water vaporizes, ‘healing them’. Healing is important so that materials can remain reliable and durable over a long life span. With multiple use of a material, its properties will degrade

over time due to fatigue and initiation of micro cracking; fatigue will worsen and cracks will propagate leading to failure of the material. Self-healing material has a built in ability to repair itself over time (Qiu, 2012).

Table 2-1 Biomimetic self-healing inspiration in novel self-healing materials

(Trask et al., 2007)

Biological attribute	**Composite/polymer engineering**	**Systems**	**Systems Biomimetic self-healing or repair strategy**
Bleeding	Capsules	Liquid based	Action of bleeding from a storage medium housed within the structure, 2-phase polymeric cure process rather than enzyme "waterfall" reaction
Bleeding	Hollow fibres	Liquid based	Action of bleeding from a storage medium housed within the structure, 2-phase polymeric cure process rather than enzyme "waterfall" reaction
Blood flow Vascular network	Hollow fibres	Liquid based	2D or 3D network would permit the healing agent to be replenished and renewed during the life of structure
Blood clotting	Healing resin	Liquid based	Synthetic self-healing resin systems designed to clot locally to the damage site. Remote from the damage site clotting is inhibited and the network remains flowing
Concept of self-healing	Remediable polymers	Solid based	Bio-inspired healing requiring external intervention to initiate repair
Blood cells	Nano-particles	Solid based	Artificial cells that deposit nanoparticles into regions of damage
Skeleton/bone healing	Reinforcing fibres	Solid based	Deposition, resorption, and remodelling of fractured reinforcing Fibres
Elastic/plastic behaviour in reinforcing fibres	Reinforcing fibres	Solid based	Repair strategy, similar to byssal thread, where repeated breaking and reforming of sacrificial bonds can occur for multiple loading cycles
Tree bark healing	-	Solid based	Formation of internal impervious boundary walls to protect the damaged structure from environmental attack

2.5.1 Concept of Self-Healing

Self-healing can be defined as the built-in ability of a material to automatically heal (repair) the damage occurring during its service life (White et al., 2001). The properties of a material degrade over time due to damage (such as microcracks) at microscopic scale. These cracks can grow and ultimately lead to full scale failure. Usually, cracks are mended by hand, which is difficult because micro cracks are often hard to detect. In the field of materials science researchers are now trying to introduce self-healing components to normal materials to obtain a self-healing system to improve the service life of materials. A material that can intrinsically correct damage caused by normal usage could lower production costs of a number of different industrial processes through longer part lifetime, reduction of inefficiency over time caused by degradation, as well as prevent costs incurred by material failure (Hager et al., 2010, van der Zwaag and Brinkman, 2015, Wool, 2008).

The dominant research on self-healing materials is done in the field of polymers. The first patent of a polymer with intentional self-healing characteristics dates back to 1966. Craven developed reversible cross-linked polymers from condensation polymers with pendant furan groups cross-linked with maleimides (Craven, 1969). These polymers could reverse to their cross linked state after cracking. Unfortunately, the potential of this route was not appreciated.

In 1994, Dry developed an active and a passive cracking repair method by smart timed release of polymerizeable chemicals from porous and brittle hollow fibres into cement matrices (Dry, 1994). As shown in

Figure 2-9 (left), the active cracking repair system contains porous fibres coated with wax and filled with methyl methacrylate. When a crack occurs, low heat is applied to the cement matrix, wax is melted and the methyl methacrylate is released into the matrix. Subsequent heating makes the methyl methacrylate polymerize to close the crack. In the passive crack filling method, loading, which causes microcracking in the cement matrix, breaks the brittle hollow glass fibres to release the chemicals, Figure 2-9 (right).

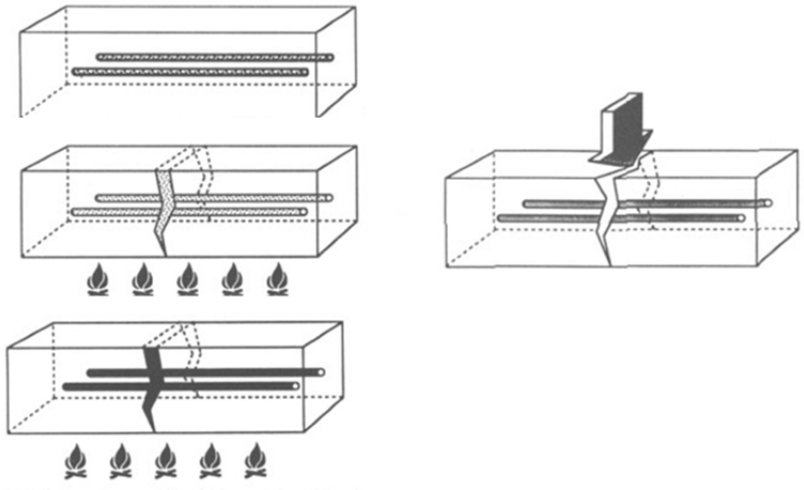

Figure 2-9 Design for timed release of polymerizeable chemicals to repair and fill cracks
(left) by melting of the coating on porous fibres, (right) the brittle fibre breaks under load (Dry, 1994)

The first completely autonomous synthetic self-healing material was reported by White et al. (2001) with an example of a polymer composite with microcapsules. This healing concept is illustrated in Figure 2-10. A microencapsulated healing agent is embedded in a structural composite matrix with a catalyst capable of polymerizing the healing agent. An approaching crack breaks the embedded microcapsules, releasing the healing agent into the crack plane through capillary action. Polymerization

of the healing agent is triggered by contact with the embedded catalyst, closing the crack faces.

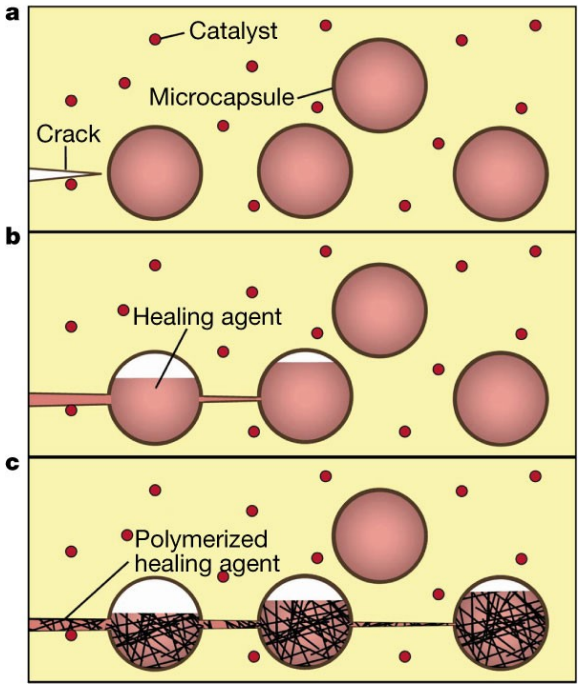

Figure 2-10 The self-healing concept with microcapsules
(White et al., 2001)

Since then, more and more research on creating self-healing materials has been conducted successfully. These self-healing materials consist of concrete (Li and Yang, 2007, Schlangen, 2013), asphalt (Little and Bhasin, 2007); polymer and composites (Andersson et al., 2007); and others.

2.5.2 Self-Healing of Asphalt Concrete

Similar to other self-healing materials, asphalt concrete can repair the damage autonomously. Asphalt concrete has a potential to restore its stiffness and strength, when subjected to rest periods. This self-healing

capability of asphalt concrete has been shown both with laboratory tests and in the field since the 1960s (Bazin and Saunier, 1967, Van Dijk et al., 1972, Francken, 1979). Bazin and Saunier (1967) found that asphalt concrete beams, tested until failure under uniaxial tensile loads could recover 90% of their original resistance when they were left to rest under pressure at a temperature of 25°C. Meanwhile, they found that fatigue damaged beam samples could regain over a half of their original fatigue life after introducing a one day rest period to the failed samples and pressing the crack faces together with a small pressure during this rest period. The recovery of both strength and fatigue life were evidence of healing caused by rest periods. After that, more laboratory experiments were done to study the strength recovery and the fatigue life extension of an asphalt mixture when rest periods were introduced in between the loadings. Laboratory experiments done by Castro and Little demonstrated that the fatigue life of an asphalt mixture could be extended when rest periods were introduced in the normally continuous loading test (Castro and Sánchez, 2006, Little and Bhasin, 2007). Healing of asphalt concrete was also shown with field experiments: Si et al. (2002) used surface wave measurements to assess the stiffness of a pavement before, immediately after, and 24h after loading passes. The stiffness recovered completely after 24 hours of rest. It has also been reported by many researchers that cracks observed in winter time disappeared in summer time. As a consequence, healing plays an important role in the shift factor required to translate the laboratory fatigue life into the in-situ fatigue life (Lytton et al., 1993).

2.5.3 Explanation of Self-Healing of Bitumen and Asphalt Mixes

Healing of an asphalt mixture is the recovery of its stiffness and strength due to closure of the cracks inside. Many researchers have reported the healing mechanisms of asphalt concrete.

Healing is usually believed to be related to the sol-gel properties of bitumen. Bitumen is traditionally regarded as a colloidal system consisting of high molecular weight asphaltene micelles dispersed or dissolved in the lower molecular weight oily maltenes (Shell, 1995). Within the sol-gel system of bitumen, the transformation from sol to gel or from gel to sol happens reversibly due to the change of temperature, stress, etc. The colloidal properties of a bitumen system change from gel-like type at low temperature to sol-like type at high temperature. When the temperature goes down, the colloidal property of bitumen will return from sol-like to gel-like. Loading causes bitumen to behave sol-like, just like water. When the loading is ended, the properties of bitumen immediately turn to gel-like. Castro and Sánchez explained the healing of asphalt mixes during rest periods by the sol gel theories. At high temperature, healing takes place due to a conversion from a sol to a gel structure of bitumen. If the rest time is sufficient, this would be almost complete. At low temperature, rest periods don't allow the healing of the structural damage created by the loading cycles and recovery would only be partial (Castro and Sánchez, 2006).

Phillips (1998) proposed a three steps diffusion model to explain the healing of bitumen: (1) surface approach due to consolidating stresses and bitumen flow, (2) wetting (adhesion of two cracked surfaces to each other

driven by surface energy density), and (3) diffusion and randomization of asphaltene structures. The first two steps cause the recovery of the modulus (stiffness) and the third step causes the recovery of the strength.

Little and Bhasin (2007) proposed a similar 3 steps model to describe the healing process of asphalt materials: (1) wetting of the two faces of a nanocrack, (2) diffusion of the molecules from one face to the other, and (3) randomization of the diffused molecules to attempt to reach the original strength of the material. Wetting is determined by the mechanical and viscoelastic properties and material constant of the bitumen (tensile strength, work of cohesion and surface free energy). The subsequent recovery of strength is determined by the surface free energy of the asphalt binder and the self-diffusion of asphalt cement molecules across the crack interface (Bhasin et al., 2008).

Little et al. (2001) separated the healing during rest periods into a short-term healing rate (healing rate occurs during the first 10s of the rest period) and a long-term healing rate (healing rate occurs after the first 10s of the rest period). Short-term healing and long-term healing were distinguished based on their relations with the Lifshitz van der Waals surface energy component and the acid-base surface energy component of the material, respectively. The short term healing was inversely proportional to the Lifshitz van der Waals component of surface energy, while the long term healing was directly proportional to the acid-base component.

Kringos et al. (2011) used a chemo-mechanical model to simulate healing of bitumen. Bitumen has the tendency to phase separation under mechanical or environmental loadings and the resultant interfaces of the

phases will attract high stresses and are prone to cracking. By increasing the temperature or inserting mechanical energy, the phases would rearrange themselves in either a new configuration or mix themselves into a more homogenous state, giving the appearance of the existence of a single phase. The material would thus close the micro cracks, and this will result into a recovery of the mechanical properties.

2.5.4 Factors Influencing Self-Healing of Asphalt Concrete

Many factors can influence the self-healing rate of asphalt concrete. These factors can be divided into three categories: bitumen properties, asphalt mixture composition and environment.

2.5.4.1 Bitumen properties

Considering the fact that asphalt concrete can restore itself because of the healing potential of the bitumen inside, there is no denying that bitumen properties play a significant role in the self-healing potentials of asphalt concrete. Many researchers reported how the bitumen properties influence its healing potential.

2.5.4.1.1 Bitumen type

Van Gooswilligen et al. (1994) studied the effect of the bitumen content and the viscosity of the bitumen on the healing of a dense asphalt concrete for a ratio of rest period over load duration equal to 25. The healing rate of the asphalt concrete increased with the increase of the bitumen content and the healing capacity of soft bitumen 80/100 pen was higher than that of hard bitumen 50/60 pen.

2.5.4.1.2 Viscoelastic properties

As sol-gel theory is often used to explain the self-healing of bitumen, the sol-gel nature of bitumen affects its self-healing rate. It is a common consensus that the viscoelastic properties, which reflect the sol-gel nature of bitumen, influence the self-healing rate of bitumen. Many researchers have proved that a sol like bitumen with a lower stiffness and a higher phase angle shows a higher self-healing capacity (Van Gooswilligen et al., 1994).

2.5.4.1.3 Surface energy density

Lytton et al. (2001) studied the micro damage healing of bitumen and asphalt concrete and established a healing model for asphalt concrete. In his model, the short term healing rate is inversely proportional to the Lifshitz-van der Waals component of surface energy density and the long term healing rate is directly proportional to the acid-base component of surface energy density.

Si et al. (2002) linked the healing rate of asphalt concrete (in terms of pseudo-strain energy recovery ratio) with its surface energy density. The inverse relationship between Lifshitz-van de Waals component of surface energy density and short term healing rate (healing occurs in the first 10 seconds of the rest periods) of asphalt concrete was reported. It is evident that Lifshitz-van de Waals behaviours is not favourable to healing of the binder. They also found that the acid-base component of surface energy density promoted the healing rate of asphalt concrete.

2.5.4.1.4 Bitumen compositions

Si et al. (2002) investigated the effects of the chemical composition of bitumen on its self-healing. They concluded that aromatics promote healing for the pi-pi interaction of the aromatic rings. Amphoterics are also important for healing, which could promote healing for the polar-polar bonds. The wax content is also helpful to healing because of the Van der Waals force of the interactions between long chains of hydrocarbons and aliphatic molecules within the wax. In addition, the heteroatom content promotes healing because sulfur, oxygen and nitrogen promote the polarity of bitumen (Si et al., 2002, Qiu, 2008).

2.5.4.1.5 Diffusion

Diffusion is one of the key factors affecting healing of asphalt concrete. One of the mechanisms of healing is the self-diffusion of the molecules across the crack surface (Bhasin and Motamed, 2011). So, the healing rate is determined by the diffusion speed (the molecular movement speed from a high concentrated region to low concentration region). Phillips also concluded that diffusion limited built-up of asphaltene structure controlled the strength recovery in healing (Phillips, 1998).

2.5.4.1.6 Ageing

Ofori-Abebresse (2006) found that the Lifshitz-van der Waals component of surface energy density increased with ageing, whereas the acid-base component of surface energy density decreased with ageing (Ofori-Abebresse, 2006). The Lifshitz-van der Waals component of the surface energy density is related inversely to the short term healing rate and the acid-base component of surface energy density is related to the long

term healing rate. As a result, the magnitude of both short term healing and long term healing would decrease with ageing. Therefore, the total capacity of healing was decreased by ageing.

2.5.4.1.7 Modifiers

An asphalt pavement with modified bitumen often has very good fatigue and rutting resistance. However, the effect of modifier on the self-healing rate of bitumen during rest periods is far from clear; different researchers have reported different effects of modifiers on self-healing of bitumen (Qiu, 2008, Qiu, 2012).

2.5.4.2 Asphalt mixture composition

The asphalt mixture composition, including bitumen content, aggregate structure characteristics and gradation, also influences the self-healing rate of asphalt concrete.

2.5.4.2.1 Bitumen content

Asphalt concrete can heal itself because the bitumen inside is self-healing. Therefore, the bitumen content plays an important role in healing of asphalt concrete. As shown in section 2.5.4.1.1, the experiments of Van Gooswilligen et al. (1994) showed that an asphalt concrete with higher bitumen contents exhibited higher healing rates.

2.5.4.2.2 Mixture gradation

Abo-Qudais and Suleiman (2005) monitored fatigue damage and crack healing of asphalt concrete by ultrasound wave velocity. The ultrasound pulse velocity was measured on the cylinder asphalt sample

before and after a fatigue test, and after rest periods. The increase of the ultrasound pulse velocity caused by rest periods was used to predict cracking and healing. The sample prepared with higher sizes of aggregates showed a higher healing rate, because the coarse gradation with less surface area has thicker asphalt film thickness and less transition zones between aggregate and asphalt, which improves the asphalt tendency towards cracks healing.

2.5.4.2.3 Structural characteristics

Kim and Roque (2006) concluded in their papers that the healing properties of asphalt mixes are more affected by the aggregate structure characteristics (which affects the aggregate interlock, the film thickness and the voids in aggregate) than by polymer modification.

2.5.4.2.4 Asphalt layer thickness

The thickness of an asphalt layer is also very important for healing. Theyse et al. (1996) indicated that the shift factor is determined by the thickness of the asphalt layer. A thicker asphalt layer is favourable for healing: the shift factor increases with the increase of asphalt layer thickness.

2.5.4.3 Environments

2.5.4.3.1 Temperature

Self-healing of asphalt concrete is a temperature dependent phenomenon. Si et al reported in their paper that the increase of the

temperature causes a significant increase in the healing rate of asphalt concrete (Si et al., 2002).

Grant concluded that the increase of the temperature increases the healing rate (recovered dissipated creep strain energy per unit time) and shortens the time needed to full healing for both coarse and fine mixtures. He implied that, the healing is immediate above a certain temperature (Grant, 2001).

Kim and Roque (2006) also showed with their work that the temperature sensitivity of the self-healing rate is highly non-linear and healing increases with the increase of temperature.

2.5.4.3.2 Loading history

The loading history is one of the major factors affecting healing in asphalt concrete (Seo and Kim, 2008). Kim and Little conducted different types of cyclic loading test with varying rest periods on notched asphalt concrete beams to identify the healing potential. It was shown that the loading history had an influence on healing of asphalt beams (Kim and Little, 1990, Kim et al., 1991). Lytton et al. (2001) developed a constitutive model to predict the damage growth and healing in asphalt concrete. This model successfully predicts damage growth and healing due to complex loading histories, in both controlled-stress and controlled-strain modes, composed of randomly applied multilevel loading with different loading rates and varying durations of rest period.

2.5.4.3.3 Rest periods

When subjected to rest periods, asphalt concrete has a potential to heal the damage, restore its mechanical properties and improve its durability

by closing the cracks inside. The beneficial effects of rest periods on healing have been shown by many researchers (Bazin and Saunier, 1967, Van Dijk et al., 1972, Francken, 1979, Lytton et al., 2001, Kim and Roque, 2006, Little and Bhasin, 2007). Rest periods help to restore the stiffness and strength, and extend the fatigue life of asphalt concrete. However, healing even occurs without rest periods (Pronk, 2005).

2.5.4.3.4 Water

Water also plays a role in healing. According to Hefer (2004), water has a negative effect on healing of adhesive bond, because water has a greater affinity for the aggregates than bitumen and therefore promotes fracture and prevents healing. However, Zollinger (2005) concluded in his thesis that water increases the bitumen's ability of long term healing (an increase in the acid-base component) and reduces its resistance to fracture (a decrease in the total fracture bond energy). As explained by Cheng (2002), the hydrogen atoms in the water have good interaction or affinity with those of the Lewis acid and base components of surface energy density of the bitumen; hence, water makes the hydrogen bonds stronger and enhances the healing capability. As the bonding of those hydrogen atoms take time, it is associated with long term healing of asphalt (Good and van Oss, 1992).

Based on the previous literature review, the factors influencing the healing rate of asphalt mixtures are summarized in Figure 2-11.

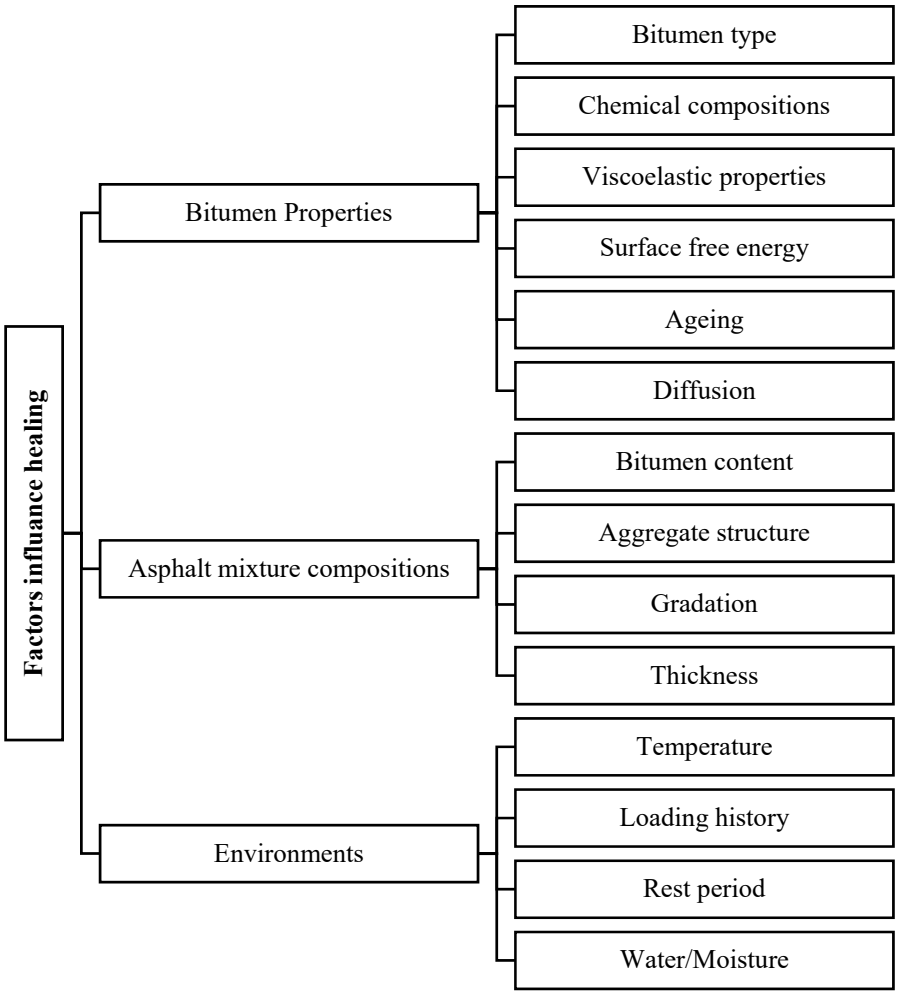

Figure 2-11 Factors influencing healing of asphalt mixtures

As discussed previously, asphalt concrete has a potential to heal itself. However, its healing rate is not sufficient at ambient temperatures, especially at low temperatures. Besides, it is not wise to stop the traffic circulation on the road to allow full healing. Thus, it is a challenging task to increase the self-healing rate of asphalt concrete in road engineering. From the literature, it becomes clear that the temperature dependent nature of healing offers a potential to heal the damage in asphalt pavement through bitumen diffusion and flow at high temperatures.

2.5.5 Novel Self-Healing Techniques for Asphalt Pavements

The self-healing capabilities of asphalt pavements have been known about for over five decades, with the ability to repair fatigue caused by ageing and external factors such as the environment. The process of self-healing can be simplified; when the faces of a microcrack are in contact, capillary action activated by surface energies occurs and diffusion of molecules from one face to another takes place, followed by the randomisation and entanglement of the diffused molecules. Natural self-healing in asphalt pavements takes several days, which in practice is impossible due to continuous flow of traffic. Researchers have targeted technologies that increase the healing rate of asphalt pavements, on which would prevent the pavement from further degradation and crack propagation (Garcia et al., 2010a).

Degradation of asphalt properties over time can result in cracking within the pavement; without rest periods under continuous loading the asphalt is unable to heal naturally, and with the influence of low temperatures and the ageing of the binder, cracks can propagate and lead to the structural failure of the pavement. Ageing is an increase in stiffness of the asphalt binder and a reduction in relaxation stresses, which makes the binder brittle. This is caused by oxidation of the mixture, where the asphaltene content increases and the maltene content decreases leading to the development of microcracks at the interface of aggregate particles (Read and Whiteoak, 2003).

Pavement maintenance historically has seen the use of surface technologies such as sealants to prevent further environmental damage on

existing cracks. Rejuvenators have also been used (extensively in the US (Boyer and Engineer, 2000)) to remediate fatigued pavements using healing agents that change the chemical composition of the bitumen. However, both of these techniques are surface treatments, which may extend the life of the pavement for several years after their use, but they are only effective centimetres from the surface and do not affect deep rooted cracks within the pavement. An experiment conducted by Chiu and Lee (2006) confirms this; they used three variations of rejuvenators on a 12 year old car park to assess their effectiveness; it was found that none of the three rejuvenators penetrated more than two centimetres into the pavement in spite of quite a high void content of almost 10%. Furthermore, rejuvenators reduce the skid resistance of roads and may have adverse effects on the environment. Two innovative techniques to increase the healing rate of asphalt pavements without the negative effects of using rejuvenators or sealants, as described above, were first introduced in Garcia et al. (2010a): a passive self-healing mechanism using embedded encapsulated rejuvenators and an active self-healing mechanism using conductive materials within the binder to induce heating.

There are three different approaches for accelerating the healing properties of asphalt concrete pavements: induction-heating, microwave heating and encapsulated healing agents. On the other hand, there are different methods used for healing different materials for which the viability has not yet been tested in asphalt concrete. Examples of these are bacteria that can seal cracks by producing calcium carbonate, or un-hydrated cementitious materials that could stop crack propagation in case of contact

with water (Garcia et al., 2011c). The un-hydrated cementitious materials could be used by their bonding abilities or produce heat that induces the healing process.

2.5.5.1 Self-healing asphalt pavements by microwave heating

Microwaves are electromagnetic waves of a similar nature to radio, visible light and X-ray waves. What differentiates them from the others is their wavelength (or, in other words, their frequency). Thus, for example, visible light has a wavelength of between $4x10^{-7}$m (violet) and $7x10^{-7}$m (red), while microwaves have wavelengths of between 3mm and 3m, which correspond to frequencies of between 100MHz and 100GHz. A microwave oven typically functions at 2.45 GHz, which corresponds to an approximate wavelength of 120mm. Use of microwaves was a technique introduced to increase temperature within the pavement and initiate the healing process. Microwaves, like induction heating, use electrically conductive materials, fillers and fibres, mixed into the asphalt material. There must be a large enough volume of conductive fillers/fibres to interact with the waves and produce heat around the microcrack (Gallego et al., 2013, Sun et al., 2014).

2.5.5.2 Self-healing asphalt pavements by encapsulated rejuvenators

It is well known that ageing of an asphalt binder can change its chemical composition, thus affecting its rheological and mechanical properties. As a binder is oxidised over time its asphaltene content increases and its maltene content decreases leading to a stiff and brittle binder, causing microcracks to develop at aggregate particle interfaces. In the past rejuvenators have been used to restore the asphaltenes and maltenes

imbalance; applying a healing agent, with a high maltene constituent, to the pavement surface. The application of rejuvenators to a pavement surface has a series of implications: reducing skid resistance of roads, environmental issues and that surface treatments are superficial only affecting a shallow skin depth (surface depth), where only a proportion of the fatigue is.

Until recently there was little research into the effects of microcapsules in an asphalt concrete environment. There have been several research efforts into using microencapsulated rejuvenators in asphalt pavements led by the likes of Garcia, Schlangen, Ven, Su and Qiu. Like the mechanism for polymer microcapsule self-healing, the principle is that with traffic loads high stresses are induced on the shell of the capsule embedded within the asphalt pavement, when the stresses on the capsule reach a certain threshold, the capsule will fracture and release the healing agent (rejuvenator) restoring the chemical imbalance of the asphalt. The specification for microcapsules set by Garcia et al. (2010b) was that, "capsules should encapsulate very viscous hydrocarbons based oils, they should not react with bitumen, they should resist the mixing process with the aggregates and the bitumen at about 180°C, and they should not be so resistant they never break". See Figure 2-12 and Figure 2-13 (Garcia et al., 2010b, Garcia et al., 2010a, Van Tittelboom et al., 2011, Garcia et al., 2011a, Su et al., 2013a, Su et al., 2013b, Su et al., 2015). Successful attempts of using polymeric capsules containing sunflower oil or waste cooking oil were investigated leading to promising low cost application and high performance self-healing (Al-Mansoori et al., 2018, Al-Mansoori et al., 2017, Su et al., 2015).

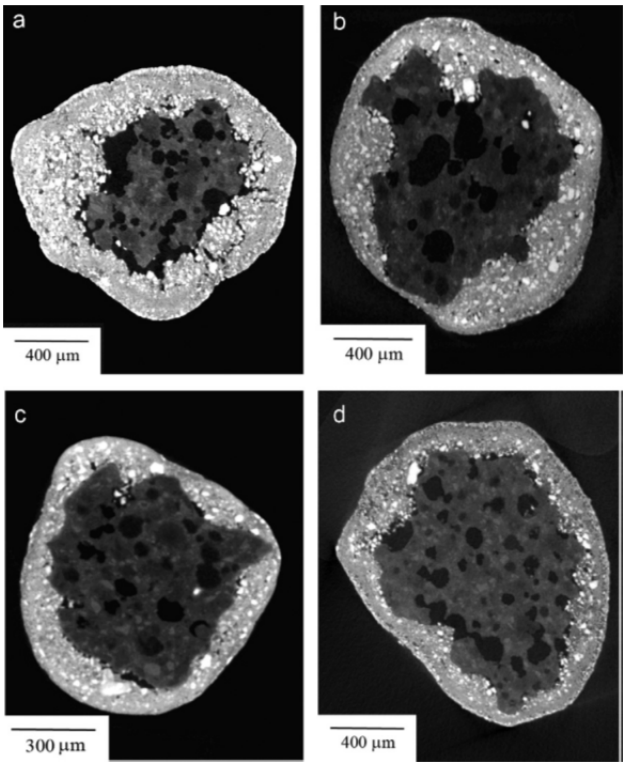

Figure 2-12 CT-scan of capsules with varying shell thickness
(Garcia et al., 2011a)

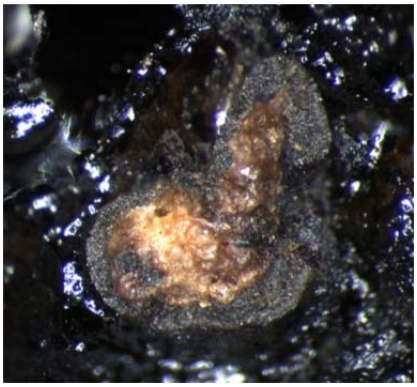

Figure 2-13 Capsule broken after an indirect tensile test
(Garcia et al., 2011a)

2.5.5.3 Self-healing asphalt pavements by induction heating

2.5.5.3.1 Induction heating and its applications

The English physicist Michael Faraday in 1831 found the principles for heating metal by induction. While testing in his research lab with two coils of wire wrapped around an iron rod, he realized that if a battery was connected to the first coil, a sudden passing electric flow could be measured in the second. No current was detected in the second coil if the battery remained connected. At the point when the battery was disconnected, a current was again detected in the second loop, in the opposite direction to the first current. Faraday reached the conclusion that an electric current can be delivered by an alternating magnetic field. Since there was no physical association between the two coils, the current in the second coil was said to be created by a voltage that was "induced". Throughout the following decades these effects were utilized to build the outline of transformers with the end goal of changing the level of voltage from one circuit to another. A by-product of this was the heat created in the metal centre of the transformer. Late in the nineteenth century the opposite was endeavoured in order to use the induction heating action for metal heating and melting (Rudnev et al., 2002, Haimbaugh, 2001).

Induction heating is the process of heating an electrically conductive metal object by electromagnetic induction. The induction part consists of an electromagnetic coil and an electronic oscillator that produces a high-frequency alternating current (AC). The alternating magnetic field generates electric currents inside the conductor called eddy currents. Because of the current flow resistance of the materials, heat is generated by the Joule

heating law. Heat may also produced, in ferromagnetic materials by magnetic hysteresis losses. The major feature of the induction heating is that the heat is produced inside the object itself, instead of by an external heat source. The metal object can be heated very rapidly. In addition, there no need for any external contact. The frequency and power of current used depends on the object size, material type and the penetration depth. Induction heating is used in many industrial processes, such as heat treatment in metallurgy and to melt metals which require very high temperatures. (Rudnev et al., 2002, Lucía et al., 2014).

2.5.5.3.2 Self-healing of asphalt pavements by induction heating

The analysis of natural healing in asphalt pavements has proved that temperature rises in the environment can reduce the viscosity of the asphalt binder and so it flows into cracks, 'healing' them. The viscosity of bitumen, as it behaves as a Newtonian fluid, can be calculated by the Arrhenius equation with the parameters of activation energy and time to reach a known reference viscosity (Garcia et al., 2011c); this provides information for the time of healing to be predicted. However, in many cases the temperature is not high enough to obtain complete recovery. Induction heating was a technique introduced to increase temperature within the pavement and hence the rate of healing. Induction heating uses electrically conductive and magnetically susceptible materials, fillers and fibres, mixed into the asphalt material. There must be a large enough volume of conductive fillers/fibres to form closed-loop circuits around the microcrack (Garcia et al., 2010a). However there is an optimum amount of fibres that should be added to the mixture. This was investigated by Garcia et al. (2011b), who state: "To find

the optimum volume of conductive particles needed, each mixture should be analysed separately by increasing the volume of fibres added until the optimum of fibres (percolation threshold) is found". The research also found that conductive fibres are much more efficient than fillers in terms of increasing conductivity. Eddy currents are induced in the closed-loop circuits, if in the vicinity of a coil, with the same frequency as the magnetic field; when these currents meet the resistance of the material, heat is produced through the loss of energy (Garcia et al., 2010a). When the bitumen is heated, it becomes less viscous and flows into the crack, see Figure 2-14.

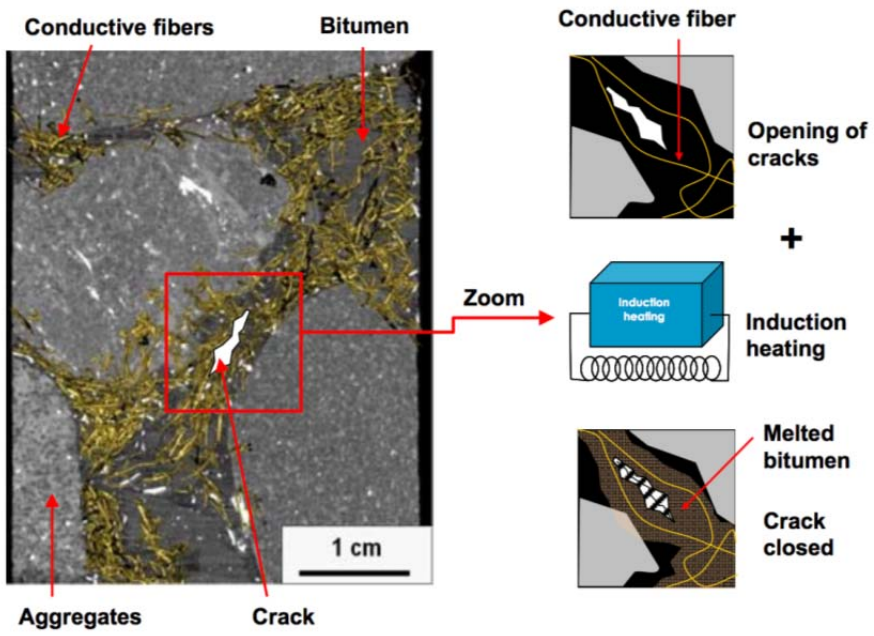

Figure 2-14 The mechanism of induction healing
(Garcia et al., 2010a)

From preliminary studies of volumes of fibres to studies into the energy input at a given magnetic field frequency, the development of induction heating has very promising results. It is well known that iron/iron

alloys respond excellently to induction heating due to their ferromagnetic nature; together with a low cost and good availability, iron particles are the ideal choice in induction heating. Steel wool (an iron alloy) has been used as a conductive material with the benefits of improving mechanical properties of the pavement, through reinforcing it and hence increasing fatigue resistance. It has been proved that the fatigue life of induction-healing pavement has been extended significantly with the application of induction heating (Liu et al., 2012). Induction healing technology was applied to its first road on the Dutch motorway, the A58 in 2010 (Schlangen et al., 2011). Experiments on cores from the road and the results coincided with those from laboratory experiments. The field cores showed good particle loss resistance, high strength, good fatigue resistance and high induction healing capacity (Liu et al., 2013); however these experiments were done in 2013, just three years after the pavement construction, where there should not be any signs of fatigue. Laboratory results of induction healing are promising, but more time needs to be given to the Dutch A58 to analyse the results of the technique of full scale; furthermore an analysis into the sustainable and economic benefits of the new technique should be carried out before further applications to roads.

Also we should address the limitation of self-healing phenomena in warm countries, like Iraq or Spain which will be evaluated in the proceeding chapters, studying the limitation of temperatures, the long-time of heating and lack of rest period.

2.6 Summary

This chapter has covered a background literature review on hot mix asphalt pavements in general and the self-healing techniques in particular as the main research subject. The next chapter will cover the materials and testing methods used throughout the research.

Chapter 3: **Materials and Experimental Programme**

3.1 Introduction

The behaviour of composite materials is largely affected by the properties of their components. This chapter describes the material used, characterisation and mixture design methodology adopted for the mixtures, together with some of their mix design related properties and standards. The main experimental procedures implemented to distinguish the mix and its component properties are reported, as well as the standard specifications used.

3.2 Materials

3.2.1 Aggregates

The aggregate used in this project is a crushed limestone (density 2.67 g/cm^3) with a nominal maximum size of 20mm obtained from Dene quarry in Derby, UK. This was collected, dried and stored in different stockpiles according to their fraction sizes, which are 20mm, 14mm, 10mm, 6mm, dust and fillers. The gradation of each nominal size is in Table 3-1. Figure 3-1 depicts the different sizes used.

Table 3-1 Gradation of Dene limestone aggregate

Sieve Size		Size 20		Size 14		Size 10		Size 6		Dust	
		Pass. (%)	Retain. (%)	Pass. (%)	Retain. (%)	Pass. (%)	Retain. (%)	Pass. (%)	Retain. (%)	Pass. (%)	Retain. (%)
31.5	Mm	100.00	0.00	100.00	0.00	100.00	0.00	100.00	0.00	100.00	0.00
20	Mm	87.65	12.35	100.00	0.00	100.00	0.00	100.00	0.00	100.00	0.00
16	Mm	39.74	47.91	100.00	0.00	100.00	0.00	100.00	0.00	100.00	0.00
14	Mm	12.89	26.85	94.98	5.02	100.00	0.00	100.00	0.00	100.00	0.00
10	Mm	0.80	12.09	25.60	69.38	97.32	2.68	100.00	0.00	100.00	0.00
8	Mm	0.54	0.26	7.61	17.99	70.19	27.13	99.83	0.17	100.00	0.00
6.3	Mm	0.49	0.05	1.95	5.66	27.72	42.47	96.22	3.61	100.00	0.00
4	Mm	0.49	0.00	0.56	1.39	3.07	24.65	24.07	72.15	97.36	2.64
2.8	Mm	0.49	0.00	0.54	0.02	1.79	1.28	4.26	19.81	88.25	9.11
2.0	Mm	0.49	0.00	0.54	0.00	1.62	0.17	2.18	2.08	74.63	13.62
1.0	Mm	0.49	0.00	0.54	0.00	1.58	0.04	1.94	0.24	53.84	20.79
0.500	Mm	0.49	0.00	0.54	0.00	1.57	0.01	1.94	0.00	40.70	13.14
0.250	Mm	0.49	0.00	0.54	0.00	1.56	0.01	1.94	0.00	32.37	8.33
0.125	Mm	0.48	0.01	0.51	0.03	1.51	0.05	1.91	0.03	26.21	6.16
0.063	Mm	0.45	0.03	0.48	0.03	1.42	0.09	1.82	0.09	20.99	5.22
Pan		0.01	0.44	0.00	0.48	0.00	1.42	0.00	1.82	0.00	20.99
Sum			100.0		100.00		100.00		100.00		100.00

Figure 3-1 Different sizes of aggregate fractions

3.2.2 Bitumen

In this study, 6 binders were used from different sources and with different penetration grads as shown in Table 3-2. Generally, the binder used for most of the experimental work was generic bitumen 40/60 pen and density 1.03g/cm^3 to ensure results consistency. The rest of the binders were used in the experimental work of Chapter 7.

Table 3-2 Bitumen types used for the present investigation

Ref.	Country	Supplier	Pen. grade	Needle pen. (10^{-1}mm)
1	UK	-	40/60	50
2	Israel	Pazkar	40/60	49
3	Netherlands	Shell	70/100	70
4	Netherlands	Shell	50/70	46
5	Netherlands	Total	40/60	44
6	Netherlands	Total	70/100	73

3.2.3 Conductive Particles

The present investigation was carried out with the following 4 different kinds of metal particles (Figure 3-2):

1. Steel grit, normally used for abrasive blasting processes, is a metallic granular carbon steel material with uniform gradation between 1 and 2mm (average diameter 1.5mm), Figure 3-2-top left.
2. Steel wool. This product was supplied as very fine fibres with diameter ranging from 16μm to 72μm (average diameter 40μm) and length from 0.15mm to 5mm (average length 1.4mm). It is used in industrial applications, such as the reinforcement of materials exposed to high levels of abrasion (for example, car brake components), Figure 3-2-top right.

3. Steel fibres from old tyres. This recycled product was selected for its low cost and environmental interest. It was obtained as fibres with maximum length 45mm (average length 22mm) and average diameter 0.13mm, Figure 3-2-bottom left.
4. Steel shavings from the metal industry. This by-product of the metal industry, such as car manufacturing and the lathing process, was supplied at zero-cost, being the most economical of the studied kinds of particles. In this case, the helical shape of the fibres did not allow an accurate measurement of lengths and diameters. On average the thickness was 0.24mm and length 25mm, Figure 3-2-bottom right.

Steel grit was used throughout the experimental work as a control conductive particle because the particles are easy to mix, homogenous in shape and size. The other types are used in Chapter 5 to compare the mechanical properties and healing of hot mix asphalt using these different particles.

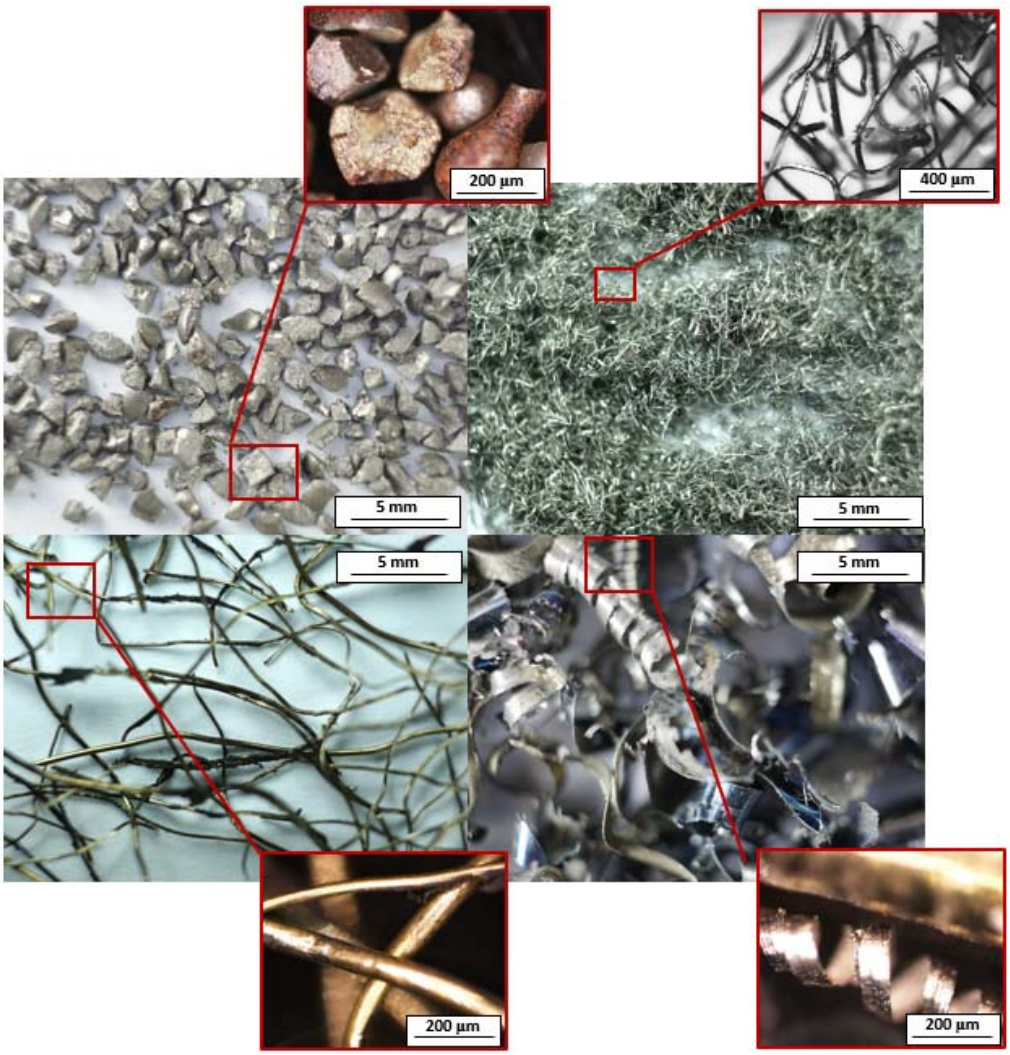

Figure 3-2 Appearance of the metal particles used in this study
steel grit (top left), steel wool (top right), metal fibres from old tires (bottom left) and steel shavings from the metal industry (bottom right)

3.2.4 Hot Mix Asphalt

Generally, three different asphalt mix gradations were used in this investigation. Dense mixes (4.5% air voids content), semi-dense (13%) and porous (21%), see Figure 3-3. The natural aggregate was limestone and using one of the bitumens as specified above (BSI, 2016a, BSI, 2016b), while the conductive component (in order to obtain an asphalt mixture that

can be heated by electromagnetic induction) was introduced in the mix by replacing the same volume of the natural aggregate in this fraction.

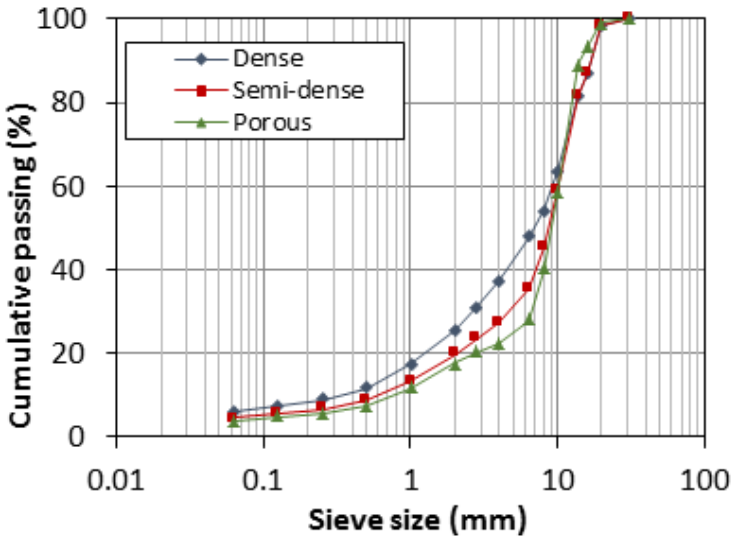

Figure 3-3 Gradation curves of dense, porous and semi-porous asphalt mixture

3.2.5 Artificial Aged and RAP Mixtures

Artificially aged hot asphalt mixes were produced for the investigation of ageing and RAP (Reclaimed Asphalt Pavement) effects on self-healing in Chapter 6. Although many methods, such as thin film oven test (TFOT), rolling thin film oven test (RTFOT), oxidative pressure ageing vessel (PAV) test and the rotating cylinder ageing test (RCAT), have been developed to produce both short-term and long-term ageing of asphalt binder (Yin et al., 2017), there is not a standard method to produce ageing in asphalt mixes. There are two main methods used to produce RAP (aged) specimens: AASHTO R30 and RILEM 206-ATB. The AASHTO method is used for long-term compacted specimens and RILEM for loose mixtures

(Kim et al., 2015). For the present investigation, the recommendations given by the International Union of Laboratories and Experts in Construction Materials, Systems and Structures (RILEM) (Airey, 2003) were followed. The method proposed by this institution consists of producing the material oxidation in an air ventilated oven. UV ageing during service life was neglected as it only affects a very thin section of the surface layer (Wu et al., 2009, Durrieu et al., 2007). The primary advantages of loose mixture aging over compacted specimen aging are: (1) air and heat can easily circulate inside the loose asphalt mixture, which allows for uniform aging throughout the mix; (2) problems associated with the loss of compacted specimen integrity (e.g., slump) during laboratory aging may be reduced; and (3) the rate of oxidation may increase due to a larger area of the binder surface being exposed to oxygen (Kim et al., 2015). The time and temperature they proposed, from the penetration and RB-softening point viewpoint and for long-term ageing, are 9 days at 85ºC. Therefore, in the present investigation, different loose mix samples were subjected to 0 (control), 3, 6, 9, 12 and 15 days in an oven at 85ºC before compaction. In order to study the effect of RAP content in the mix, loose HMA made with fresh bitumen was mixed with 20%, 40%, 60%, 80% and 100% of RAP (loose mix aged for 15 days in oven) and then compacted.

3.3 Test Specimens Preparation

Hot mix asphalt, mastic and bitumen samples were prepared. For the hot mix asphalt: slabs, beams, cylindrical and semi-cylindrical specimens were manufactured. There was a need for a variety of specimen due to the

test requirements and configurations. Mainly, beams and semi-cylindrical samples were used for the healing test, cylindrical samples used for the mechanical and volumetric test and slabs were used for the skid resistance test. Smaller portions from the previous samples were cut to size for the CT-scan test. Bitumen samples were prepared through extraction from the tested samples or fresh to perform rheology and binder properties tests. Finally, mastic samples were mixed for the thermal expansion test.

Control samples without any additives were manufactured alongside those with metallic inclusion and with different bitumen types as required for each of the research stages.

3.3.1 Slabs and Beams

Aggregates were oven heated for 2 hours before mixing. The required bitumen and conductive particles were added in a drum mixer at 160^{o}C, then mixed for 3mins. Asphalt mixture was then compacted in a slab mould by means of roller compactor until the mixture reached the target air voids content, according to the British Standard BS EN 12697-33:2003 (BSI, 2003c). The dimensions of the slabs were 310x310x50mm^3. After a 24hr cooling time, eight 150x70x50mm^3 prismatic samples (beams) were saw cut from each slab. Finally, a notch was cut at the midpoint in the direction of the loading from the central axis of the beams, with a width of about 2mm and a depth of about 10mm, see Figure 3-4.

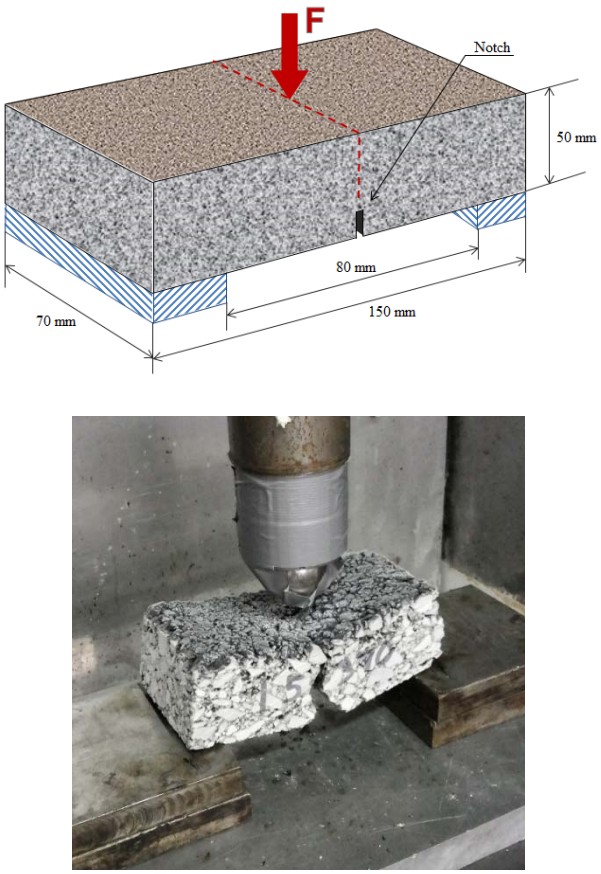

Figure 3-4 Prismatic test specimen and 3-point bending test

3.3.2 Cylindrical and Semi-Cylindrical

A dense aggregates gradation, based on British Standard BS EN 13043:2002 (BSI, 2002) was used for all the cylindrical specimens used in the research. Materials were heated for 2hrs before mixing and mixed for 3min in a drum mixer at 160°C. Cylinders of 101.6mm diameter and approximately 50mm height were compacted by applying 75 Marshall Hammer blows to each face of the samples. Semi-cylindrical test specimens were obtained by cutting the cylindrical test samples in half and making a notch at their base with 50mm length, 2mm width and 5mm depth, see Figure 3-5.

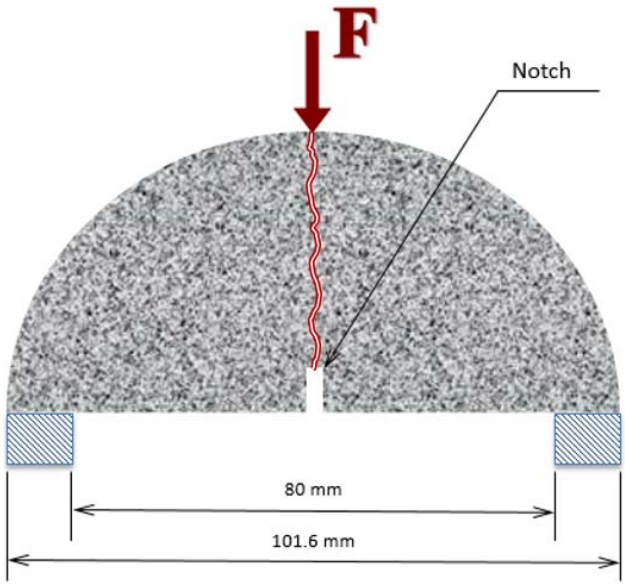

Figure 3-5 Semi-cylindrical test specimen and 3-point bending test

3.4 Testing Procedures

3.4.1 Self-Healing Test

First, the self-healing samples were tested under the three-point bending configuration at -20±2°C to produce brittle cracks, without permanent deformation (García et al., 2015). In order to obtain the failure strength of each sample, the tests were carried out under strain control conditions, with an increasing load ramp at a deformation rate of 50mm/min. The ultimate force applied at the moment of break was registered, F_i. During each test, a complete vertical crack from the notch to the load application point was produced. Then both separated halves were stored at 20±2ºC for at least 4 hours.

Later, the two halves of the samples were gently put together into a non-conductive silicone mould, and healed by means of induction or infrared heating, depending on the research stage. Furthermore, the surface

temperature of the test samples was constantly monitored. Once the healing and another 4hrs cooling were finished, the samples were stored at -20°C and tested again under three-point bending. The healing ratio (S(τ)) of asphalt beams was defined as the relationship between the ultimate force measured in the test specimens after the breaking and healing processes Fb(τ), and the ultimate force of the test specimens during the first three point bending test, Fi, where τ is a parameter that gives an idea of the amount of energy applied to the asphalt concrete test sample during the healing process (defined in Section 3.5).

$$S(\tau) = \frac{F_b(\tau)}{F_i} \qquad 3.1$$

Induction heating experiments were performed with a 6kW induction heating generator. The electromagnetic field was obtained by circulating an alternating current through a 15x15cm^2 pancake coil composed of three windings. The air temperature during the tests was 20°C. The distance from the upper side of the test samples to the coil was 2cm, the working frequency was 348kHz. Moreover, the current was set to 80A, and the power to 2800W during the experiments, see Figure 3-6 (left). The test specimens were exposed to induction heating for times that ranged between 15s and 240s.

Moreover, in order to simulate heating of pavements by solar radiation in Chapter 4, the test samples were exposed to the infrared light generated by a set of 250W infrared lamps at 30cm, 70cm, and 110cm from the surface of the test specimens, for times that ranged between 5min's and 4days. During the test, the beams were embedded in white sand (Catsan® cat

litter) with the exception of their upper surface, to minimise the radiation intake from their sides, see Figure 3-6 (right).

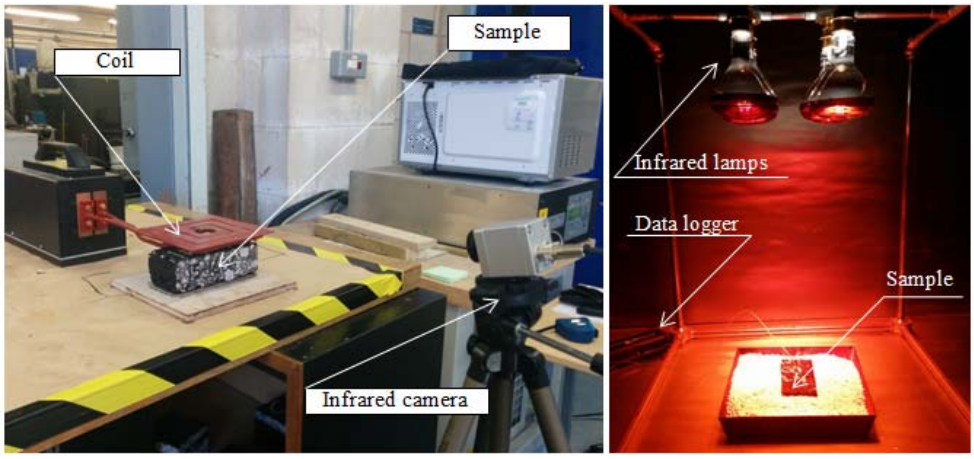

Figure 3-6 Healing procedures
by induction heating (left) and infrared radiation (right).

3.4.2 Test Temperature Registering

Using a 320x240pixels, full colour infrared camera for the test samples exposed to induction heating the surface temperature was recorded in real time. Four points representing the upper, lower, middle and maximum temperatures were chosen. For the infrared healing, a J-type thermocouple was placed in the upper and lower geometrical centre of the prismatic test specimens. The thermocouples were connected to a data logger (Omega OMB-DAQ-54) that allowed continuous measurements at 1min intervals. Only the surface temperatures of the heated samples were measured. There was a difficulty of record the specimen's internal temperature without damaging the samples. There is no direct or indirect method to achieve that.

3.4.3 X-Ray Computed Tomography (CT scan) and Image Processing

Blocks of dense asphalt concrete were cut to a size suitable to be examined in a XRadia Versa XRM-500 scanner operated at 80kV and 120μA. The blocks were mounted on a rotational table at a distance of 11.8mm from the X-ray source and the distance between the X-ray source and the X-ray detector was 1155mm. It was ensured that the focal spot size of the X-ray tube was about 2μm and therefore, a spatial resolution of 4μm was achieved.

Reconstructions of the CT-scan images were prepared by segmenting the materials found in a specific volume, based on simple thresholding. With this simple method, aggregates, steel particles, bitumen and air voids could readily be separated, showing the particles' real configuration and the cracks evolved during the healing process. The software tools used for this reconstruction were ImageJ and Meshlab.

3.4.4 Volumetric Properties

A volumetric analysis was carried out in order to determine properties, such as (1) bulk specific gravity (G_{mb}), (2) air voids content (V_a), (3) voids in mineral aggregate (VMA), and (4) voids filled with asphalt (VFA), calculated as follows (BSI, 2012a, BSI, 2003a):

$$G_{mb} = \frac{A}{(B - C)} \qquad 3.2$$

$$V_a = 100 * \frac{(G_{mm} - G_{mb})}{G_{mm}} \quad 3.3$$

$$VMA = 100 - \frac{(G_{mb} * P_a)}{G_{sa}} - \frac{(G_{mb} * P_s)}{G_{ss}} \quad 3.4$$

$$VFA = 100 * \frac{(VMA - V_a)}{VMA} \quad 3.5$$

where A is the weight of specimen in air (g); B is the weight of surface-dry specimen in air (g); C is the weight of specimen in water (g); G_{sa} is the bulk specific gravity of aggregate; P_a is the aggregate percent by total weight of asphalt mixture; G_{ss} is the bulk specific gravity of steel; P_s is the steel percent by total weight of asphalt mixture and G_{mm} is the maximum specific gravity of asphalt mixture, calculated as (BSI, 2009b):

$$G_{mm} = \frac{A}{\big(A - (C - B)\big)} \quad 3.6$$

where in this case, A is the weight of oven dry sample in air (g), B the weight of container in water (g) and C the weight of container and sample in water (g).

3.4.5 Mechanical Properties

3.4.5.1 Indirect tensile strength

The indirect tensile strength was obtained according to the British Standard BS EN 12697-23 (BSI, 2003b) at a temperature of 25±2°C. Thus, a group of three cylindrical specimens was subjected to an increasing diametrical compression at a deformation rate of 50±2 mm/min until

fracture occurred. The ITS was obtained for each specimen with the following equation:

$$ITS = \frac{2 * P}{D * H} \quad 3.7$$

where P is the peak vertical load (kN), D is the diameter (mm) and H is the height of the cylindrical specimens (mm). The final value of ITS was considered as the average value of the three tested specimens.

3.4.5.2 Resistance to water damage

Once the indirect tensile strength tests has been carried out under dry conditions, as described in the previous point, a homologous 3-samples group was tested according to the Standard BS 12697-12 (Method A) (BSI, 2008b). In this case, the set of samples were placed on a perforated shelf in a vacuum container filled with distilled water at 20±5ºC to a level of 20mm above the upper surface of the test specimens. Then a vacuum was applied to obtain an absolute pressure of 6.7±0.3kPa within 10±1min and maintained for 30±5min. Then, the pressure was released to atmospheric pressure and the samples were submerged in water for another 30±5min. At this point, samples whose volume was increased by more than 2% were rejected and substituted for new conditioned samples. The samples were placed in a water bath at 40±1°C for a period of 68h to 72h.

The conditioned specimens were brought to the testing temperature of 25±2°C and subjected to an increasing diametrical compression at a deformation rate of 50±2mm/min until fracture occurred and the average

value of indirect tensile strength was obtained. The retained indirect tensile strength ratio (ITSR) was calculated as:

$$ITSR = 100 * \frac{ITS_{wet}}{ITS_{dry}} \quad 3.8$$

where ITS_{wet} is the indirect tensile strength of the conditioned group (MPa) and ITS_{dry} the indirect tensile strength of the group that was not submerged.

3.4.5.3 Stiffness modulus

The stiffness modulus was obtained according to the Standard EN 12697-26 (Annex C) (BSI, 2012b), involving the application of 5 semi-sinusoid impulses with a total duration of 3s that consisted of a rise time of 124ms and a viscoelastic deformation recovery, conducted in a regime of deformation control (5μm). For each load pulse, the modulus was calculated as:

$$S_m = \frac{F(v + 0.27)}{(z * h)} \quad 3.9$$

where S_m is the stiffness modulus (MPa), F represents the peak value of the applied vertical load (N), z is the amplitude of the horizontal deformation obtained during the load cycle (mm), h is the mean height of the cylindrical specimen (mm) and ν is Poisson's ratio, assumed as 0.35. Groups of 5 similar samples were tested, calculating the stiffness modulus as the average of all of them.

3.4.5.4 Bitumen mixture particle loss resistance (Cantabro test)

Particle loss resistance tests were chosen to measure if the metallic fibres and particles chosen affected in any way the ravelling capacity of the asphalt mixture. The tests were carried out according to British Standard BS EN 12697-17:2004 (BSI, 2004). For this purpose, 5 cylindrical test samples for each material studied were stored at a temperature of 20°C for 24h before testing. Afterwards, each sample was subjected to 300 revolutions at 30rpm in a Los Angeles drum without steel balls. The mass of the test specimens before and after testing was noted and the particle loss resistance was calculated using Eq. 3.10.

$$Particle\ loss = \frac{(w_1 - w_2)}{w_1} \qquad 3.10$$

where w_1 is the initial sample weight, measured in kg and w_2 is the final sample weight, measured in kg.

3.4.5.5 Skid resistance

The pendulum skid resistance test was carried out according to British Standard BS EN 13036-4:2011 (BSI, 2011). The method consists of a small rubber slider at the end of a free-swinging pendulum. The tester measures the frictional resistance between the slider and the contact area of a wetted pavement surface. The test was performed at a temperature of 20±2°C using a wide slider and the sliding length was 126±1mm. The test was performed five times, re-wetting the surface and the slider before each attempt, and recording the results each time. The procedure was repeated twice in different slabs to confirm the results. Then the average values were

calculated by using Eq. 3.11, which represents the Pendulum Test Value (PTV):

$$PTV = \frac{\sum(v_1 + v_2 + v_3 + v_4 + v_5)}{5} \quad 3.11$$

where v_1 to v_5 are individual values for each swing.

3.4.6 Environmental Performance- Leaching Behaviour

The only environmental hazard that might arise from the addition of metal particles to asphalt mixes, is the dissolution of certain metals that can be carried by the rain water draining through the pavement. In order to assess that, two methods were used: (a) rolling bottle test and (b) up-flow percolation test (Figure 3-7).

The first produces one standard value that could be compared to those limits established by different waste leaching specifications. The latter produces a curve of concentration over percolation time, which allows the determination of: (1) the time needed to reach a steady-state concentration; (2) the time needed to reach the standardised value given by the roller bottle test; and (3) the time needed to exceed the limits established by the specifications. The tests were carried out as follows:

3.4.6.1 Rolling bottle test

This test was carried out according to Standard BS EN 12457-4. Hence, 90±5g of loose and dry asphalt mix were introduced in 1L glass bottles with 900±10ml of rain water collected in the Area of Nottinghamshire (liquid/solid ratio of 10). The bottles were then closed and

rolled for 24±0.5h at 10rpm. After the test, eluates were filtered on a 0.45mm porosity Millipore membrane and then analysed.

The analysis was done using an ICP-OES (PerkinElmer Optima 3300 DV) with autosampler (AS90 Plus) and controlled with Perkin Elmer Winlab software. The ICP operational conditions were: RF power=1300W, Plasma gas flow=15L.min^{-1}, Auxiliary gas flow=0.5L.min^{-1}, Nebulizer gas flow=0.8L.min^{-1}, Sample flow rate=1mL.min^{-1}, Wash time=300s, Read delay=90s, Replicate readings=3.

Calibration standards were prepared from single element standard solutions (Romil PrimAg) diluted with 10% HNO_3 (69.5% AnalaR). All solutions were prepared using Milli-Q ultrapure water (18.2MΩ.cm^{-1}). All the plastic and glassware were cleaned by soaking in dilute HNO_3 and then rinsed with ultrapure water prior to use.

3.4.6.2 Up-flow percolation test

This test was performed based on Standard BS EN 14405-2017. In this case, 1kg of loose asphalt was introduced into 5cm diameter by 35cm high columns. A peristaltic water pump was used to supply over 10days a continuous and constant rain water flow of 15mL/min to the bottom inlet of the column. Once the water reached the top outlet, the rain water was collected into a 1.5L reservoir before being recirculated by the pump. Eluates were collected at different times over the 10days and filtered on a 0.45mm porosity Millipore membrane before being analysed as described before.

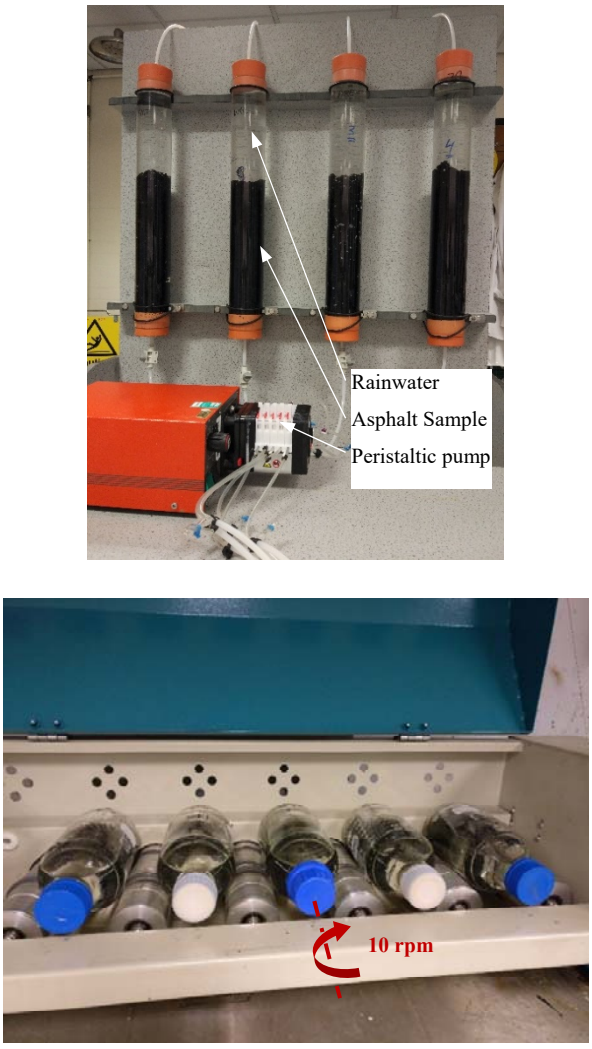

Figure 3-7 Leaching test
Up-flow percolation test (left) and rolling bottle test (right)

3.4.7 Bitumen Rheology Tests

The rheology of bitumen was examined using a dynamic shear rheometer (Bohlin Gemini HR^{nano}) according to BS EN 14770:2012 (BSI, 2012c). The tests were carried out over a range of oscillatory frequencies (from 0.1Hz to 10Hz) and temperatures (5°C to 80°C every 5°C). 8mm-diameter parallel plates were used for temperatures below 40°C with 2mm gap and 25mm-diameter plates with 1mm gap for higher temperatures. To

ensure the linear viscoelastic behaviour of the samples, the strain amplitude was fixed at 1%.

The results obtained from this test were the complex viscosity (η*) and complex modulus (G*) for each frequency and temperature. Using the principle of time-temperature superposition, the so-called master curves could be constructed by fixing a reference temperature (40°C) and shifting the data with respect to time until the curves merge into a single smooth function. The obtained master curves could be mathematically modelled by a sigmoidal function described as:

$$\log|E^*| = \delta + \frac{\alpha}{1 + e^{\beta} + \gamma(\log t_r)} \qquad 3.12$$

where t_r is the reduced time of loading at the reference temperature; δ is the minimum value of E*; the sum δ+α is the maximum value of E* and the parameters β and γ describe the shape of the sigmoidal function. Data shifting is made by using a shift factor, whose form for a certain temperature of interest (T) is:

$$a(T) = \frac{t}{t_r} \qquad 3.13$$

where t is the time of loading at the desired temperature and t_r is the reduced time of loading at the reference temperature.

3.4.8 Generic Composition of Bitumen (SARA-Analysis)

In collaboration with the Belgian Road Research Centre (BRRC), the Thin-Layer Chromatography system used was an Iatroscan® TLC-FID

analyser MK-6s from SES GmbH Analytical Systems (Bechenheim, Germany). Quartz rods (Chromarod, 10 in a holder), coated with a thin layer of silica were used for fraction separation. Flame ionization detection (FID signals) allowed the quantitative detection of peaks (SARA-fractions) in the obtained chromatograms (details in IATROSCAN MK-6/6s Catalog) (SES_GmbH-Analytical_Systems, 2017). Figure 3-7 illustrate the test set-up as used at BRRC.

The test protocol used is largely based on the procedure described in IP469 entitled 'Determination of saturated, aromatic and polar compounds in petroleum products by thin layer chromatography and flame ionization detection'. The latter protocol was already published in 2001 by the former Institute of Petroleum (IP) in the UK (Energy_Institute, 2006). However, in order to optimize the separation into the four SARA-fractions, the analysis is carried out at BRRC in two steps:

Step 1: elution of the maltene fraction while using a polar solvent (95:5 dichloromethylene/ methanol) allowing the determination of the non-eluted asphaltene fraction (bath 1).

Step 2: elution of the saturate fraction while using heptane as solvent (bath 2), followed by the elution of the aromatics by using 80:20 toluene/heptane (bath 3). Subsequently, by calculation the content of resins is determined (difference of the non-eluted fraction after applying bath 2 and the asphaltene fraction as obtained in step 1.

Figure 3-8 TLC-FID Iatroscan® equipment used at BRRC laboratories.

3.4.9 Asphalt Mix Thermal Expansion

A Thermomechanical Analyser instrument (Q400 TMA), with a temperature range of 10-50°C, heating rate of 10°C/min and measurement resolution of 0.02µm (Figure 3-8), was used to test the thermal expansion for the bitumens (TA-Instruments, 2006). The samples were prepared by mixing each binder with the same amount of 6mm limestone gradation and dust to produce a mastic consistency mix. The samples were then cut, moulded and polished to reach the instrument required sample dimension (25mm height and 10mm diameter). Three samples were tested for each bitumen and the average was taken to determine the coefficient of expansion and the melting point.

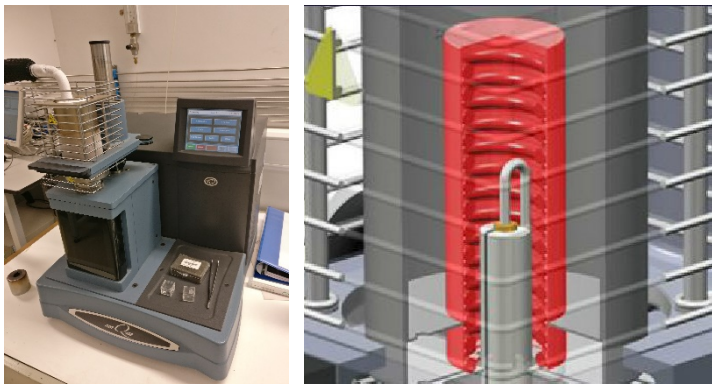

Figure 3-9 Thermomechanical Analyzer (Q400 TMA) setup and illustration of sample chamber.

3.5 Theoretical Framework

3.5.1 Energy Needed for Healing

As has been reported in previous research, asphalt self-healing does not happen only during the heating periods, but also during cooling (Garcia, 2012) (see Figure 3-10). The analytical relationship between time and temperature can be obtained for heating and cooling by integrating Newton's law of heat transfer:

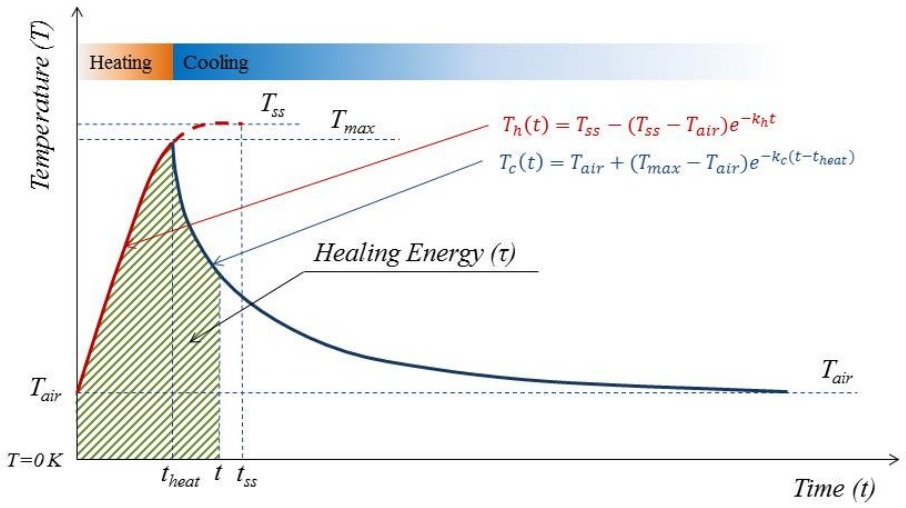

Figure 3-10 Temperature changes during the heating and cooling processes

$$mc\frac{dT}{dt} = -k\,A(T - T_c) \qquad 3.14$$

where k is a heat transfer coefficient (s^{-1}), which depends of the area of the beams exposed to the environment, mass of the test samples and specific heat capacity. As the heating and cooling rates may differ during the heating and cooling periods, the heat transfer coefficient has been noted as k_h for the heating period and k_c for the cooling period. m and c are the mass and mass specific heat capacity respectively. Moreover, T (K) is the temperature of asphalt mixture; and T_c (K) is a fixed temperature that can be the ambient temperature (T_{air}) during cooling, or the steady state temperature reached by the asphalt mixture during heating (T_{ss}). Thus, after integration of Eq. (3.14), expressions (3.15) and (3.16) were obtained for heating and cooling:

$$T_h(t) = T_{ss} - (T_{ss} - T_{air})\,e^{-k_h t} \qquad 3.15$$

$$T_c(t) = T_{air} + (T_{max} - T_{air})\,e^{-k_c(t - t_{heat})} \qquad 3.16$$

Parameters k_h and kc can be obtained by fitting the experimental temperature-time curves to these equations and t_{heat} is the time for heating the test sample.

On the other hand, after a certain time healing, t (s), the total healing energy, τ(t), could be calculated as the area under the temperature-time curve (Figure 3-10), being its units K.s (Garcia, 2012). In order to obtain an analytical expression for τ(t), the heating and cooling curves were integrated again obtaining Equation (3.17) and (3.18) for heating (τ_h) and cooling (τ_c), respectively:

$$\tau_h(t) = T_{ss}.t + \frac{T_{ss} - T_{air}}{k_h}(e^{-k_h t} - 1) \quad ; t < t_{heat} \tag{3.17}$$

$$\tau_c(t) = T_{air}.(t - t_{heat}) + \frac{T_{max} - T_{air}}{k_c}\left(1 - e^{-k_c(t - t_{heat})}\right) \quad ; \quad t > t_{heat} \tag{3.18}$$

Finally, the total healing energy needed for healing has been calculated as follows:

$$\tau(t) = \tau_h(t_{heat}) + \tau_c(4h) \tag{3.19}$$

In this study, 4 hours was the cooling time: i.e. the time after heating that the samples were left at room temperature. After this time, they were stored at -20°C.

3.5.2 Asphalt Self-Healing Theory

In Garcia et al. (2013) it is explained that healing of cracks in asphalt mixture starts when both faces of a crack are in contact. Then, bitumen can drain from the mixture into the cracks, healing them. In Garcia et al. (2013) the capillary phenomena were studied through a modification of the Lucas–Washburn equation (Arpaci et al., 1999, Hamraoui and Nylander, 2002, Washburn, 1921, Duarte et al., 1996). This research will follow this theory. For this reason, the main forces that affect the cracks during self-healing are due to the equilibrium of surface tension, gravity and dissipation force caused by the movement of bitumen against the walls of the crack. According to Garcia et al. (2013), after solving the balance of forces and

integrating, the healing level $S(\tau)$ can be predicted using the following equation:

$$S(\tau)=\frac{C_1}{F_0}.e^{-D\tau}\left(-1+e^{\frac{D\tau}{2}}\right)^2 \quad 3.20$$

where $S(\tau)$ is the healing ratio or percentage of recovered strength after the healing treatment (%), F_0 is the initial 3-point bending strength of the test samples (kN), τ is the energy applied during the healing (K.s) and D and C_1 are parameters that can be calculated as:

$$D=\frac{\rho g r}{\beta} \quad 3.21$$

$$C_1=8.\frac{\sigma_u.C}{L.H} \quad 3.22$$

where ρ is the density (kg/m^3), g is gravity (m^2/s), r is the width of the crack (m), β is a dimensionless parameter that takes into account possible sources of energy losses, σ_u is the maximum force resisted by the beam (N), L is the span of the beam (m), H is its height and C is a material constant with units (m^2). Furthermore, the D value is an indication of the healing rate; when its value increases, the healing happens faster.

3.6 Summary

This chapter has discussed the different materials and the main experimental procedures used throughout the research. In the next chapter a comparison between induction and infrared heating with different air voids asphalt mixes is studied.

Chapter 4: **Effect of Air Voids Content on Asphalt Self-Healing via Induction and Infrared Heating**

4.1 Introduction

Asphalt roads are composed of aggregates and bitumen. After some years in use, they can develop micro-cracks, which if they are not treated can grow further and affect the safety and comfort of traffic. As bitumen is a very viscous fluid at the ambient temperature (Read and Whiteoak, 2003), it tends to flow to the lower parts of the asphalt layers under the effect of gravity (Garcia, 2012). Furthermore, if there are cracks open, these will be filled by bitumen and repaired. For these reasons, cracks in asphalt roads can self-heal. Bitumen drains from the asphalt mixture into the cracks until the pressure and surface tension of bitumen filling the cracks equals that in the asphalt mixture (García et al., 2015). However, cracks can self-heal only if asphalt roads are not exposed to traffic loads that may open them even more (Menozzi et al., 2015). Although asphalt self-healing can be recorded at the ambient temperature, bitumen needs several weeks to completely fill a crack (Qiu, 2008).

Asphalt self-healing can be artificially accelerated by using induction heating (Garcia et al., 2013). This method involves the addition of electrically conductive particles, such as steel wool fibres, to the mixture and heating them by means of an alternating magnetic field produced by an electric coil (Garcia et al., 2012). The heat in the fibres transmits to bitumen, reducing its viscosity, differently than with solar heating, where the heat is

transmitted by radiation from the surface to the bottom of the road. The temperature reached by the fibres depends on their diameter, material composition and length (Garcia et al., 2012), and cracks can be fully closed in seconds or minutes if the global temperature of asphalt mixture is increased above a threshold between 30°C and 50°C, depending on the type of bitumen used (García et al., 2015).

On the other hand, there are certain zones in the world where roads are exposed to very intense solar radiation, and can reach temperatures of 70°C (Ongel and Harvey, 2004), which are much higher than needed for asphalt induction-healing (Liu et al., 2011). In spite of this, cracks normally continue growing until roads degrade so much that they need to be replaced. This research aims at finding why roads exposed at very high environmental temperatures do not self-heal completely even if long resting times are provided, while cracked roads treated at the same temperature using induction heating may heal almost completely in seconds.

With this purpose, (1) asphalt beams with different gradations and containing steel grit were fabricated, (2) broken under three point bending, (3) exposed to induction or infrared heating, for different times and (4) broken again under three point bending. Healing recovery has been represented versus the total energy needed for heating the beams and the causes for the accelerated healing recovery have been analysed through the model proposed by Garcia in (Garcia, 2012) and Computed Tomography Scans of the test samples before and after healing.

4.2 Procedure

4.2.1 Samples

The investigation in this chapter was carried out on asphalt mixture test samples with 3 different gradations: dense (4.5% air voids content), semi-dense (13%) and porous (21%). The natural aggregate was limestone, while the conductive component was metal grit of 1 mm diameter. Metal grit was introduced in the mix by replacing the same volume of the natural aggregate in this fraction. The volumetric content of metal grit in the mix was fixed at 4%, which is 11.2% in weight. Finally, the selected binder was a 40/60 pen and its content was 4.7%. Prismatic beams of asphalt mixture were used as described in Chapter 3: Section 3.2 and 3.3.

4.2.2 Self-Healing Test

Following the self-healing procedure shown in Section 3.4.1, the prisms were healed by means of induction or infrared heating. Furthermore, the surface temperature of the test samples was constantly monitored by using a full colour infrared camera for the test samples exposed to induction heating and by using a J-type thermocouple, Section 3.4.2. Although a significant gradient of temperature is expected from the surface to lower layers, only the temperature of the upper side was introduced in the model. This will allow correlations with experiments in real roads in further investigation, it not being possible to measure the temperature of lower layers without affecting the material. In addition, the methodology detailed in Theoretical Framework, Section 3.5, was designed to establish a fair

comparison between the results of both heating methods. As long as both of them are treated in the same way (in this case just considering the temperature on the upper side) the comparison will be reliable.

4.2.3 Bitumen Rheology

In order to assess whether bitumen ageing was induced during the healing process, 5 samples of bitumen were recovered by rotary evaporator from beams of dense asphalt mixture exposed to infrared radiation during 0min, 200min, 1day, 2days and 4days. The rheology of bitumen was examined following Section 3.4.7.

4.2.4 X-Ray Computed Tomography (CT scan)

A beam made of dense asphalt concrete was examined by X-ray computed tomography, Section 3.4.3, after being cracked and subjected to infrared radiation for periods of 0min, 200min and 4days. Reconstructions of the air voids were prepared. Aggregates, steel particles, bitumen and air voids could be readily separated, showing how the cracks evolved during the healing process.

4.3 Results and Discussion

4.3.1 Heat Transfer and Maximum Temperature Reached by the Test Samples

The Newtonian heat transfer coefficients during heating (k_h) and cooling (k_c) were obtained by fitting Equations 3.15 and 3.16 to the temperature-time curves obtained experimentally for each test sample. The

average values for all the tests conducted can be seen in Table 4-1. The differences in the heat transfer coefficient for heating and cooling came from two factors: the heating speed, where induction heating heats the sample in seconds in contrast to infrared in hours; the heat target, where induction heating targets the bitumen covering the heating fibres. Therefore, during cooling the heat dissipates to the surrounding aggregate and then to the room temperature, whereas in infrared radiation, the specimens (aggregate and the bitumen) heat together. Furthermore, it should be remembered that all recorded temperatures were at the surface of the specimen and not inside.

Table 4-1 Heat transfer coefficient values obtained for asphalt mixtures with induction and infrared heating

Air voids content (%)	Induction heating		Infrared heating					
			30 cm		70 cm		110 cm	
	Heating	Cooling	Heating	Cooling	Heating	Cooling	Heating	Cooling
4.5	3.1E-03	1.2E-03	1.5E-04	2.6E-04	1.5E-04	3.1E-04	1.4E-04	2.7E-04
13.0	3.4E-03	1.2E-03	1.4E-04	2.8E-04	1.6E-04	2.7E-04	1.5E-04	2.9E-04
21.0	3.3E-03	1.1E-03	1.3E-04	2.8E-04	1.4E-04	2.9E-04	1.2E-04	3.0E-04

First and regarding the infrared heating results, it can be observed that the distance between sample and lamps did not significantly affect the heating transfer coefficients, as they are an intrinsic property of the material, independent of the temperature of the test. However, as the air voids content became higher, the k_h values reduced while the k_c values tended to increase. The reason for this is the lower thermal conductivity and specific heat capacity of porous asphalt mixture versus denser materials (Hassn et al., 2016).

In addition, it is noticeable that the k_c values were significantly higher than the k_h values, which made the cooling process faster than the

heating. The reason for this behaviour is that during infrared heating, the energy was induced into the test samples through their upper side and conducted to the rest of the test samples while during cooling, the energy was dissipated to the environment through all the faces of the test samples.

Regarding the induction method, heating and cooling occurred faster than with infrared radiation. In the case of induction heating, only the metal particles were directly heated and the heat was transferred first to the bitumen and then to the aggregates. As bitumen coated the metallic particles, it reached higher temperature than the aggregates. As a result of the short heating times, the temperature of aggregates remained lower than the temperature of the binder and cooling of asphalt mixture was faster than with the infrared heating method.

4.3.2 Energy Approach and the Concept of Critical Energy

Figure 4-1 (top) shows the healing level evolution with time obtained for (1) dense, (2) semi-dense and (3) porous asphalt samples exposed to (a) induction and (b) infrared heating. It can be observed that in all the cases studied, the test samples exposed to induction heating healed in 1–2min, while test samples exposed to infrared needed several hours for healing. The difficulty of using this graphic to study asphalt self-healing is that each material analysed had different thermal conductivities and energy inputs.

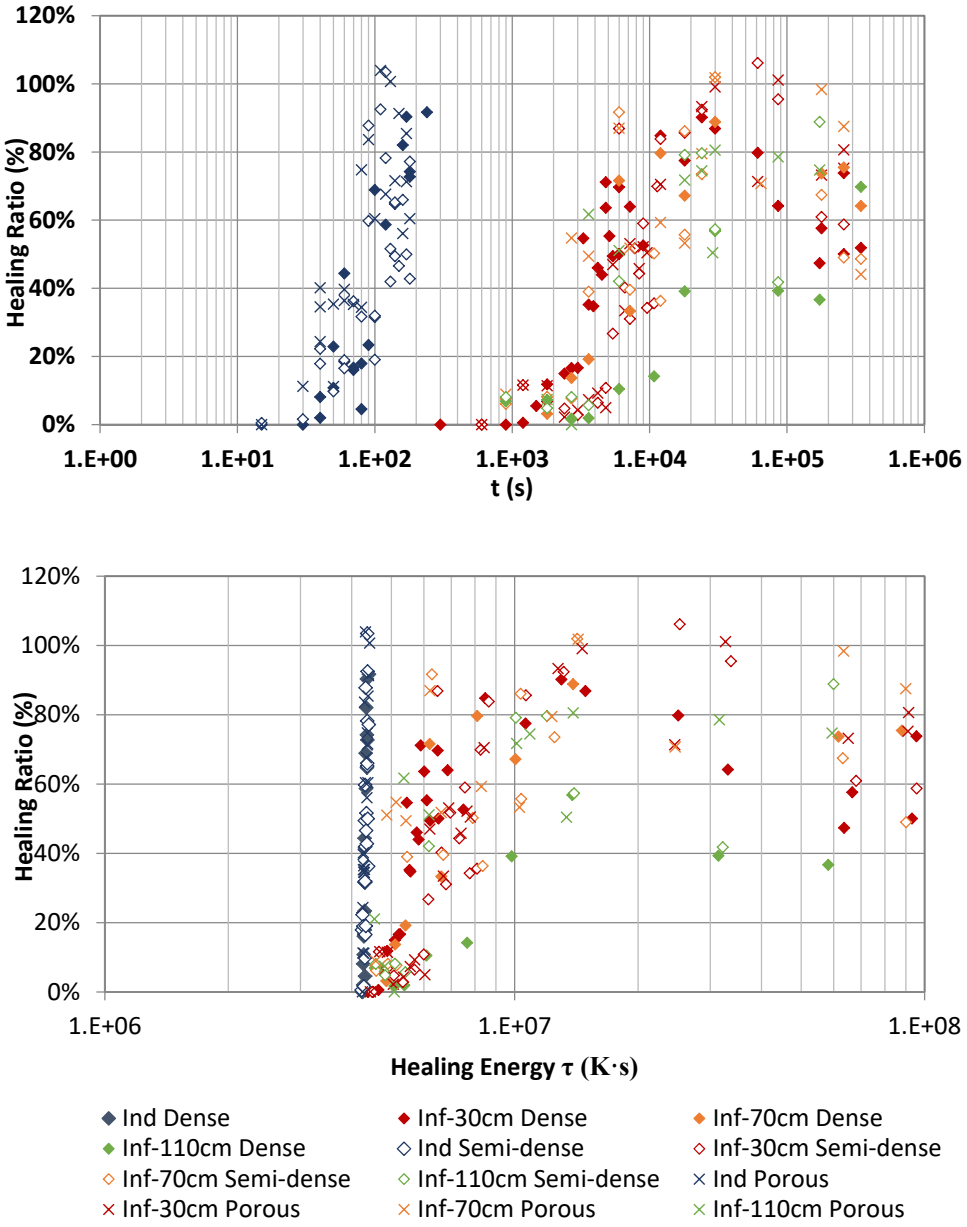

Figure 4-1 Induction and infrared Data
At different distances and with different gradations. Data represented as a function of time (top) and healing energy (bottom)

To compare asphalt self-healing of different test samples heated at different temperatures, the time considered during the healing period was transformed into an indicator which will called healing energy. This approach highlighted the existence of a critical energy (τ_c) that triggered the

beginning of the healing process (Figure 4-1, bottom). Until this energy level was reached, healing did not happen.

Moreover, the critical energy for self-healing has been obtained by fitting the healing level-energy data in Figure 4-1 (bottom) with Equation 3.20, and obtaining the energy at which the healing level reaches 1% (see Figure 4-2). It was found that the average critical energy necessary for induction heating was lower (approximately $42.5*10^5$K.s) than for infrared radiation (approximately $46.0*10^5$K.s), which made induction more efficient than infrared for asphalt self-healing. This greater efficiency could be due to the fact that the binder in the whole test sample was directly heated by induction heating, while the heat provided by infrared radiation had to be conducted from top to bottom to heat the binder alongside the aggregate. Furthermore, Figure 4-2 shows that the critical energy was independent of the infrared heating power and aggregate gradation.

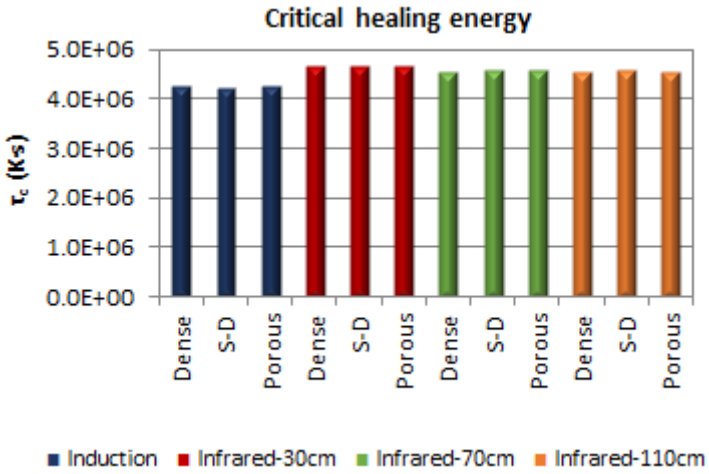

Figure 4-2 Critical energy that triggers the beginning of the healing process (τ_c) with induction and infrared radiation

4.3.3 Effect of Induction and Infrared Heating on Asphalt Self-Healing

To evaluate the experimental healing results, Equation 3.20 was used to fit the healing level-energy data in Figure 4-1 (bottom). Figure 4-3 (Top) shows an example of dense asphalt mixture heated using induction energy and infrared lamps at 30cm from the test samples. Note that in Figure 4-1 and Figure 4-3 the healing level of the test samples heated under infrared reaches a maximum and then decreases. The reasons for this will be explained in the next sections. All the curves obtained for the rest of the mixtures have been represented in Figure 4-3 (Bottom).

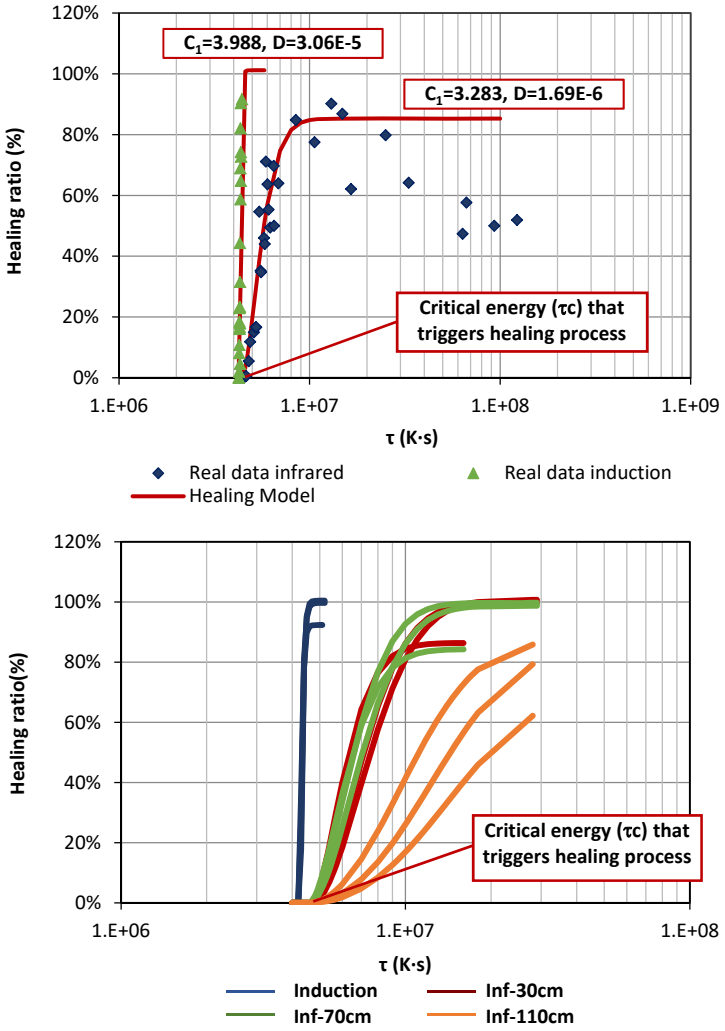

Figure 4-3 Fitting of healing model to experimental data
Dense asphalt, healed for different induction and infrared times (infrared lamps at 30 cm) (top) and curves obtained after fitting Eq. 3.20 to all the experimental results in Figure 4-1 (bottom).

Furthermore, the C_1/F_i-ratio (%) is a parameter that defines the highest healing level reached by asphalt mixture and has been represented in Figure 4-4 (Top). This figure shows that: (1) the maximum healing level was lower for dense asphalt mixtures since the high packing of aggregate particles makes them more prone to crack, while the weak points in porous samples are the binder connections between the aggregate particles (e.g. the healing level reached by test samples exposed to induction was 92.3% for dense asphalt, 99.7% for semi-dense and 100.4% for porous asphalt); and

(2) the maximum healing level reached by test samples was very similar for all the heating modes, except for test samples heated by lamps at 110cm (e.g. the healing level reached by dense asphalt mixture was 92.3% for dense test samples under induction heating, 86.3% for test samples under infrared heating with the lamps at 30cm, 84.3% for test samples under infrared heating with the lamps at 70cm, and 69.4% for test samples with the lamps at 110cm).

In addition, Figure 4-4 (Bottom) shows the D-values. They are indicators of the healing rate: healing happens faster in mixtures with higher D-values. It can be observed that experiments with higher healing levels, i.e. asphalt samples exposed to induction heating, showed also higher D-values, while the values were approximately constant in test samples exposed to infrared heating.

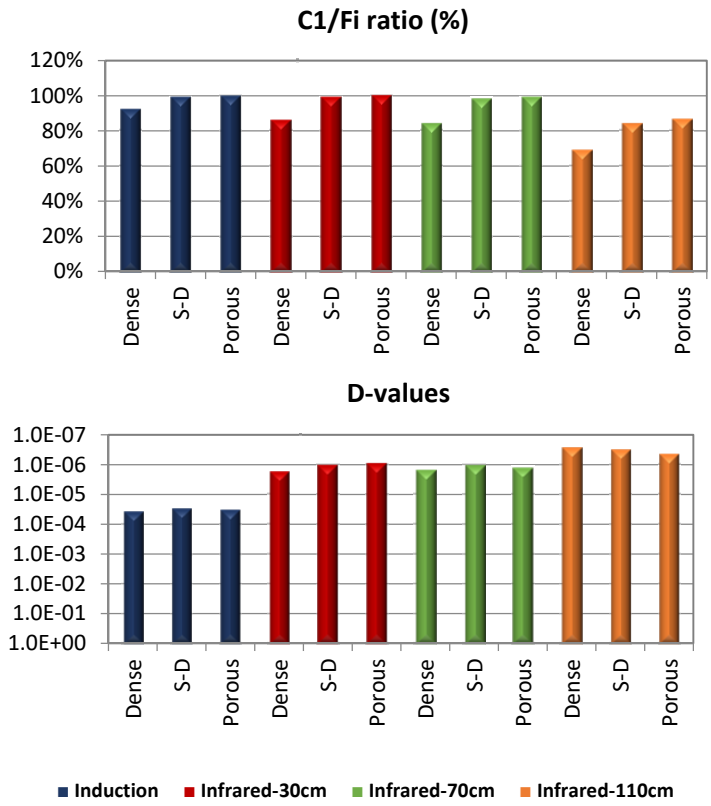

Figure 4-4 C_1/F_i-values of dense, semi-dense (S-D) and porous mixtures
Healed with induction and infrared radiation (top). D-values obtained for dense, semi-dense (S-D) and porous mixtures, healed with induction and infrared radiation (bottom)

Furthermore, Figure 4-5 (Top) shows the temperature of asphalt mixture at the maximum healing level, while Figure 4-5 (Bottom) shows the τ parameter at the maximum healing level. It is interesting to observe that while the temperature reached by test samples exposed to induction was the highest, the total energy used for healing these test samples was the lowest. Moreover the total energy used for healing test samples exposed to infrared heating was nearly constant and independent of the maximum temperature reached by the test samples. This shows that under the same heating mode, the energy used to heal asphalt test samples to a certain level is approximately constant.

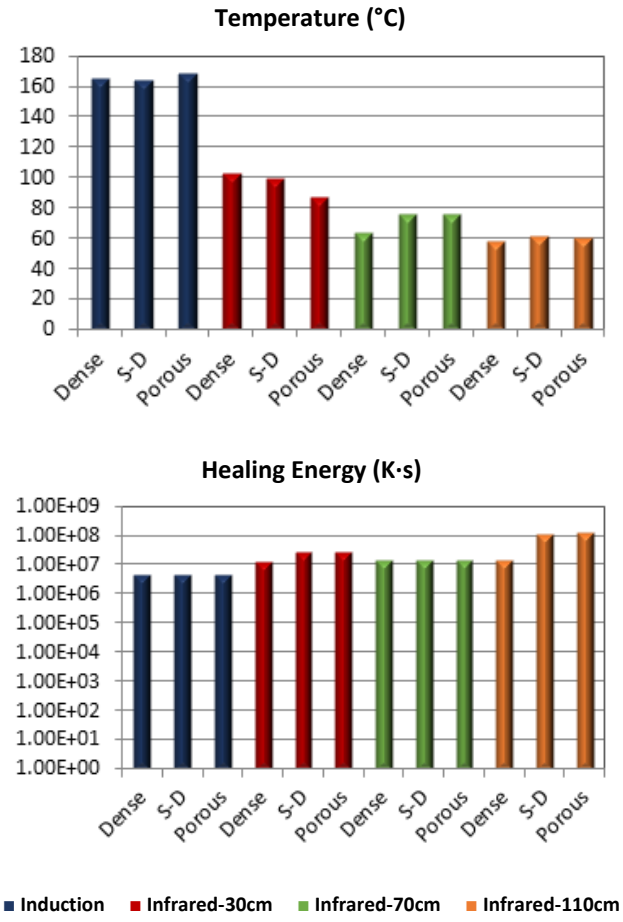

Figure 4-5 Temperature and healing energy (top) and (bottom) respectively, observed at the moment of maximum healing ratio

These results show that the temperature or time heating are not the most important factors affecting self-healing, but the heating mode.

4.3.4 Damage Produced by Overheating the Test Samples

The healing ratios of test specimens exposed to induction heating increased continuously with the time heating (see Figure 4-1). The longest induction heating test lasted 240s, when the bitumen started smoking. On the other hand, it could be observed that the time to heal completely the test samples exposed to infrared was the same as the time until the test samples

reached the steady state temperature. After the test samples reached the steady state temperature, the healing level decreased. As an example, Figure 4-6 shows the temperature-time (Top) and healing level-time (Bottom) relationships for dense asphalt mixture exposed to infrared heating, with the lamps at 30cm from the surface. It can be observed that the maximum heating ratio was 90% reached in a time between 300min and 500min. However, after heating the samples for 4 days at the steady state temperature, 105°C, the healing ratios fell to values around 50%.

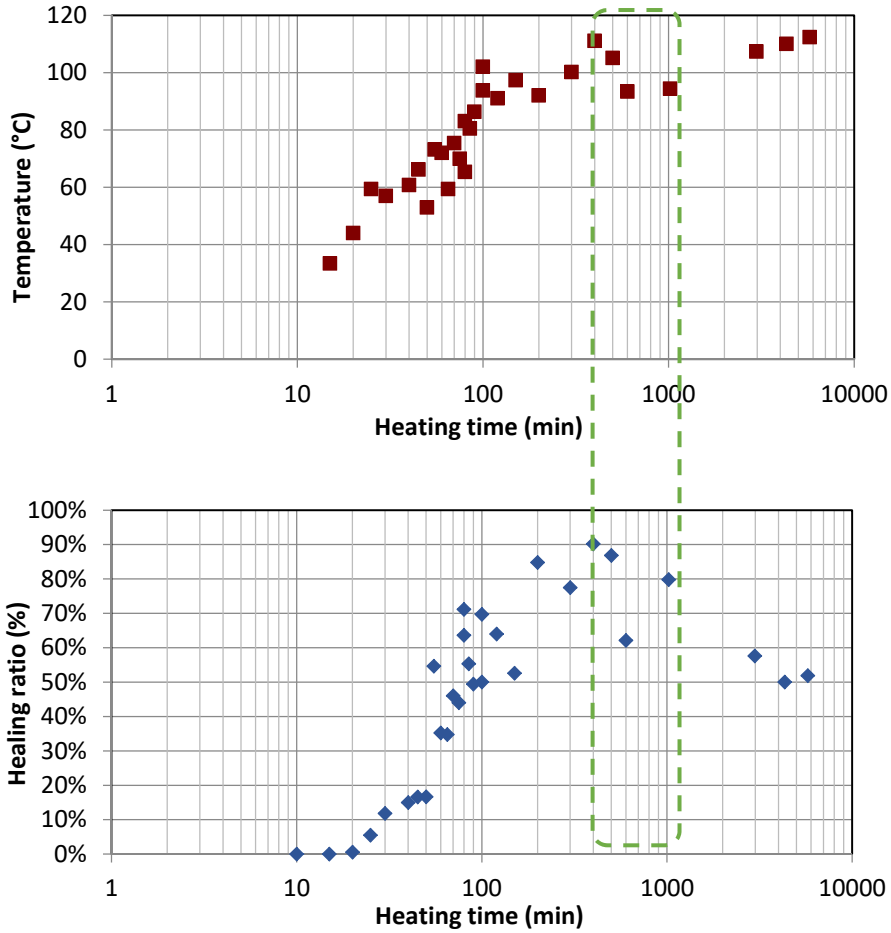

Figure 4-6 Curves of maximum temperature and healing ratio (top) and (bottom) respectively, obtained for a series of dense mix asphalt samples healed by infrared lamps at 30cm

This effect cannot be predicted by the healing model in Equation 3.20, which can only predict increasing healing values (Figure 4-1 (Top)). Therefore, there must be at least another factor, different from surface tension, hydrostatic forces and energy dissipation due to friction that affects asphalt self-healing and acts differently for induction and infrared heating methods.

4.3.5 Rheology of Bitumen from Asphalt Samples Exposed to Infrared Heating

A reason for the decrease of healing levels after reaching the steady state temperature may be bitumen ageing. To examine this, bitumen was extracted from test specimens exposed to infrared during 0min, 200min, 1day, 2days and 4days and the rheology and flow behaviour index (n) (see Figure 4-7) were compared. The flow behaviour index (n) describes the thickness or pumpability of the fluid, and is somewhat analogous to the apparent viscosity. It indicates the degree of non-Newtonian characteristics of the fluid and it is a relationship between the shear stress and shear rate. When (n) is 1 the fluid is Newtonian. If (n)>1 the apparent viscosity increases as the shear rate increases. If 0<(n)<1 the apparent viscosity decreases as the shear rate increases. The distance between the sample and the infrared lamps was set at 30cm.

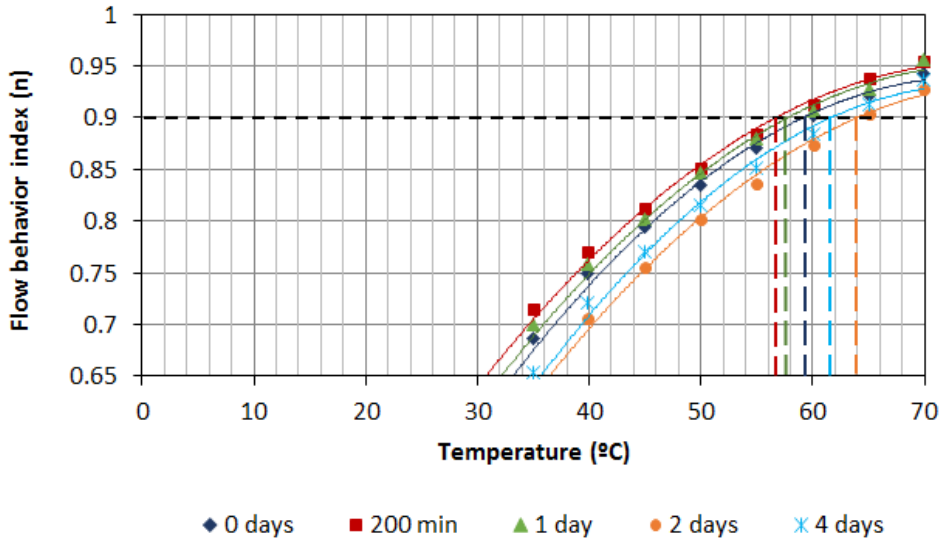

Figure 4-7 Flow behaviour index (n)
of bitumen recovered from samples subjected to infrared radiation over different periods of time

In references (Heyes et al., 1994, Sung et al., 2005) a value for n of 0.9 was proposed as the threshold flow behaviour index to initiate self-healing. Although this value is now obsolete after the introduction of the critical energy, it is still interesting as a reference to consider ageing in the test samples. As can be seen in Figure 4-7 it was found that n reached a value of 0.9 at very similar temperatures for all the studied samples, between 56.5°C and 64.0°C, without following any specific trend. Therefore, the ageing of bitumen can be rejected as an explanation for the decrease of healing ratios.

4.3.6 Evolution of the Internal Structure of Asphalt Mixture Exposed to Infrared Heating

Once the hypothesis of bitumen ageing was rejected, CT-Scans of the test samples were obtained in order to find whether the decrease in healing ratios is produced by physical changes in the internal structure of the material. Figure 4-8 shows the internal air voids structure of asphalt mixture (1) after cracking, (2) after heating with infrared lamps at 30cm for200 min and, (3) after 4 extra days exposed to infrared radiation.

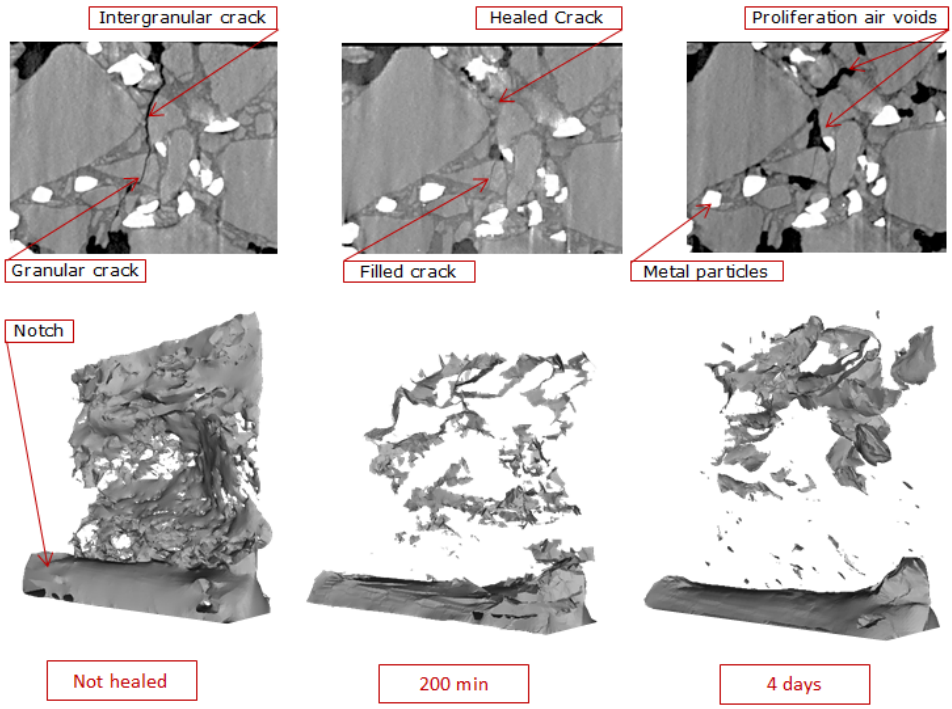

Figure 4-8 CT-Scans of the same section observed right after the crack happening
(left), after being healed with infrared radiation for 200 min (centre) and after 4 days (right). Down, the 3D-views of the crack, representing the air voids as solids

The CT-Scans show an almost-complete healing of the samples after 200min, produced by the flow of bitumen into the crack. This moment corresponds to the maximum healing level (Figure 4-6). However, after exposing the samples to 4 extra days of infrared radiation, the air voids increased in the upper part of the test specimens, which corresponds to the decrease of the healing ratios observed in Figure 4-1 Also Figure 4-8 shows that cracks in aggregates can be also filled by bitumen. Finally, it could be observed that after 4days heating, the upper part of the specimen looked porous, while the bottom had a much higher content of bitumen than before heating.

4.3.7 Results and Discussion

To explain asphalt self-healing, let us imagine asphalt mixture as a porous medium where bitumen is contained in the inter-aggregate space. During the heating phase, the binder reduces its viscosity, draining from the mixture into the cracks due to the combination of surface tension, hydrostatic forces, gravity and energy dissipation forces due to friction. This flow stops once these forces are in equilibrium, but as (1) the coefficient of thermal expansion of bitumen is $6*10^{-4}$/°C (Read and Whiteoak, 2003), more than one order of magnitude higher than the coefficient of thermal expansion of asphalt mixture, $3*10^{-5}$/°C (Read and Whiteoak, 2003), and (2) the viscosity of bitumen is temperature-dependent, the equilibrium cannot be reached until asphalt is not under steady-state conditions.

In the induction method the metallic particles may reach temperatures of more than 100°C in seconds. As bitumen coats the particles it reaches the same temperature, which causes its thermal expansion and viscosity reduction. As a consequence, internal pressure develops and bitumen is pushed to flow into the cracks (Figure 4-9).

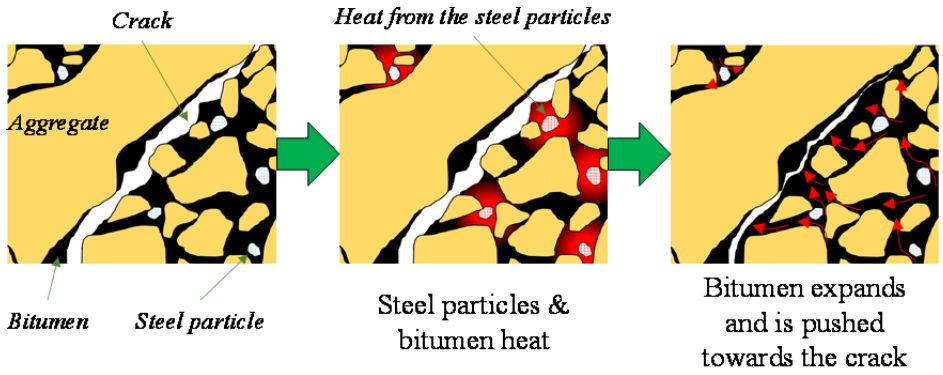

Figure 4-9 Schematic representation of the induction-healing process
(Garcia et al., 2013)

In the case of infrared (or solar) radiation, thermal energy is induced in the material through the upper face of the test samples and conducted downwards by the aggregates and bitumen. As a result, (1) the temperature of bitumen increases more slowly with infrared than with induction, (2) the critical energy (τ_c) is higher because aggregates must be also heated and (3) self-healing occurs at a slower rate (h versus min/s). Rapid heating is clearly preferable over the prolonged and slow heating mainly because of low energy requirement.

Moreover, self-healing happens while the temperature of asphalt mixture is increasing, because bitumen contained in the inter-aggregates space is pressurized as a consequence of continuous thermal expansion. Once the temperature of the test specimens reaches steady-state condition, the pressure in bitumen dissipates. In addition, due to the reduction of viscosity during heating, bitumen is able to flow downwards by gravity. This hypothesis can only be definitively proven through new complex numerical modelling and experiments in future research. However, in the current research it was observed, indeed, that the time for the maximum healing level of asphalt mixture corresponded with the time when the temperature reached steady state condition (see Figure 4-6). This could be an indication that pressure caused by thermal expansion dissipated and the main force affecting the movement of bitumen was gravity. As a consequence, the bitumen is accumulated in the bottom sections of the test specimens and new air voids are generated in the upper sections (see Figure 4-8).

4.4 Summary

This chapter has compared two heat sources to use to promote the self-healing in one type of steel fibre enriched asphalt mixture and its energy effectiveness, using infrared radiation, to mimic the solar radiation, and induction heating. Furthermore, it has discussed the effect of air voids on the self-healing. The next chapter will discuss the principal concepts and implementations of using four different types of steel fibres to address their effect on the mechanical properties of the mix alongside their self-healing properties.

Chapter 5: **Mechanical Properties and Self-Healing of Asphalt Mix with Different Types of Electrically Conductive Particles**

5.1 Introduction

To develop a sustainable uses loop that converts all the valuable metallic fibres and particles, which are landfilled as waste materials, into new high-value products, this chapter investigates the use of low-cost waste metal particles as an additive to asphalt mixtures and compares the results to those obtained without additions and with the addition of commercial fibres. One of the types of waste metal particles considered is steel fibres from old tyres. The European Union has dedicated great effort to reduce the amount of scrap tyres disposed in stockpiles and landfills. Hence, from 1994 to 2010, the amount of recycled tyres increased from 25% of annual discards to nearly 95%, with roughly half of the end-of-life tires used for energy, mostly in cement manufacturing (European Tyre and Rubber Manufacturers' Association (ETRma, 2011)), (Sienkiewicz et al., 2012). However, in countries, such as USA, in 2015 still 67 million tyres remained in stockpiles (Rubber Manufacturers Association (RMA, 2016)). Finding new ways of recycling this material can help to improve the situation. Something similar happens with the other types of metal waste considered in the present research: steel fragments produced during machining processes in the metal industry, such as drilling or shaping. Also known as "borings" or "swarf" this material is usually recycled in Basic oxygen steelmaking (BOS) or electric arc furnaces (EAF) through processes which involve great energy

consumption. More sustainable applications for these by-products would help to reduce the amount of steel disposed in landfills.

According to Kandhal (1993), the use of recycled waste in asphalt materials might raise some engineering concerns (e.g. impact on production and lower recyclability and quality), environmental (e.g. fumes production, hazardous leaching, difficult handling and processing), and economic (e.g. higher price, disposal costs, salvage values, and lack of incentive). In addition, in road applications, the most significant impacts are produced during activities, such as bitumen production, crushing of aggregate and materials transport, which produce a large part of the emissions to the atmosphere (Katz, 2004, Mroueh et al., 2001, Ponte et al., 2017, Horvath, 2004, Chiu et al., 2008, Horvath, 2003). Based on this, the researcher has identified the main impacts that might arise from the addition of waste metal particles to asphalt roads: (1) possible presence of dissolved metals in leached rain water; (2) detriment of mechanical performance and service life; (3) additional costs and environmental impact from transportation of metal particles; and (4) reduction of road safety (e.g. reductions in skid resistance or production of emerging spikes from the road surface). Hence, the main objective and innovation of the present research is to study the extent of these problems and determine if the addition of secondary metal products to asphalt is feasible, not only to enhance its mechanical properties but also to improve its self-healing capacity. In addition, based on obtained results, recommendations to design and produce cleaner roads through the use of waste metal particles will be elaborated.

5.2 Procedure

5.2.1 Samples

A dense aggregate gradation was used for all the asphalt mixtures in this chapter. The aggregates were crushed limestone and the binder was bitumen 40/60 pen and its content was 4.7% in all the mixtures; see Chapter 3: Section 3.2 and Section 3.3.

Four different kinds of metal particles and fibres were used: (i) Angular carbon steel grit particles, (ii) Steel wool, (iii) Steel fibres from recycled tyres, (iv) Steel shavings, as described in Section 3.2.3.

Metallic fibres and particles were simply included in the asphalt mixture, without replacing aggregates or adding extra bitumen in the following percentages by total mass of asphalt mixture: 0.15%, 0.23%, 0.30%, 0.38% and 0.45%. The reason for this was the high imprecision of finding the right proportion of aggregate removal, due to the variable aspect ratio of the fibres. The maximum value of 0.45% was selected, as higher contents of tyre fibres tended to produce clusters during mixing and compaction processes.

Two types of specimen were fabricated: (i) Cylindrical and (ii) Semi-cylindrical test specimens; see Section 3.3.2.

5.2.2 X-Ray Computed Tomography (CT) Scans

To analyse fibres and air voids distributions, X-ray micro tomography was used. For that, cylindrical asphalt samples of 101.6mm

diameter and 50mm height were used. Reconstructions of the fibres and air voids were prepared, as described in Section 3.4.3.

5.2.3 Volumetric properties of asphalt mixture

A volumetric analysis was carried out in order to determine (1) bulk specific gravity (G_{mb}), (2) air voids content (V_a), (3) voids in mineral aggregate (VMA), and (4) voids filled with asphalt (VFA) of asphalt mixture, tested for each fibre type and content according to the Standard BS EN 12697-5:2009 (Procedure A: Volumetric procedure), shown in Section 3.4.4.

5.2.4 Mechanical Properties

5.2.4.1 Indirect tensile strength (ITS)

The indirect tensile strength was obtained for a group of three dry cylindrical specimens for each type and content of conductive particles. The final value of ITS was considered as the average value of the three tested specimens, Section 3.4.5.1.

5.2.4.2 Resistance to water damage

Once the ITS Tests had been carried out under dry conditions, an equivalent 3-samples group was produced for each type and content of metal fibres and particles and tested under wet condition according to the Standard BS 12697-12 (Method A). To evaluate the water damage, the conditioned specimens were tested for indirect tensile strength and the indirect tensile strength ratio (ITSR) was calculated, Section 3.4.5.2.

5.2.4.3 Stiffness modulus

The stiffness modulus was obtained following the procedure in Section 3.4.5.3 for each type and content of metal particles; 5 samples were tested. The stiffness modulus was calculated as the average of the 5 results.

5.2.4.4 Particle loss resistance

Particle loss resistance tests were performed as shown in Section 3.4.5.4 according to British Standard BS EN 12697-17:2004. The mass difference of the test specimens before and after testing was noted and the particle loss resistance was calculated.

5.2.4.5 Skid resistance

The pendulum skid resistance test was conducted as explained in Section 4.4.5.5. Two flat 300x150x50mm^3 asphalt slabs for each of the four types of steel particle and a control slab (without steel) were manufactured. The samples with fibres were manufactured with 0.45% volumetric content of fibres, the highest of all those studied in the present investigation.

5.2.5 Temperature and Induction Heating Measurements

The surface temperature evolution of asphalt test samples during induction heating was measured using an infrared camera, as specified in Section 4.4.2. The induction heating experiments were performed using the procedure shown in Section 4.4.1. The air temperature during the tests was 20°C.

5.2.6 Asphalt Self-Healing Measurements

The self-healing procedure was applied according to the method defined in Section 4.4.1. Three semi-circular asphalt samples were tested for each type of metal particle studied. Finally, a healing ratio (HR) was calculated and registered.

5.3 Results and Discussion

5.3.1 Length of Fibres

Figure 5-1 shows the cumulative Weibull distribution function for the length and width of the four types of metal particles used in the present investigation. The probability curves were calculated as:

$$p = \left(\frac{i - 0.5}{n}\right) \quad 5.1$$

where p is the cumulative probability of obtaining a certain particle length, n is the number of measured particles and i is the rank of a given particle once the sizes are sorted in increasing order. The results were also obtained for the particles extracted from compacted asphalt samples, which made possible the analysis of particle size change due to shear and bending stresses applied during the manufacturing process.

As can be seen, steel grit and tyre fibres are very stable against such stresses but steel wool and shavings reduce their size significantly. Hence, in average terms, steel wool reduced its length by 49.5% and its width by 16.6% while shavings reduced length and width by 72.2% and 11.8% respectively. This means that although initially, tyre fibres and shavings

have similar dimensions, the average size of the shavings contained in a compacted asphalt sample is 30% smaller, which can affect both mechanical and conductive properties of asphalt mixes.

Finally, as explained in Garcia et al. (2012), the decrease in fibre length is directly correlated to their capacity to resist tensile forces. For the case of steel wool, this can be related to its smaller cross sectional area (diameter within the range of 14µm to 72µm), while for the shavings, it might be related to the damage caused by the highly-aggressive machining process through which they were obtained.

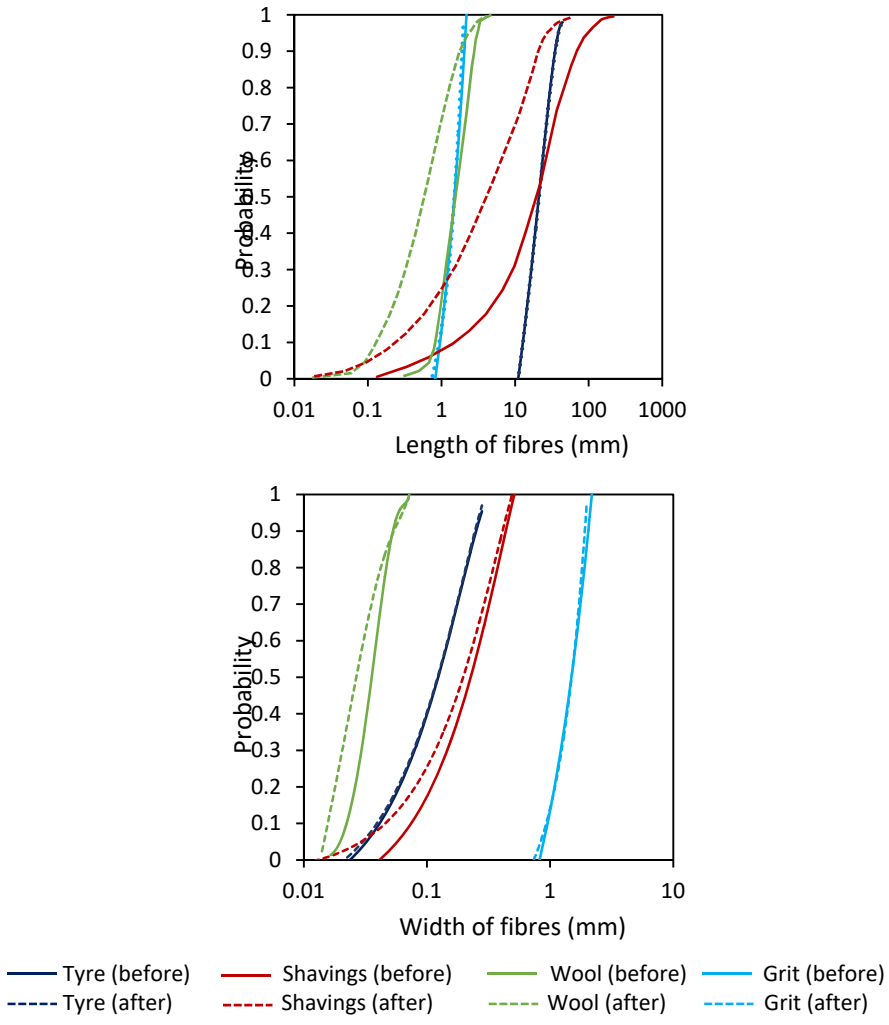

Figure 5-1 Probability distribution of the length of metal particles before and after asphalt samples manufacturing

5.3.2 Volumetric properties of asphalt mixture

Figure 5-2 shows how the type and content of metal particles in the mix affects the bulk density and air voids content. A statistical 2-way ANOVA (variables type and content of metal particles) was carried out after checking that all results presented normal distribution (Shapiro-Wilk test for sample size N<50) and variance homogeneity (Levene test).

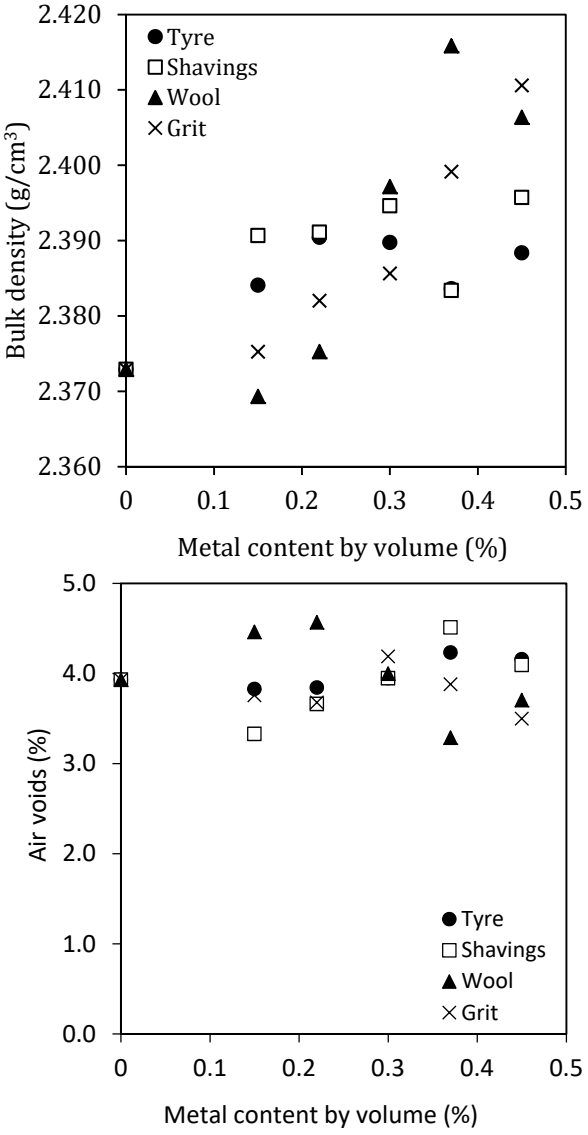

Figure 5-2 Volumetric properties of asphalt mixtures with different types and contents of metal particles
(every point is the average value obtained for 3 specimens)

Results show the content of metal particles affects the bulk density of mixes at a confidence level of 95% ($p_{content}$=0.014<0.05) due to the high specific weight of steel, almost 3 times higher than aggregates. Nevertheless, for the small contents considered for the present investigation, such increases were small, 1.2% higher for mixes with 0.45% of steel, than for control mixes without steel. In addition, no statistically significant differences were found when changing the type of metal particles.

The statistical analysis also showed that air voids content is independent of both content and type of metal particles. Taking both results into account, it can be concluded that an increase in metal content, slightly increases the density of the mixes but it does not affect their compaction level and internal structure.

5.3.3 Homogeneity of the Mix

The distribution of metal particles and air voids can be seen in Figure 5-3, based on observations and calculation carried out by CT-Scan, Figure 5-4. The distribution of fibres is, in general, homogenous with the height and does not present segregations of significant cluster formations. It could also be checked that the cumulative content divided by the total volume of the sample, averaged at the added content of 0.3% (0.31% for steel grit, 0.28% for steel wool, 0.37% for tyre fibres and 0.30% for shavings) which was useful to prove the method was well calibrated.

Regarding the air voids content, all results averaged at the target content of 4.5% used to manufacture the specimens (4.55% for steel grit, 4.58% for steel wool, 4.40% for tyre fibres and 4.24% for shavings). This

value was also observed by volumetric testing as shown above (Figure 5-2). In addition, it can be seen that the distribution of air voids in samples with tyre fibres is much more irregular than for the other types of metal particles. Since there is not any clear parallelism between the curves of fibres and air voids contents, it can be said that such irregularity is not caused by the formation of clusters, but by a greater difficulty to mix and compact this type of long and hard fibre.

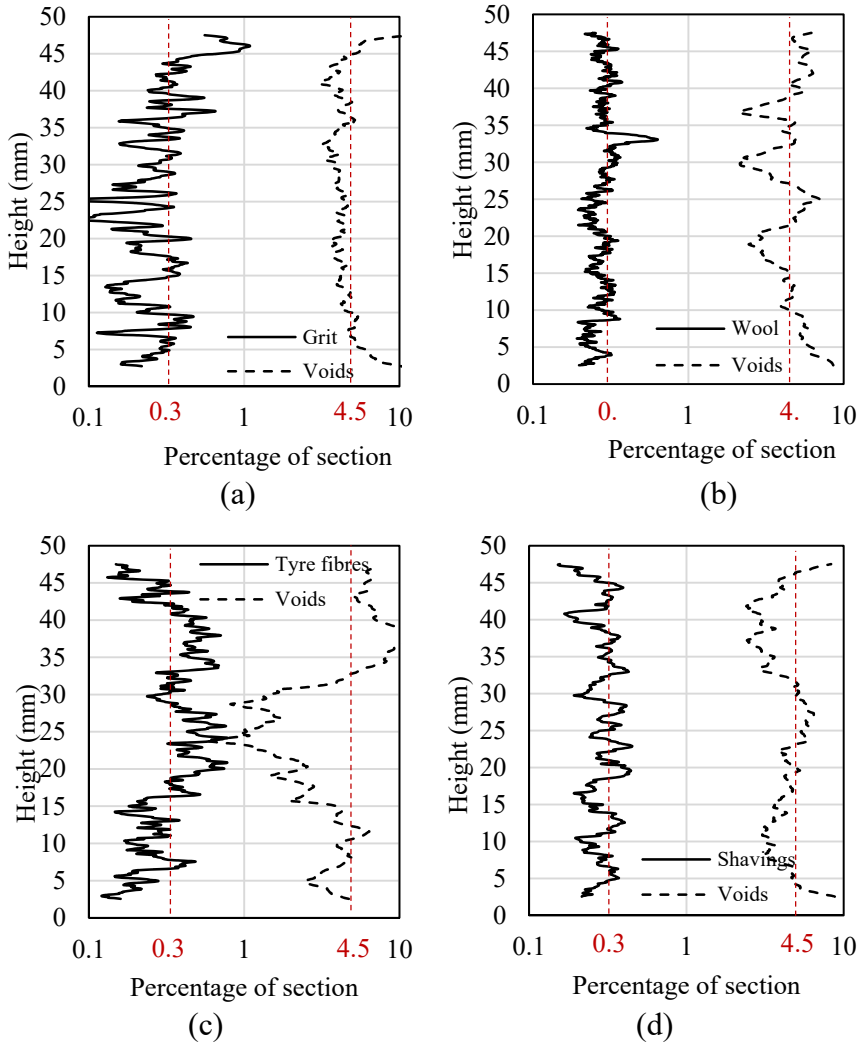

Figure 5-3 Distribution of fibres and air voids inside asphalt samples
with 0.3% of (a) steel grit, (b) steel wool, (c) tyre fibres and (d) shavings

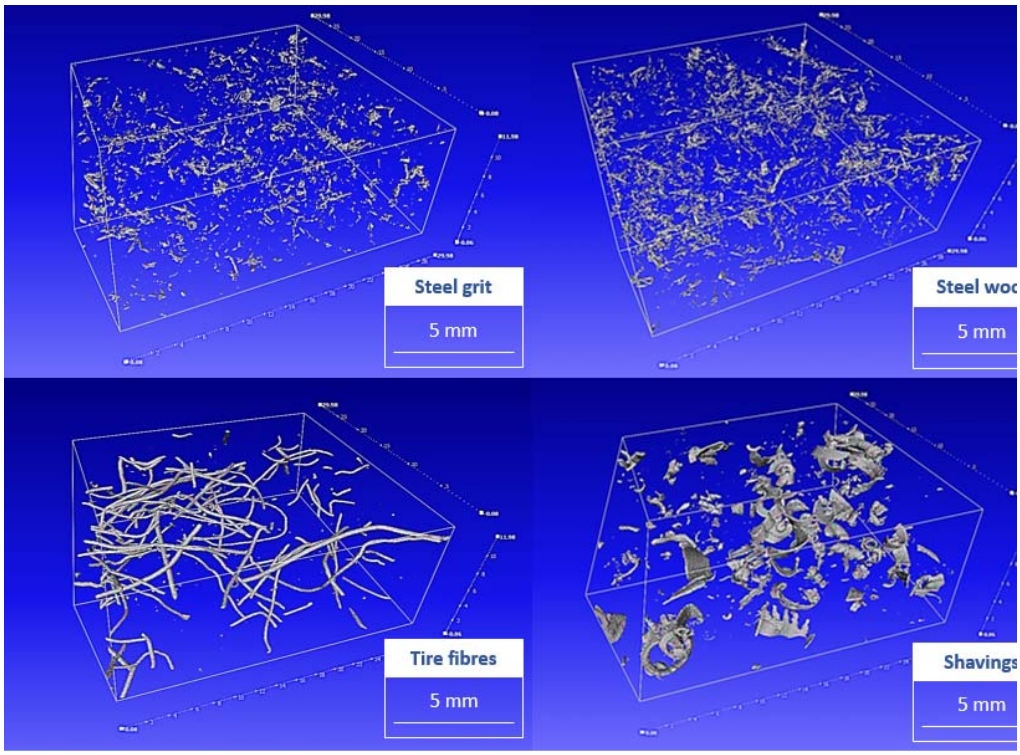

Figure 5-4 Reconstructed CT-scans images of the HMA specimens after compaction
with 0.3% of steel grit, steel wool, tyre fibres and shavings respectively

5.3.4 Leaching Behaviour

Leaching tests have shown traces of Nickel (<0.075mg/kg), Cobalt (<0.025mg/kg), Palladium (<0.05mg/kg), Antimony (<0.375mg/kg), Selenium (<1.75mg/kg), Molybdenum (<0.04mg/kg) and Tungsten (<0.02mg/kg) in the recycled fibres from tyres and shavings. Traces of Arsenic (<0.36mg/kg) and Chromium (0.025mg/kg) were also found in all the samples due to the contamination of the rain water.

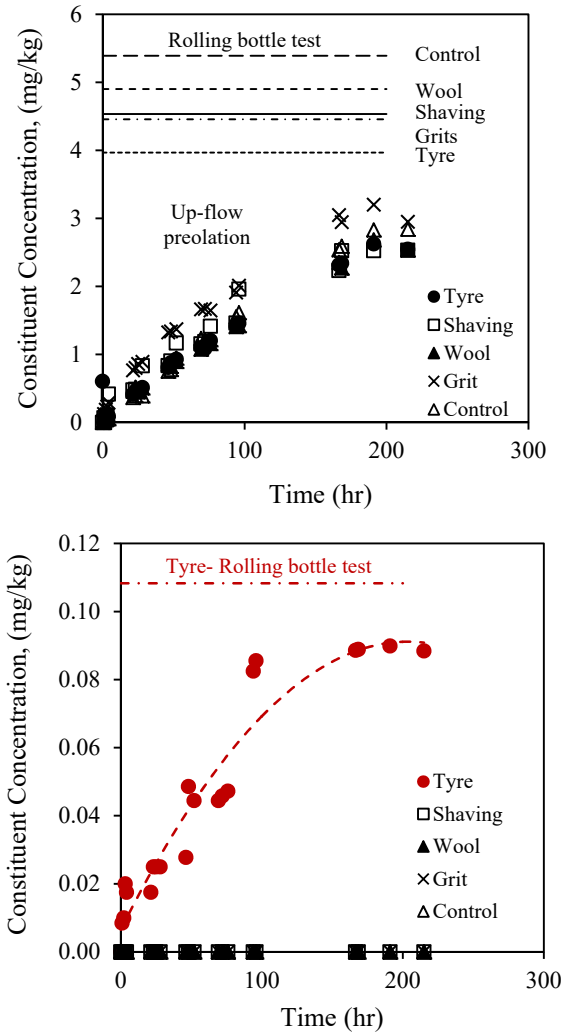

Figure 5-5 Results of rolling bottle test and up-flow percolation test
For the elements Barium (top) and Iron (bottom)

The only metals observed in significant concentrations were Aluminium, Barium, Iron, and Zinc. In general, and as can be seen in Figure 5-5 (top) for the example of Barium, all the samples performed very similarly between them and also similarly to control mixes with no fibres. The observed concentrations reached a steady state in the up-flow percolation test after around 170h from the beginning of the test. Such steady state values were always lower than the values obtained by the rolling bottle test and significantly lower than the limits established in

specifications, such as (Water_UK, 2018, Lenntech, 1998). For the example shown of Barium, such limit is 20mg/kg of dry sample, four times higher than the maximum value obtained experimentally.

Fibres from old tyres also produced a significantly higher concentration of iron than other types, as can be seen in Figure 5-5 (bottom). Although the obtained values do not pose any problem in terms of legislation, it explains why this type of fibre tends to rust through oxidation, a phenomenon observed after introducing the samples in water.

5.3.5 Indirect Tensile Strength (ITS)

In this case, the indirect tensile strength (Figure 5-6) is affected, at a confidence level of 95%, by both type and content of metal particles (p_{type}=0.011 and $p_{content}$=0.028, both lower than 0.05). Specifically, a Scheffe post hoc test showed that although there is no significant difference between the behaviour of mixtures with tyre fibres, shavings and steel wool, the strength of samples with steel grit became significantly improved. This indicates these particles, with shape very similar to the aggregate grains, forms part of the structural skeleton of asphalt samples improving their load capacity.

In general, all types of particles scored higher values than the 0%-control samples for the considered metal contents, which highlights the beneficial effect of adding metal particles to asphalt mixtures. However, they also showed the highest values at around 0.3% metal content, indicating that higher contents might lead to reductions in strength.

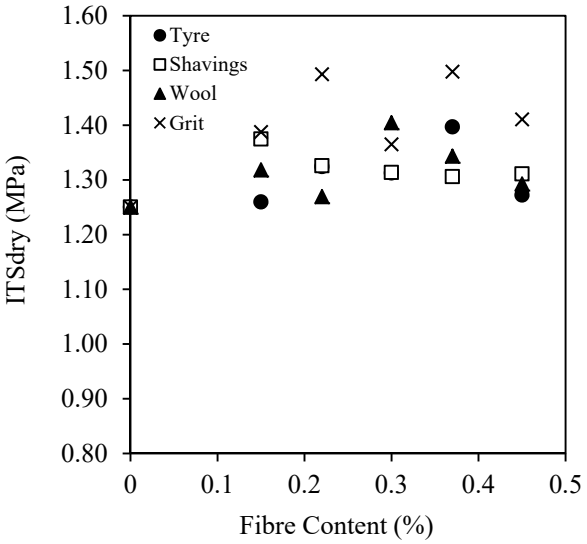

Figure 5-6 Indirect tensile strength of asphalt mixtures with different types and contents of metal particles.

5.3.6 Resistance to Water Damage

Resistance to water damage (Figure 5-7) does not significantly depend on the fibre content but it depends strongly does on the type of fibre at a confidence level of 99% (p_{type}<0.001). While long fibres, such as tyre fibres and shavings perform very similarly to control mixes, the addition of steel wool and especially steel grit worsened average mix resistance by 8.5% and 13.3% respectively.

It is remarkable that, while steel grit produced the highest results of resistance in dry condition (Section 5.3.5), it also produced the worst results when samples were conditioned in water. As a consequence, they also obtained the lowest results of retained strength. This behaviour could mean loss in mastic cohesion. The longest fibres (from tyres and shavings) would contribute to resist tensile stress produced through the mastic but the small wool fibres and especially the rounded grit would not be able to contribute in this sense. Another plausible explanation would be a loss in particle-binder adhesion, which would especially affect the grit due to its rounded

shape. In any case, such behaviour makes this type of fibre particularly suitable for lower layers (e.g. base layer), where the material is well protected against water damage and where the contribution to the mechanical performance is very important.

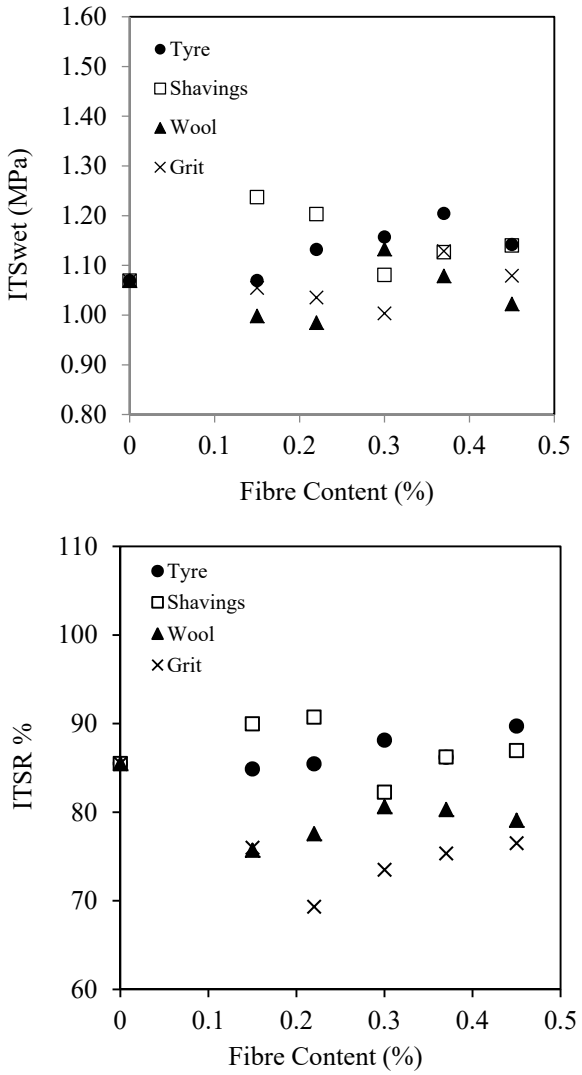

Figure 5-7 Wet indirect tensile strength and resistance to water damage (ITSR) of asphalt mixtures with different types and contents of metal particles.

5.3.7 Stiffness Modulus

Stiffness (Figure 5-8) is affected by metal particle content, according to the statistical analysis carried out at a confidence level of 95% ($p_{content}$=0.031). As in the case of indirect tensile strength, the results show

an optimum content around 0.3%, which produces the highest results. In general, the results obtained with metal particles were higher than with control mixes, although the maximum increase obtained for the optimum content was just 12%. Hence, the addition of fibres, in the range of the studied contents, can be considered as a positive contribution to get stiffer mixtures, although no great increases are expected.

On the other hand, stiffness does not significantly depend on the selected type of fibre at a confidence level of 95% (p_{type}=0.076), which means that all the studied types performed in a very similar way.

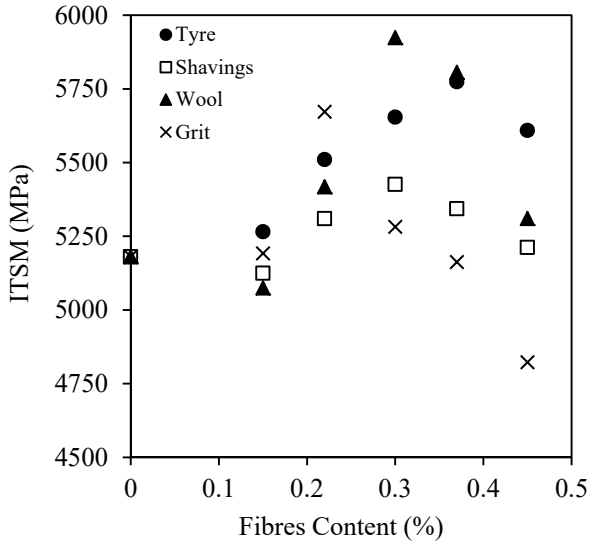

Figure 5-8 Indirect tensile stiffness modulus (ITSM) of asphalt mixtures with different types and contents of metal particles.

5.3.8 Particle Loss Resistance

The results of the Cantabro test show that the length of steel particles, when they are fibre-shaped, is an important factor affecting the resistance to particle loss. Hence, the longer they are, the lower the resistance is. As can be seen, in Figure 5-9, compared to mixes with steel wool, the particle loss increased 6.2% with shavings and 55.8% with tyre

fibres. This behaviour can be related to an increasing possibility of cluster formation close to the surface, as the length of the fibres increases.

In addition, although the size of steel grit is comparable to the length of steel wool fibres, it produced 27.3% greater loss, probably due to its rounded shape and lower particle-binder adhesion, as already mentioned above.

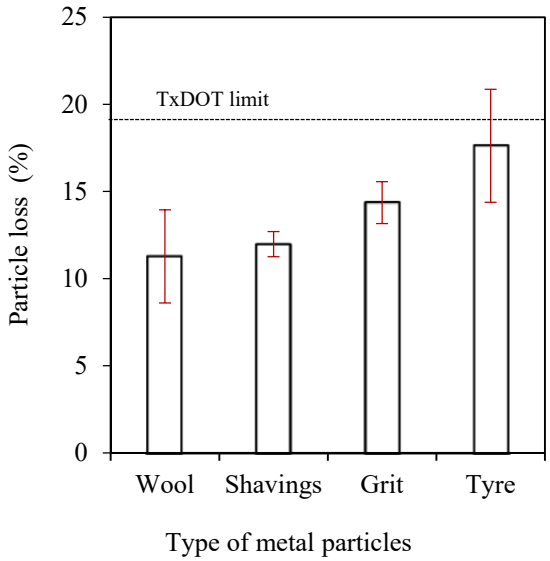

Figure 5-9 Results of particle loss (Cantabro test)
of asphalt samples containing 0.45% (by volume) of different types of metal particles.

Despite the previous considerations, all the samples met the critical value of 20% required by different Specifications (A. Ongel, 2007, Department_of_Transport_and_Main_Roads, 2017, BSI, 2016b), such as TxDOT Surface Aggregate Classification (SAC). As a consequence, although grit and tyre fibres would be more recommendable for lower layers, not subjected to traffic abrasion, all of them are suitable for any use.

5.3.9 Skid Resistance

European Standard EN 1436 (BSI, 2008a) has a range of Skid Resistance Classes ranging from S0 to S5. While there is no requirement for S0 material, the skid resistance value needs to be at least 65 in order to obtain the top S5 classification. As can be seen in Figure 5-10, all the fibres obtained values higher than 70, demonstrating they can be generally used even in pavements with high quality requirements.

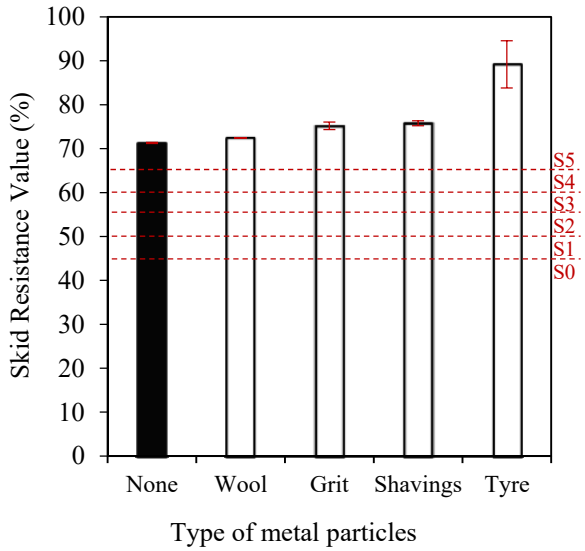

Figure 5-10 Results of slip/skid resistance of asphalt samples
Containing 0.45% (by volume) of different types of metal particles and classification of materials according to Standard EN 1436.

In addition, it can be seen that compared to control mixes without metal particles, it is possible to increase skid resistance by adding small particles, such as steel wool (1.5% higher than control mix), steel grit (5.5%) and shavings (6.3%). However, the greatest increase was obtained by adding tyre fibres (25.1%), highlighting that the length of fibres is an important factor also affecting this mechanical property. The higher difficulty of mixing tyre fibres and their greater length, produce the partial

exposure of sharp spikes in the surface that increase skid resistance. However, it can also compromise the safety of road users. As this is an issue only observed with tyre fibres, their use is advised for lower pavement layers, with a protective superficial layer placed on top manufactured with other sorts of metal particles.

It should be clarified that the results in Figure 5-10 refer to the first day in service or a virgin specimen. In other words the comparison made among the different steel particles has not been done in terms of evolution of the skid resistance with accumulated traffic.

5.3.10 Temperature and Induction Heating Measurements

By subjecting the samples to induction heating, it could be observed that there is a clear correlation between the temperature reached by the samples after a given time (Figure 5-11 shows the case of 100s) and the metal content present in the mix, when using shavings, steel wool and grit. From these types of particle, once again, steel wool and grit behaved in a very similar way obtaining temperatures slightly higher than 100ºC. On the other hand, the temperature of mixes with shavings remained in general below 50ºC. This poorer behaviour indicates that asphalt layers containing this type of fibre should be placed as close as possible to the road surface, as the heating effect decreases exponentially with the distance to the induction coil (Garcia et al., 2012).

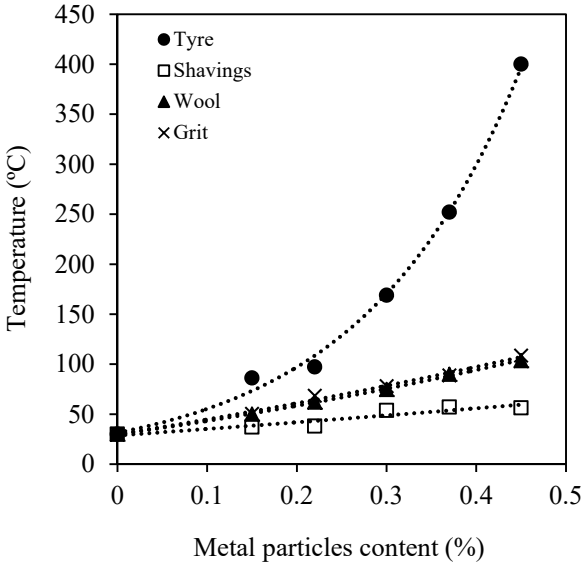

Figure 5-11 Temperature of samples with different contents metal particles after being heated for 100s

On the other hand, samples containing tyre fibres increased their temperature exponentially with the fibre content, reaching after 100s, temperatures above 400ºC. Such a high temperature exceeds the fire point of bitumen causing its ignition. Due to this, this type of fibre is, again, especially suitable for lower pavement layers, where the action of the coil is much weaker.

5.3.11 Asphalt Self-Healing Measurements

Figure 5-12 shows the healing ratios (% of initial strength recovered) after subjecting the samples to 100s of induction heating. As can be seen, the healing ratios depend directly on the metal particles content for all the considered types. Hence, by increasing metal content from 0.15% to 0.45%, healing ratios increased 13% for tyre fibres, 41% for shavings and 56% for steel grit. But especially remarkable is the case of mixes with steel wool, where an increase of 104% was obtained.

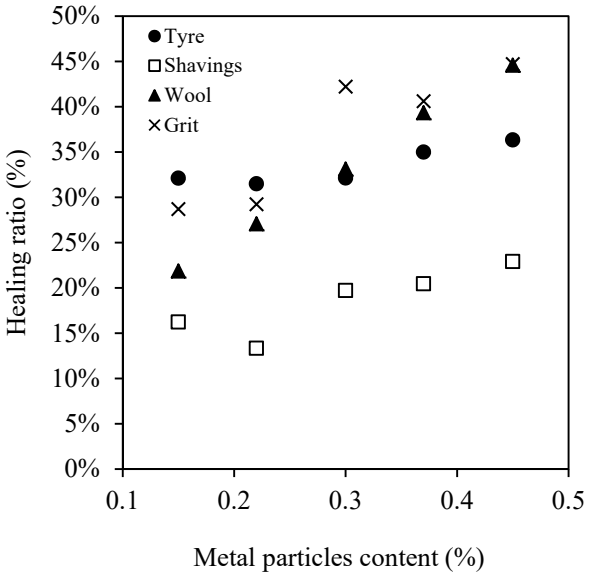

Figure 5-12 Relationship between the healing ratio and content of metal particles after 100s of induction heating

It can be also observed that all types of metal particles performed very similarly with the exception of the shavings which, in average terms, produced healing ratios 46% lower. Since it has been seen above that its heating capacity is poorer than other types of particles, lower healing ratios were also expected. In fact, it would be also reasonable to expect higher healing ratios for tyre fibres, as their heating capacity is superior to others. However, due to their great length and stiffness, after initially breaking the sample and before applying electromagnetic induction, it was very difficult to put the two halves back together due to interference in between the fibres. As a consequence, the healing was less effective. To support this, it can be observed that samples with the lowest tyre fibre contents (0.15% and 0.22%) produced higher healing ratios than samples with other types of particles but as the content increased (more fibres interfering) the performance became poorer. Since in a real road, the cracks to be healed have reduced size and both sides separate from each in the range of microns,

this problem is not likely to happen. Quite the opposite, it would be expected that tyre fibres produced the highest healing ratios of all the studied types of particles.

5.4 Discussion

Previous results (summary in Table 5-1) showed that, in general, the addition of the studied metal particles did not significantly affect the volumetric, leaching and mechanical properties of the mixes, although some slight improvements in ITS and stiffness were obtained, as well as skid resistance. Moreover, the addition of waste particles produced a similar effect to commercial metal products and other additives found in the literature, such as coal waste powder (Modarres and Rahmanzadeh, 2014, Modarres et al., 2015). In addition, the amount of metal needed in the mix is so low (less than 0.5% in total mix) that no significant extra cost or environmental impact from transportation are expected compared to the impacts already produced by the rest of materials. Consequently, from the point of view of Cleaner Production, by adding these small amounts of recycled fibres from old tyres or steel shavings, it is possible to build roads with enhanced service life and induction-healing capacity, increasing road safety and reducing maintenance costs, environmental impact and traffic disruptions. Based on previous results and in order to optimise this Cleaner Production, the following considerations can be taken into account.

The healing capacity of the material can be increased by increasing the amount of metal particles, which would also slightly improve the strength of the mixtures. However, the resulting mixes would have higher

density and lower resistance to water damage (especially if steel grit is used). As an alternative, it would be enough to increase the healing energy by increasing the current intensity through the induction coil (in this case only 80 A were used) or the heating time (for the present research no times longer than 100 s were studied).

Table 5-1 Effect of adding different types of conductive particles on the studied properties

		Type of fibre			
		Grit	**Wool**	**Tyre**	**Shavings**
Volumetric properties	- Density	▲	▲	▲	▲
	- Air voids	●	●	●	●
	- Homogeneity of mix	●	●	▼	●
Leaching properties	- Up-flow percolation	●	●	●	●
	- Rolling bottle test	●	●	●	●
Mechanical properties	- Indirect tensile strength	▲▲	▲	▲	▲
	- Resistance to water damage	▼▼	▼	●	●
	- Stiffness modulus	▲	▲	▲	▲
	- Particle loss resistance	▼	●	▼	●
	- Skid resistance	▲▲	▲	▲▲▲	▲▲
Healing properties	- Induction heating capacity	▲▲	▲▲	▲▲▲	▲
	- Self-healing properties	▲▲▲	▲▲	▲▲*	▲

▲Increase ▼Decrease ● No significant effect (x1 – Slight effect; x2 –Moderate effect; x3 – Strong effect)
*Due to test configuration, results in real roads are expected to be better that those observed in the present investigation

From the studied types of fibre, the use of fibres from old tyres can be recommended for non-superficial layers. Due to the emerging sharp spikes that can be found on the surface even after compaction, this type of fibre could involve safety issues for road users when used in superficial layers. In addition, their high iron content makes them susceptible to corrosion by oxidation in the presence of water, and their use is advised in

lower and denser layers, more protected from water action. On the other hand, these fibres have great heating potential which can be translated into higher healing ratios even when they are placed far from the induction coil (lower layers). At the same time, they slightly improve mechanical properties, such as ITS and stiffness, not producing any detrimental effect on the resistance to water damage, which makes them very suitable for structural layers, such as bases and sub-bases. In addition, their waste nature makes them a cheaper and more sustainable product whose use can contribute to reduceing the ecological impact of roads without increasing the costs and needs of raw materials in a significant way. Therefore, its use in the thickest layers the base is advisable in order to maximise all this economic and ecological potential.

For superficial layers (surface and binder layers), the most suitable type of fibre is steel wool. This commercial product might add a significant extra cost to the mix production but it produced the highest resistance to abrasion and slightly improved the skid resistance without reducing too much the resistance to water damage (as for instance does the grit). All of these features make them very convenient for superficial layers that will be in direct contact with traffic and weather agents.

The metal shavings can add great value to asphalt mixes from an economic and ecological point of view, as they are waste products that can be obtained at low cost. Since they do not produce any detriment on the resistance to abrasion and can even improve mechanical properties, such as ITS, stiffness and skid resistance, their use could be suitable for any layer of asphalt pavement. However, the heating capacity and, as a consequence, the

results for the healing potential they can offer was lower than for the rest of fibres. Therefore, they should be used as close as possible to the surface and induction coil.

On the other hand, the steel grit behaved very similarly to the steel wool, probably because of the reduced particle size of both materials. In addition, they produced the best healing and ITS results. However, its rounded shape might cause lower particle-binder adhesion, which would explain the sharp reductions in resistance to water damage and resistance to particle loss. Due to this, the use of steel grit is more advisable in lower layers (base and sub-base), where they can contribute to the structural performance of the pavement while being protected from water damage. Nevertheless, its use does not lead to any significant benefit, compared to tyre fibres.

Finally, it must be added that for the present study, the waste metal particles were supplied in very good condition, not containing significant amounts of impurities or clusters. The use of other types of metal forms or supplied in different conditions (e.g. metal fibres from concrete containing cement paste or fibres from old tyres containing rubber fragments) might lead to material behaviours different to that obtained in the this study. For these reasons, in order to apply the present conclusions to a practical case, it is recommended that metal particles are as similar as possible to those used in the present paper and treated (if necessary) to be free from impurities.

5.5 Summary

This chapter describes the mechanical properties and self-healing capabilities of four different steel fibre asphalt mixes. In the next two chapters the effect of bitumen on the self-healing will be covered. Chapter 6 will cover the aging effect, taking into account the compaction level of the mixes. Chapter 7 will cover the effect of using 5 types of virgin bitumen on the self-healing form mechanical, rheological and chemical points view.

Chapter 6: **Effect of Ageing and RAP Content on the Self-Healing of Asphalt**

6.1 Introduction

Within the framework of pavement engineering, durability was defined as the ability of a material to resist effects of water, ageing and temperature variation, in the context of a given amount of traffic loading, without significant deterioration for an extended period (Scholz, 1995). This property of the materials constituting different road layers, is often insufficient for the purpose for which they were designed. As an example, according to Interim Advice Note 157/11 (Highways_England, 2011), asphalt surfacings, such as the Thin Surface Course Systems (TSCS), have a service life of 7-15 years, considerably lower than the expected 10-20 years. Most reductions in the service level of roads and the most aggravating pavement distress for traffic safety (Yang et al., 2015) are caused by chemical degradation of bitumen as it becomes brittle due to environmental conditioning (Read and Whiteoak, 2003), loss of binder-aggregate adhesion due to moisture penetration (Zheng et al., 2013), thermal effects (Zborowski and Kaloush, 2011) and traffic loads (Mobasher et al., 1997). When these agents persist over time, cracks propagate throughout the material producing aggregate losses and the eventual formation of potholes (Miller and Bellinger, 2014).

In addition, ageing occurring in the binder due to the presence of oxygen, ultraviolet radiation, and changes in temperature produces, in general, a hardening process related to decreases in penetration grade,

increases in softening point and viscosity and, usually, increases in penetration index (PI) (McKay et al., 1978, Reerink, 1973, Griffin et al., 1959, Simpson et al., 1961). Some authors consider this a beneficial phenomenon in structural layers, since it increases their stiffness and load spreading capability, resulting in longer service life (Scholz, 1995). However, in surface layers, it usually leads to fretting and/or cracking (Scholz, 1995).

It is evident that self-healing treatments are only necessary once the cracks have been produced in the pavement, which normally happens after years of service life. In other words, they are necessary when the bitumen constituting the pavement is already aged and its viscosity increased. As viscosity is one of the main parameters that directly affects the healing properties of asphalt, the healing capacity of an asphalt mix can significantly change from the moment when the road is constructed to the moment when healing is applied. A similar phenomenon happens when a new pavement is built incorporating RAP, as the old binder contained in these particles is aged and its hardening can continue even upon reclamation (De Lira et al., 2015).

Despite these considerations, the vast majority of research found on asphalt healing was carried out on samples with fresh bitumen (Ayar et al., 2016), and it is not clear whether the conclusions are still valid for the moment when the pavement needs to be healed. The aim of the present investigation is to study how the ageing phenomenon and the incorporation of aged material into new asphalt affect the self-healing properties of pavements.

6.2 Procedure

6.2.1 Materials and Samples

As illustrated in Chapter 3: Section 3.2 and 3.3, hot mix asphalt (HMA) was used for the investigation in this chapter with 4.7% content of bitumen 40/60 pen and target air voids content of 4.5%. The aggregate was limestone with a continuous gradation. In order to obtain an asphalt mixture that can be heated by electromagnetic induction, steel grit was introduced in the mix by replacing the same volume of natural aggregate in this fraction. The volumetric content of 0.4% (1.12% by mass) was fixed for all the samples, Section 3.2.3. Aged mix and RAP used for the present research was artificially produced according to the procedure described in Section 3.2.5.

As summarised in Table 6-1, the present research involves the study of two different types of material: (a) HMA samples subjected to an ageing process after compaction, to simulate the effect of progressive ageing happening in a pavement during its service life; and (b) samples made of a mix of HMA and aged RAP to simulate the effect of introducing recycled material into new mixes. For the first case, loose mix was subjected to a certain ageing process of 0 (control), 3, 6, 9, 12 or 15 days in an oven at 85ºC before compaction. For the second case, loose HMA made with fresh bitumen was mixed with 20%, 40%, 60%, 80% and 100% of RAP (aged for 15 days) and then compacted.

All the samples were 150x70x50mm3 beams obtained from 310x310x50mm^3 slabs with a 2mm thick and 5mm deep notch at the

midpoint of the bottom surface to ensure that all samples cracked around the same point, Section 3.3.

Table 6-1 Summary of studied materials

Mix	RAP content in mix (%)	Ageing after compaction (days)	
1	0	0	New road (control)
2	0	3	Effect of ageing process during the service life of the road
3	0	6	
4	0	9	
5	0	12	
6	0	15	
7	20	0	Effect of mixing aged material (RAP) with new material for a new road
8	40	0	
9	60	0	
10	80	0	
11	100	0	

6.2.2 Bitumen Rheology

Changes in rheology due to ageing or RAP incorporation have been studied by recovering the binder of test samples after compaction and after being subjected to the corresponding ageing process. The bitumen was tested using a dynamic shear rheometer, shown in Section 3.4.7.

The results obtained from this test were the complex viscosity (η^*) and complex modulus (G^*) for each frequency and temperature. Using the principle of time-temperature superposition, the so-called master curves could be constructed.

6.2.3 Testing of Asphalt Self-Healing

Following the healing process described in Section 3.4.1, the healing properties were assessed using the induction heating method (times ranged from 30s to 180s). The temperature of the samples was monitored during induction heating by using an infrared camera, Section 3.4.2. The healing

ratio (HR) was calculated giving an idea of the percentage of initial strength that was recovered by the application of the healing process.

6.3 Theoretical Framework

Although the same induction energy is applied for the same time to different samples, they do not always heat in the same way, as factors such as fibres and air voids distribution vary from one sample to another. For this reason, it is not totally accurate to simply correlate the observed healing level to the heating time. The concept of Healing Energy (τ) was developed, obtaining a parameter that depends on both heating time and the temperature reached, described in details in Section 3.53.5. This model was used to fit the experimental data and simplify the comparison between different materials. Figure 6-1 shows, as an example, the case of model fitting to experimental results obtained for the mix aged in an oven at 85°C for 3 days. The same procedure was followed for the rest of the cases.

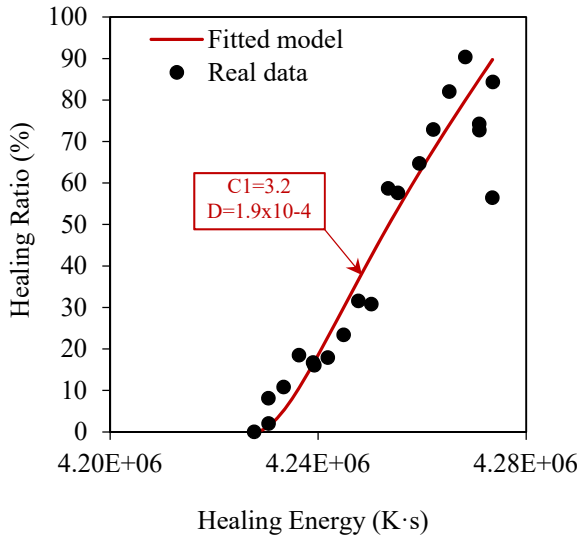

Figure 6-1 Example of model fitting to real data
Case of samples aged in an oven at 85ºC for 3 days

6.4 Results and Discussion

6.4.1 Rheology of Recovered Bitumen

The rheology of bitumen recovered from asphalt samples aged for 0, 3, 6, 9, 12 and 15 days, as well as from samples including 0%, 20%, 40%, 60%, 80% and 100% of RAP was studied through dynamic modulus tests and the representation of resulting master curves (Figure 6-2). As can be seen, both ageing and RAP addition increase the stiffness at low reduced frequencies, while the asymptotic value at high frequencies (known as Glassy Modulus, G_g) remains invariable. In order to study this change in the shape of master curves, and based on the Christensen-Anderson (CA) model, the crossover frequency was defined as the frequency in a master curve at which the phase angle is equal to 45º. Then, the R-value, the log distance between the glassy modulus and the dynamic modulus measured at the crossover frequency, was obtained. In general, for non-modified binders, the R-value increases and crossover frequency decreases after ageing (Rowe et al., 2016). Hence, when both parameters are represented together, the effect of ageing can be identified by a characteristic shifting of data downwards to the right.

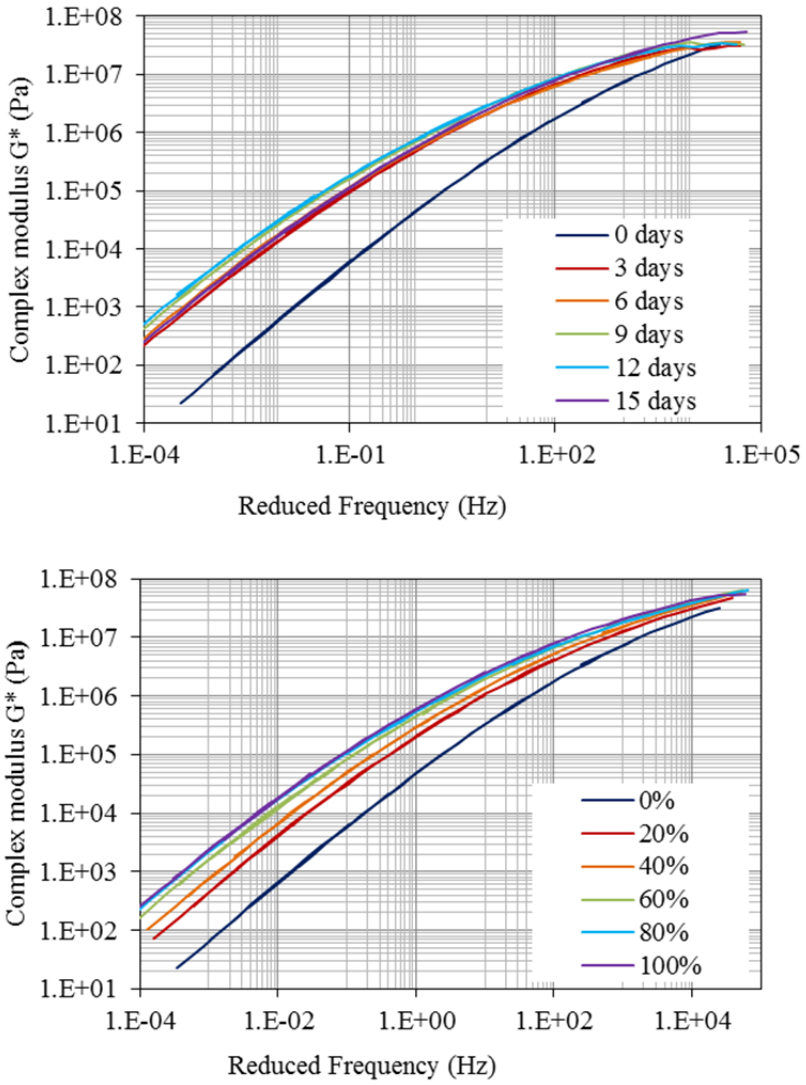

Figure 6-2 Master curves obtained for bitumen recovered from asphalt samples
aged for different times (top)
and containing different RAP percentages (bottom)

As can be seen in the R-value vs. crossover frequency diagram (Figure 6-3), the results follow the mentioned trend downwards to the right, giving evidence of the significant ageing of the binder. In addition, it is noticeable that all the points are significantly separated from the control mix, which indicates that just 20% RAP content, or 3 days ageing in an oven are enough to produce a great effect on results. After these values, the points tend to progressively get closer, the effect of ageing being less

noticeable. In addition, the effect of adding RAP seems weaker, as 80% RAP addition is equivalent to around 3 ageing days in an oven at 85ºC.

The stiffening of bitumen and the reduction of its viscosity makes its flow through cracks and air cavities more difficult, unless greater energy is applied. As a consequence, it can be expected that, as long as ageing and RAP content increase in the mix, healing performance decreases.

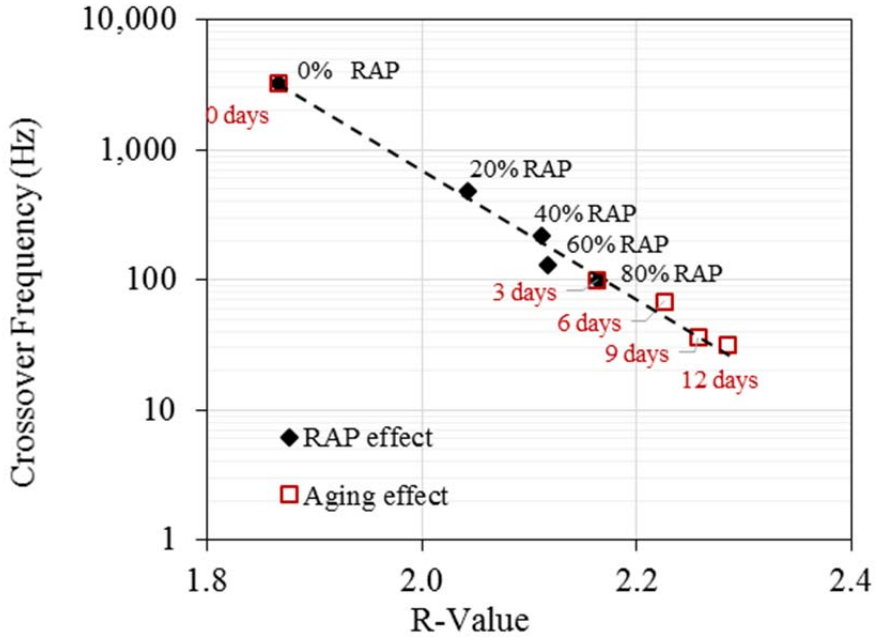

Figure 6-3 R-value versus crossover frequency for bitumen recovered from asphalt samples
aged for different times (red)
and containing different RAP percentages (black)

6.4.2 Compaction Level of Mixes

The previously mentioned stiffening of binder can produce increases in mix viscosities, the mixing and compaction operations being more difficult. As a consequence, samples might be manufactured with increasing air voids content as long as the ageing or RAP content increase. In order to evaluate this, densities of the studied samples were obtained (Figure 6-4) and, as can be clearly observed, there is indeed an inverse correlation

between the ageing level of the material and its density. In this case, the effect of adding RAP is again less severe (lower density reduction) and the mix with 80% RAP content produced densities similar to the mix aged for 3 days. How this might affect healing performance is discussed in Section 6.4.4.

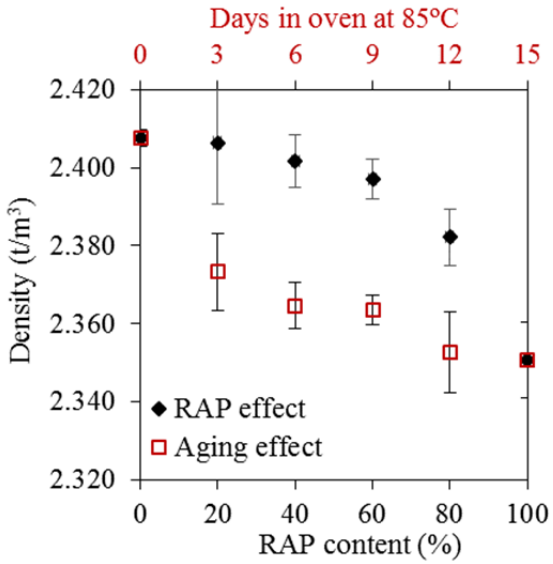

Figure 6-4 Effect of ageing time and RAP content on density of compacted samples

6.4.3 Effect of Ageing and RAP Content on Healing Performance of Asphalt Mixes

In Figure 6-5, the relationship between healing ratios and healing energy is shown for samples previously aged in an oven for different times (0, 3, 6, 9, 12 and 15 days) and manufactured with different RAP contents (0%, 20%, 40%, 60%, 80% and 100%). It is known that, the viscosity of bitumen decreases, and thermal expansion increases, when healing energy is applied (Gomez-Meijide et al., 2016). This supports the observations

reflected in Figure 6-5, where the healing ratios increased following a quasi-linear trend in both cases. In Table 6-2, the following parameters that define these curves are summarised:

1. Critical energy defined as the minimum energy at which the obtained healing ratio is different to zero.
2. Healing level obtained for the reference healing energy of $4.26*10^6$ K.s.
3. After fitting the model described in Equations 3.20 to 3.22 to experimental results, parameters C1/Fi and D could be obtained, giving an idea about the maximum healing ratio that can be achieved and how fast it can be reached (slope of the curves).

6.4.3.1 Effect of ageing on self-healing properties of hot mix asphalt

As can be seen in Figure 6-5 (top) and Table 6-2 (top), the critical energy was very similar for all the samples (circa $4.23*10^6$K.s) but still with a slightly increasing trend depending on the ageing degree, hence, 0.1% more energy was required for the samples aged for 12days than for those not aged. The slopes of the curves also depended significantly on the ageing degree of the material. As a consequence, the healing level obtained for the reference healing energy of $4.26*10^6$K.s also decreased with ageing, from 66.7% (samples with fresh bitumen) to 22.6% after 9 ageing days. After this time, results seem to stabilise around 20%, which would indicate that a residual minimum healing is always achievable, independent of the ageing degree.

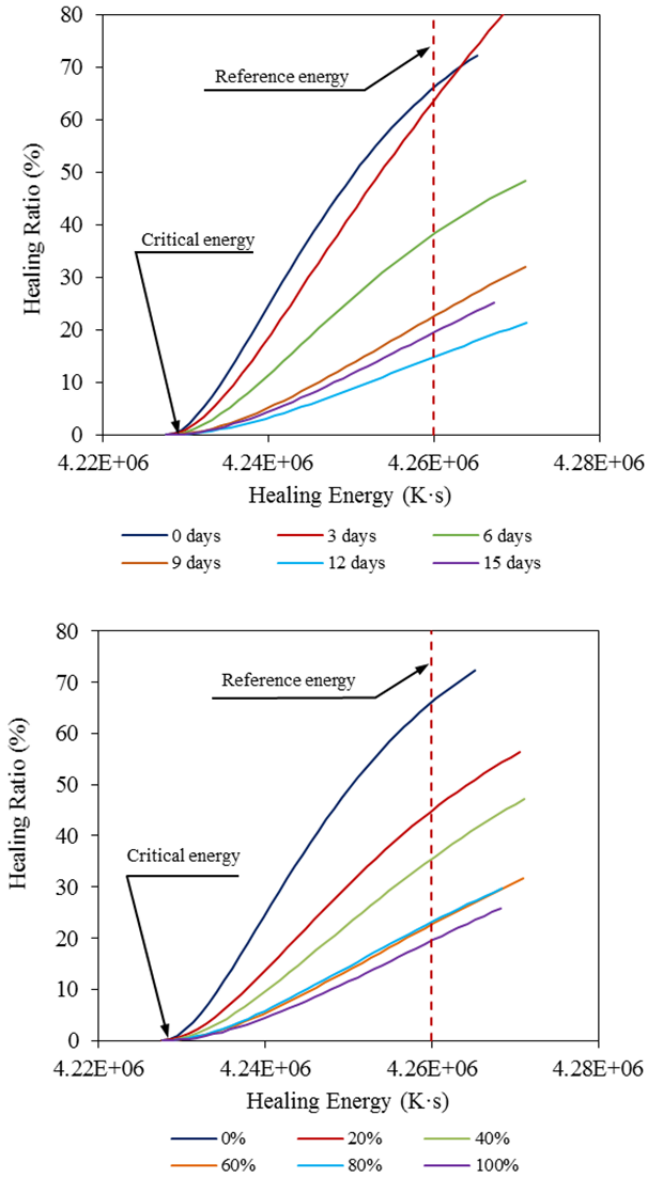

Figure 6-5 Evolution of healing ratio with the healing energy for samples
aged over different times in an oven at 85ºC (top)
and manufactured with different RAP contents (bottom)

Table 6-2 Healing results for samples
Aged for different times in an oven at 85ºC (top)
and manufactured with different RAP contents (bottom)

Ageing	Critical energy (K.s)	Healing for $42.6*10^6$ K.s	C_1/F_i	D
0 days	4229490	66.7%	0.907	1.19E-04
3 days	4230006	65.5%	0.775	1.09E-04
6 days	4230687	38.3%	0.674	0.87E-04
9 days	4232605	22.6%	0.711	0.51E-04
12 days	4233984	14.8%	0.517	0.48E-04
15 days	4233082	19.5%	0.654	0.49E-04

RAP content	Critical energy (K.s)	Healing for $42.6*10^6$ K.s	C1/Fi	D
0%	4229490	66.7%	0.907	1.19E-04
20%	4230289	46.0%	0.790	0.87E-04
40%	4231107	35.6%	0.762	0.71E-04
60%	4232499	22.7%	0.642	0.56E-04
80%	4232220	23.2%	0.573	0.63E-04
100%	4233082	19.5%	0.654	0.49E-04

The C1/Fi–value is close to 1 when the mix was not aged, meaning that almost 100% of initial strength can be achieved if enough energy is applied. However, as long as ageing increases, C1/Fi decreases to values close to 60%. In other words, the maximum achievable healing reduces, no matter the amount of energy that is applied. A similar trend was found for the D-parameter. Hence, increases in ageing time produce strong decreases in the slope of the curve (D-value after 9 days is 57% lower than control non-aged mixes). This means that the process is slower, and it needs more energy to reach a desired healing level.

Both previous considerations indicate that ageing not only reduces the maximum healing that can be achieved, but also increases the amount of energy necessary to reach it. In other words, the process not only becomes less effective but also less energy efficient, the ageing process develops with time. This agrees with previous research, such as Bhasin et al. (2011), in which the authors observed that the ageing reduces the healing potential of asphalt mixtures, as asphalt molecules becomes further oxidized and less active to heal the microcracks. Other authors, such as Shen and Sutharsan (2011) go even further stating that low temperature, high loading frequency, and the effect of ageing, or the combination of these factors can result in a negligible healing effect.

6.4.3.2 Effect of RAP content on self-healing properties of hot mix asphalt

The same analytical procedure applied in the previous section was used to evaluate the effect of introducing different amounts of RAP (0%, 20%, 40%, 60%, 80% and 100%) on the healing capacity of resulting asphalt mixes (Figure 6-5 (bottom) and Table 6-2 (bottom)). In this case, the critical energy for all the samples was also very similar and close to $4.23*10^6$K.s, although again, an increasing trend could be observed (0.1% higher with 100% RAP content than with 0%). Furthermore, for the same healing energy of $4.26*10^6$K.s, the obtained healing ratios decrease as the RAP content increases, from 66.7% in control samples to values close to 20% for contents higher than 60%. As previously observed, the decreasing trend seems to stabilise around 20%. This reinforces the idea of a minimum residual healing that can always be obtained independently from the ageing level of the material.

Again, a decreasing trend was observed in C1/Fi (from higher than 90% to values close to 60% with 100% of RAP) and D-values (53% lower with 60% of RAP than with 0%). Following the same reasoning as for the previous case, it can be concluded that the maximum achievable healing is reduced as the RAP content increases, while the energy needed to reach it increases. Therefore, the same conclusion as for the previous case can be obtained for mixes with RAP, that RAP content reduces both effectiveness and energy efficiency of healing processes in asphalt mixtures. This also agrees with previous research, such as Dinh et al. (2018) in which the authors also shared that the presence of RAP in asphalt mixes containing

6% steel wool fibres causes the ineffectiveness of induction healing treatments.

6.4.3.3 Comparison between ageing and RAP effects

Figure 6-6 shows the relationships between the parameters considered in this investigation and both ageing days and RAP content. It must be noticed that the point of zero ageing days and 0% of RAP, which corresponds to a control mix, is the same. Also, the points corresponding to 15 ageing days and 100% RAP content are the same, as the RAP was aged for 15 days.

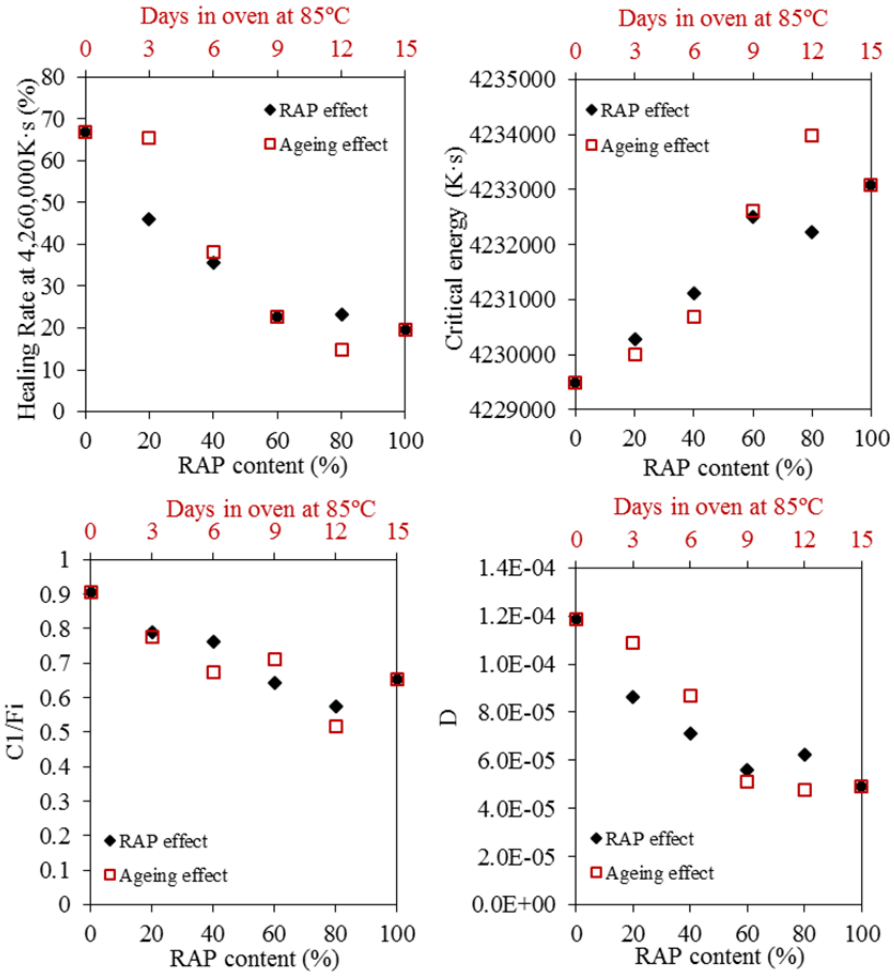

Figure 6-6 Characteristic parameters of healing performance Correlated to ageing days in an oven at 85ºC and RAP content in mix.

As can be seen, the effects of ageing the material and adding RAP to the mix are practically the same for the studied parameters. Thus, an empirical correlation between both factors could be obtained to estimate the equivalent ageing (EA) in an oven at 85ºC to that produced by introducing, into the mix, a given RAP content (RC):

$$EA(days) = 0.15\ RC\% \qquad 6.1$$

In addition, both trends registered sharp decreases for RAP contents between 0% and 60%, and 0 and 9days. However, once such values were reached, the performance reduction became significantly less pronounced indicating that a minimum healing can always be expected in both cases.

6.4.4 Effect of Compaction Level on Healing Properties

It was seen in Section 6.4.2 that the compaction level of samples reduces when ageing or RAP content is increased. As this can produce distortions in previous healing results, the correlation between compaction level and healing performance was obtained by manufacturing 5 new series of samples, all of them with fresh binder but compacted with different numbers of passes of the roller compactor. Thus, samples with 5 different air voids contents were obtained: 0.5%, 4.5%, 13.2%, 20.4% and 26.5%. Within each series, each sample was subjected to a different healing energy, obtaining 5 new healing-energy curves (Figure 6-7).

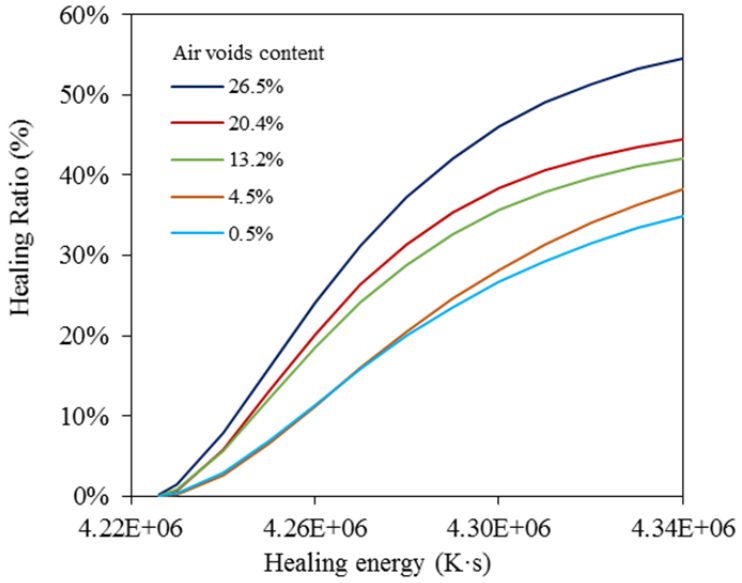

Figure 6-7 Effect of compaction (air void) on the healing energy.

Results showed that increases in air voids contents reduce the healing- energy and increase the D-parameter (greater efficiency). At the same time, the maximum healing level that can be obtained also increased (greater effectiveness). In essence, higher air voids contents do not worsen healing results. Quite the opposite, they improve them. It must be noticed that this does not mean that samples with lower compaction resist higher loads, but they can recover a greater percentage of their initial strength. As can be seen in Table 6-3, the strength is 73.1% higher for samples with 0.5% air voids than with 26.5%.

Table 6-3 Initial strength and maximum healing obtained for samples with different compaction

Air voids content	Initial strength (kN)	Maximum healing (%)
0.5%	6.867	32.5%
4.5%	5.684	42.2%
13.2%	5.524	40.2%
20.4%	4.931	45.5%
26.5%	3.966	48.3%

The researcher believes that porous mixes are easier to heal, as cracks tend to occur through the bitumen/mastic placed in the contact points between aggregate particles. On the contrary, in dense mixes, the higher level of packing makes cracks more likely to happen through aggregate particles (Figure 6-8). Although these cracks can be filled by expanding bitumen during heating, the strength will never be the same as that obtained by non-cracked particles. In addition, the flow of bitumen through the interstitial pore network (which might include eventual cracks) is more difficult in dense mixes, as cavities have smaller average diameter and interconnectivity (Aboufoul and Garcia, 2017). This produces greater energy dissipation by friction of bitumen against cavities/cracks' interior surfaces (Garcia et al., 2013) and reduces the healing capacity of the mix.

Since stiffer bitumen produced samples with greater air voids content, better results could be expected with aged bitumen. However, as seen in previous sections, experimental observations indicated quite the opposite. For this reason, it can be concluded that the detrimental effect of having an aged (stiffer) binder that needs to flow through pores and cavities is stronger than the beneficial effect of increasing air voids content. As a result, the effectiveness and energy efficiency of the healing treatments are reduced.

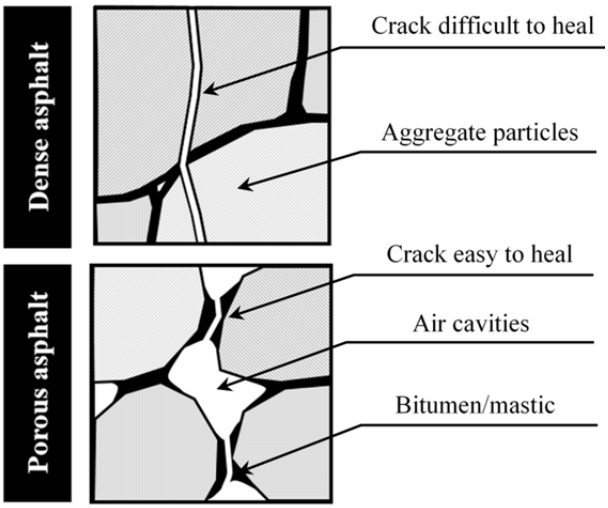

Figure 6-8 Schematic internal structure of asphalt mixes
Dense (top) and Porous mixes (bottom).

6.5 Summary

This chapter has described the hot mix aging and RAP effect on the self-healing abilities, taking into account the compaction level of the mixes. Chapter 7 will cover the effect of using 5 types of virgin bitumen on the self-healing from mechanical, rheological and chemical points view.

Chapter 7: **Mechanical, Rheological and Chemical Binder Properties Effect on the Self-Healing of Asphalt Mixes**

7.1 Introduction

It is known that the main factors affecting this technology are the heating time and temperature reached (Moreno-Navarro and Rubio-Gámez, 2016, Gomez-Meijide et al., 2016, Moreno-Navarro et al., 2017), as well as the air voids content in the asphalt mix (Salih et al., 2018). However, it is not clear yet how the intrinsic properties of bitumen affect the healing performance of the mix when subjected to electromagnetic induction. This chapter aims at finding how far the fact of choosing a specific type of bitumen can improve the capability of asphalt mixtures to self-heal.

With this purpose, asphalt samples were manufactured with five different types of bitumen, from different sources and with different penetration grades, covering the conventional range of binders that are normally used in Europe. For each binder, mechanical, rheological, compositional and thermal properties were obtained and correlated through statistical analysis to the healing performance of asphalt beams made with them.

7.2 Procedure

7.2.1 Materials and Test Specimens

In this investigation, 5 different bitumens were used from different sources and pen grades. The hot-mix asphalt samples for induction self-

healing were manufactured using limestone natural aggregate, with continuous and dense gradation. The target air voids content was set to 4.5%. The binder content was fixed at 4.7%. Finally, the conductive particles used for induction heating were steel grit, as shown in Section 3.2. Metal grit was introduced in the mix by replacing the same volume of the natural aggregate in this fraction. The volumetric content of metal grit in the mix was fixed at 4%, corresponding to 11.2% by weight. Asphalt mixture was mixed in the laboratory and 150x70x50 mm^3 prismatic samples (beams) were used, as described in Section 3.3.

7.2.2 Testing of Asphalt Self-Healing Properties

Asphalt self-healing was assessed through a 3-step test using the induction heating method for times that ranged between 15s and 240s. During the process, the surface temperature of the test samples was constantly monitored by using a full colour infrared camera and the healing ratios were calculated, as described in Sections 3.4.1and 3.4.2.

7.2.3 Testing Binder Properties

7.2.3.1 Bitumen rheology

The rheology of the 5 types of bitumen was studied following the procedure in Section 3.4.7. The complex viscosity (η*) and complex modulus (G*) for each frequency and temperature obtained by this test were used to construct the master curves, using the principle of time-temperature superposition, fixing a reference temperature (in this case 40ºC) and shifting

the data with respect to time until the curves merge into a single smooth function.

7.2.3.2 Determination of the generic composition of the bitumens

The composition of the bitumens was determined by performing SARA (saturates, asphaltenes, resins, aromatics) tests as shown in Section 3.4.8.

7.2.3.3 Asphalt mix thermal expansion

The thermal expansion for the 5 types of bitumen was tested by using a Thermomechanical Analyser instrument (Q400 TMA), see Section 3.4.9. The samples were prepared by mixing each binder with the same amount of 6 mm limestone gradation and dust to produce a mastic consistency mix. Three samples were tested for each bitumen and the average was taken to determine the coefficient of expansion and the melting point.

7.3 Theoretical Framework

7.3.1 Energy Needed for Healing

The healing process of cracked asphalt material occurs during the heating and the cooling period of the samples, as long as the temperature remains above a critical threshold. Moreover, the effectiveness of the healing process increases with the temperature and heating time. However, not all the samples reach the same temperature despite being heated for the same time. For this reason, and in order to better compare healing results, the concept of healing energy was used as defined in Section 3.5.1.

7.3.2 Asphalt self-healing theory

As noted in Section 3.5.2, the healing process of a cracked asphalt mixture starts when both faces are in contact and the bitumen starts to flow from the mix to fill the gap and heal it. The present chapter follows this theory. According to the model, the healing happens until equilibrium is reached between surface tension, hydrostatic pressure, gravity and energy dissipation due to friction. This model was fitted to the experimental data in order to better clarify the trends followed by the results.

7.4 Results and Discussion

7.4.1 Healing Properties

Figure 7-1 shows the experimental results of healing ratio obtained when different healing energies (as described in Section 7.3 theoretical framework) are applied. Moreover, the model given by Equations 3.20 to 3.22 was fitted to experimental data by using Excel's Optimization Solver function by minimising the squared error between the model and the experimental values. The fitted parameters C1/Fi and D are shown in Table 7-1. The fact that all types of bitumen obtained C1/Fi higher than 0.9 gives an idea that healing ratios higher than 90% can be expected if enough healing energy is applied.

The actual estimation, given by the top horizontal asymptote is also included in Table 7-1, all being very close to 100%. As an exception, bitumen Total 70/100 obtained a maximum healing slightly lower (90.0%) but also the highest D-value, which indicates that such a maximum is

expected to be reached with lower healing energy. In other words, this binder is less effective but also more energy efficient.

These maximum values are expected when a great amount of energy is applied. However, in order to compare the binders' performance within the range of operational healing energy, the healing ratio after 4.3MK·s was also included in this study. Such healing energy corresponds to circa 150s heating under the described test conditions, although it depends on the temperature that the samples actually reach. As can be seen, the values are ranked between 46% and 56% and bitumen Total 70/100 obtained one of the highest values, due to the greater D-value (slope of the curve). As this is paradoxical with respect to the explanations given in the previous paragraph about the maximum healing (asymptote), only the criteria of healing ratio after 4.3MK·s will be considered from this point on, as it is more realistic.

Results also show a direct correlation between healing energy and healing ratio. Thus, the healing performance can be improved by increasing the applied energy, which means not necessarily increasing the heating time. This could be also achieved by increasing the induction power (for the present research 80A were used in a device with maximum capacity 450A).

Taking into account the overall results, it could be stated that the most advisable bitumen in terms of healing performance is the Shell 50/70, as it: (1) presented one of the lowest critical energies; (2) obtained the highest healing results for the range of operational healing energies (around 4.3MK·s); and (3) offers practically 100% healing if enough energy is applied.

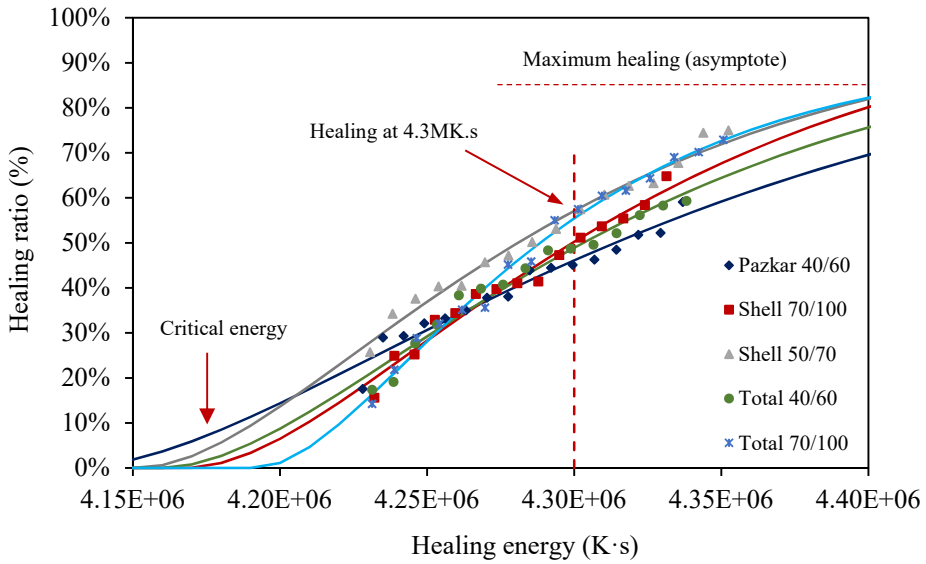

Figure 7-1 Relationship between the healing ratio and the healing energy and fitting of the model to the experimental data for 5 types of bitumen.

Table 7-1 Healing results obtained with different binders

Binder property	Pazkar 40/60	Total 40/60	Shell 50/70	Shell 70/100	Total 70/100
C_1/F_i	0.999	0.988	1.001	1.051	0.926
D	$1.3 \cdot 10^{-05}$	$1.7 \cdot 10^{-05}$	$1.9 \cdot 10^{-05}$	$1.8 \cdot 10^{-05}$	$2.7 \cdot 10^{-05}$
Maximum healing (%)	99.9%	96.7%	97.1%	103.9%	90.0%
Healing ratio after 4.3 MK·s	46.1%	47.9%	55.5%	50.2%	53.9%
Critical energy (MK·s)	4.15	4.18	4.17	4.18	4.20

7.4.2 Binder Properties

7.4.2.1 Rheology properties

In order to quantify both elastic and viscous properties of the five studied bitumens, DSR tests were performed obtaining the complex shear modulus (G*), which can be considered the sample's total resistance to deformation when repeatedly sheared. Also the phase angle (δ), or lag between the applied shear stress and the resulting shear strain, was obtained.

In general terms, a larger phase angle, means that the material behaves more as a viscous fluid, instead of an elastic solid.

Figure 7-2 shows the obtained master curves, as well as the curves of phase angle vs. reduced frequency. As can be seen, although the rheology of the five types of bitumen is very similar, stiffness tends to decrease and the phase angle increase with higher penetration grades (coefficient of linear correlation found $R^2 = 0.781$). The correlation with healing properties will be presented within the Discussion section.

In addition, Figure 7-3 shows the temperature dependency of the five binders by means of isochronal plots of complex modulus (G*) and phase angle (δ) versus temperature at a reference frequency of 1.58Hz. The results show that, as expected, increases in temperature reduce binder stiffness and enhance the viscous behaviour. However, they also show a shift (crossing of curves) in complex modulus and phase angle curves for bitumen Pazkar 40/60 at a temperature between 35ºC and 40ºC. For higher temperatures, this bitumen reaches higher stiffness than expected compared to other bitumens with similar penetration, such as Total 40/60 and Shell 50/70. It was checked that this range of temperatures (35ºC-40ºC) was reached after applying around 4.26MK·s. As can be seen in Figure 7-3, at that point, the curve corresponding to Pazkar 40/60 also crosses the other curves, passing from a better to a worse healing behaviour. It is not clear what produced this behaviour in bitumen Pazkar 40/60, but it seems clear that the fact of increasing its stiffness produced a reduction in healing performance.

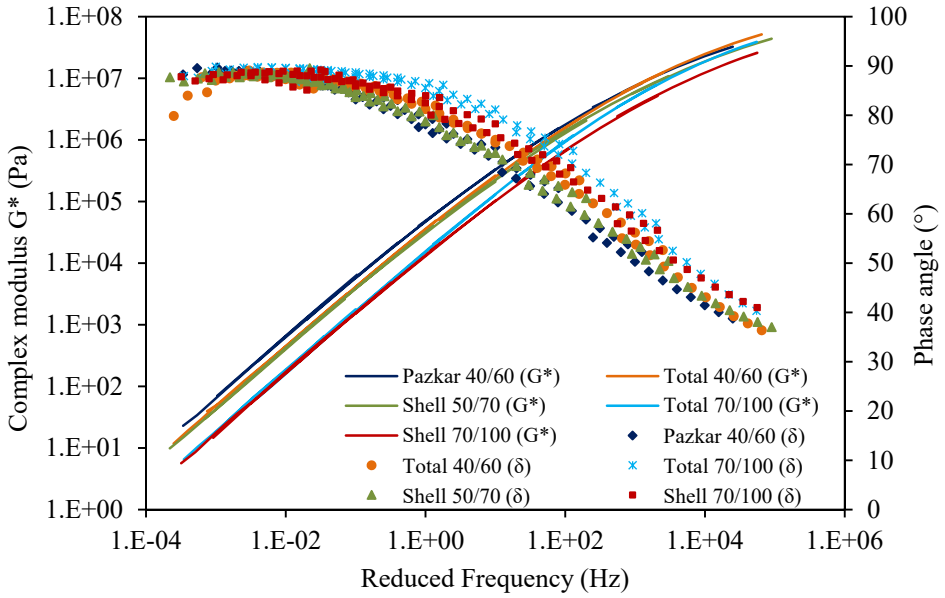

Figure 7-2 Master curve for the five types of binders-Frequency.

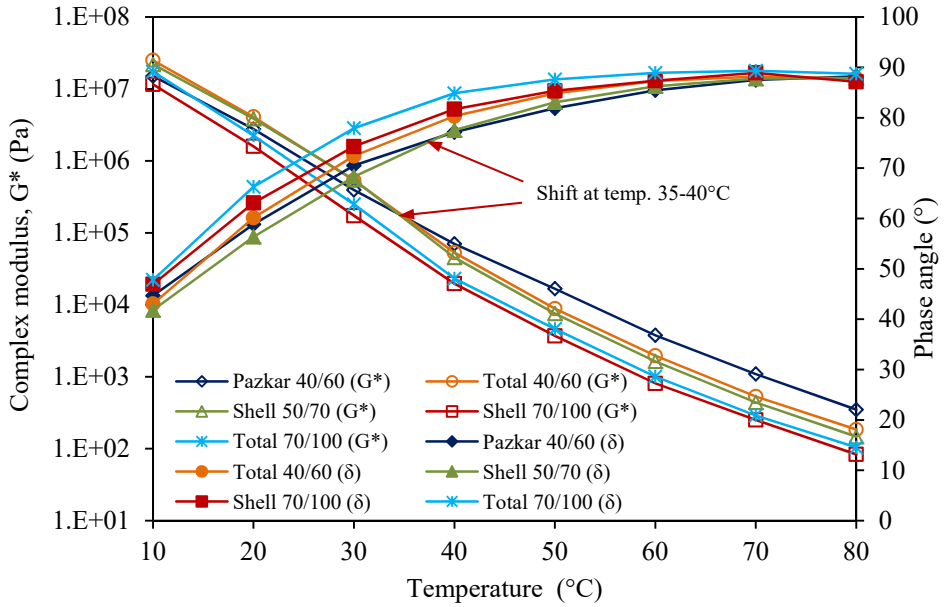

Figure 7-3 Master curve for the five types of binders-Temperature.

7.4.2.2 Composition

The generic composition of all five paving grade bitumens was determined by separating SARA fractions: Saturates, Aromatics, Resins and Asphaltenes. Results are expressed for each fraction as a percentage of the

total of all four SARA fractions. As the test was carried out by using multiple chromarods in parallel, results were calculated as the average value of eight individual measurements. It can be said that the precision of the measurements is very good as the standard deviations determined allow calculating relative errors for individual SARA fractions below 5%. This latter value is in line with test results obtained previously at BRRC for paving grade binders of the classes 35/50, 50/70 and 160/220.

These results were also used to calculate the colloidal stability index I_c as introduced by Gaestel et al. (Le Guern et al., 2010, Paliukaite et al., 2014) to describe the behaviour of bitumens in terms of their 'sol'-'gel' structure:

$$I_c = \frac{(Asphaltenes + Saturates)}{(Aromatics + Resins)} \qquad 7.1$$

Bitumens characterised by a 'gel' structure produce a higher I_c value, in general, for road bitumens, ranging between 0.2 and 0.5. A summary of the results obtained for the five bitumens considered in the present study is also included in Table 7-2.

Table 7-2 Overview of SARA fractions

Content	Pazkar 40/60	Shell 70/100	Shell 50/70	Total 40/60	Total 70/100
Asphaltenes	15.8% ± 0.4%	13.7% ± 0.3%	15.8% ± 0.6%	15.5% ± 0.6%	11.0% ± 0.4%
Resins	35.6% ± 1.3%	37.7% ± 2.0%	35.9% ± 1.3%	36.1% ± 1.5%	33.1% ± 1.6%
Aromatics	41.8% ± 1.4%	43.3% ± 1.8%	43.2% ± 1.5%	43.3% ± 1.8%	51.1% ± 2.1%
Saturates	4.9% ± 0.2%	5.3% ± 0.2%	4.7% ± 0.2%	4.9% ± 0.2%	4.1% ± 0.2%
Ic Index	0.267 ± 0.017	0.235 ± 0.017	0.259 ± 0.019	0.257 ± 0.021	0.179 ± 0.015

In general, it can be noticed that the generic composition of all bitumens is very similar, with the exception of bitumen Total 70/100, which has a lower asphaltene content (27.6% lower than the average of the rest of

the bitumens) and a higher aromatics content (19.1% higher). These contents are consequently reflected in an Ic index of 0.179 ± 0.015, 29.7% lower than the average of the others, which indicates that bitumen Total 70/100 is softer (more 'sol' like) than the other four bitumens. As this type of bitumen also gave lower healing results, the presence of asphaltenes and aromatics might cause a significant impact on bitumen performance, but this kind of correlation analysis between bitumen properties and healing parameters will be tackled in Section 7.5.

7.4.2.3 Thermal expansion

Results of thermal expansion with test temperature can be seen in Figure 7-4 for the five types of bitumen studied. As can be seen, all curves can be divided into 4 stages depending on their slope. During the first stage, the slope of the curve increases with temperature, while during the second stage the slope remains quasi-steady. The slope in this quasi-linear part is directly related to the coefficient of thermal expansion. In the third phase, the slope reduces again until the maximum thermal expansion is reached. From this point onwards, the consistency of the mix reduces and the height decreases again, producing in the curves a negative slope. The temperature at which this point is produced is also known here as the melting point. Both the thermal expansion and melting point are represented in Figure 7-4.

A statistical linear regression analysis was undertaken showing that, indeed, the linear correlation between both parameters is weak, with an obtained R^2 = 0.680. The penetration grade of bitumen is not better correlated either to the thermal expansion (R^2 = 0.069) or to the melting point (R^2 = 0.403). In fact, as can be seen in Figure 7-4 and Figure 7-5, the

maximum thermal expansion was achieved by bitumens from different sources and very different penetration grades (Shell 70/100 and Total 40/60).

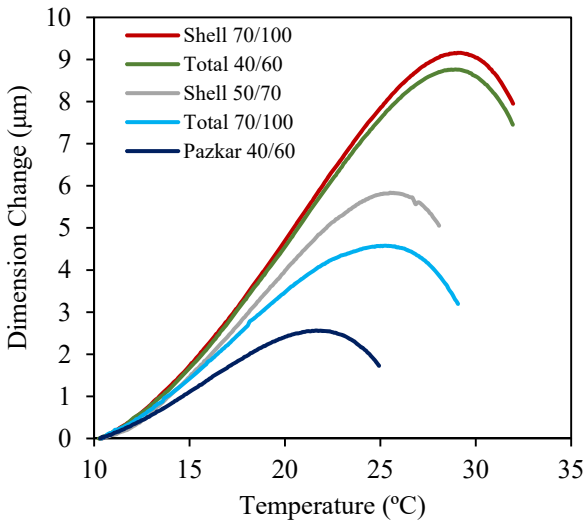

Figure 7-4 Thermal expansion curves for the five binders-fines mastic.

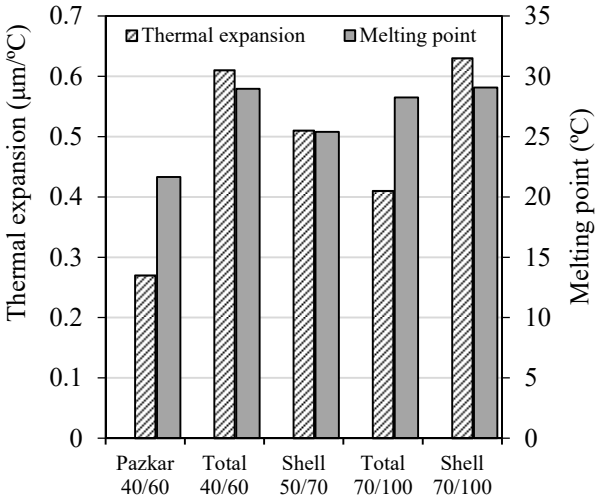

Figure 7-5 Thermal expansion and melting point of the studied bitumens-fines mastic.

7.5 Discussion

A Pearson's statistical analysis was carried out correlating previous results with the following healing parameters: critical energy, healing obtained when a healing energy of 4.3MK·s is applied, and model fitting parameters C1/Fi and D. The R^2-parameters of linear correlation can be seen in Table 7-3.

Table 7-3 Correlation coefficient R^2 between binder properties and healing parameters

Binder property	Critical energy	Healing 4.3 MK·s	C_1/F_i	D
Type of bitumen				
- Pen grade	0.618	0.192	0.027	0.542
Rheology				
- Complex modulus	0.303	0.321	0.035	0.270
- Phase angle	0.868	0.192	0.255	0.8012
- Viscosity	0.481	0.451	0.004	0.508
Composition				
- Asphaltenes cont.	0.687	0.169	0.299	0.766
- Resins cont.	0.183	0.117	0.953	0.497
- Aromatics cont.	0.703	0.284	0.648	0.926
- Saturates cont.	0.265	0.284	0.927	0.627
- Gaestel Index I_c	0.737	0.237	0.401	0.864
Thermal properties				
- CTE*	0.189	0.037	0.183	0.005
- Melting point	0.712	0.085	0.002	0.289

*CTE: Coefficient of Thermal Expansion

The penetration grade did not significantly correlate with any of the healing parameters considered ($R^2 < 0.9$), especially those which define the healing effectiveness ($R^2 = 0.192$ and $R^2 = 0.027$ for healing after 4.3MK·s and C1/Fi respectively). Although seeing Figure 7-6 (top), it might seem the correlation level is high, from a statistical point of view, this correlation also was non-significant ($R^2 = 0.618$).

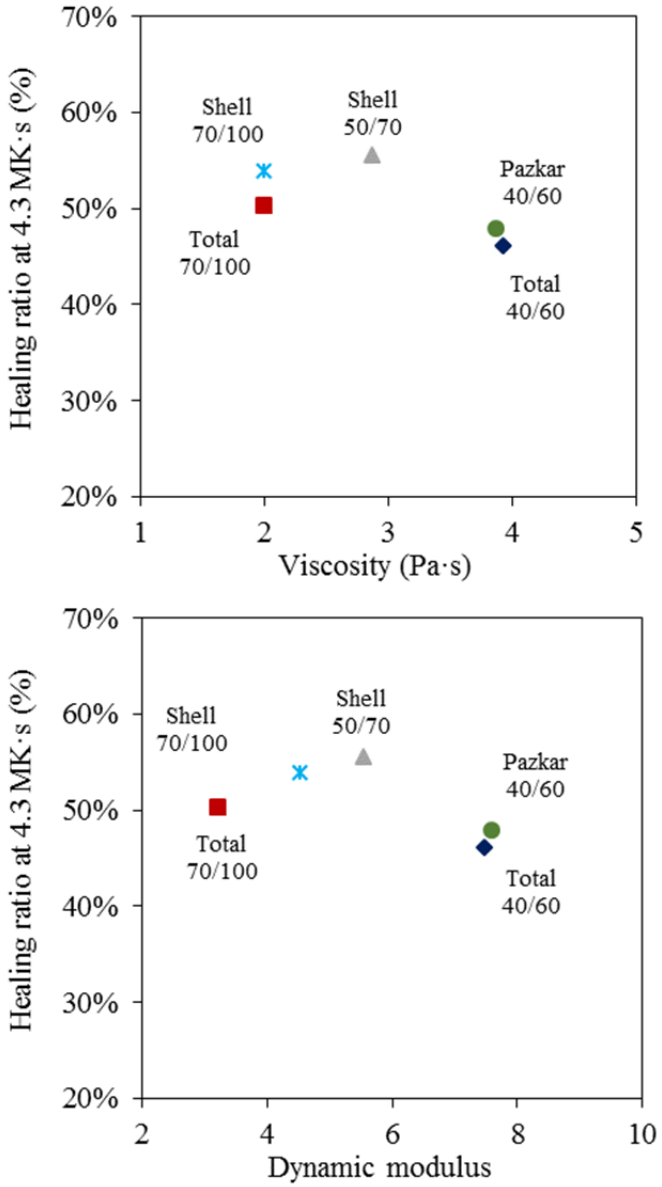

Figure 7-6 Correlation between penetration grade and critical energy (top) and maximum healing ratio (bottom).

Regarding rheology properties, all the bitumens again performed very similarly although, in general, a higher penetration grade leads to a higher phase angle and lower stiffness. For the statistical Pearson's correlation analysis, the reference values considered were the dynamic modulus and phase angle at a reduced frequency of 103Hz, as well as the viscosity at 80ºC. As can be seen in Table 7-3, none of them produced a significant effect on the healing capacity of the binders (R^2<0.9). Therefore,

it can be stated that the rheology of the binder does not significantly affect the healing performance of the mix.

In terms of composition, it can be seen how, in general, no strong correlations were found. As exceptions, it can be seen that the contents of Resins and Saturates tend to improve the effectiveness of the expected healing process when great healing energy is applied (higher C1/Fi), but not for the operational range of energy considered in this research (for energy around 4.3MK.s). Also it seems that the content of Aromatics tends to increase the efficiency of the process, as it is correlated to the D-parameter (R^2=0.926). However, there is a certain correlation between D and the critical energy (R^2=0.8113) which means that the higher D is, also the higher the critical energy. As a consequence, curves resulting in a higher slope (higher D) will also tend to present higher critical energy. In other words, it cannot be stated that the process is actually more energy-efficient.

Finally the coefficient of thermal expansion and the melting point are not linearly correlated to the type of bitumen (R^2=0.692 and R^2=0.403), nor to the healing properties (R^2<0.9).

Although previous analysis showed that there is practically no linear correlation between bitumen properties and healing parameters, it was found that some properties do present non-linear correlations. These properties are coefficient of thermal expansion, viscosity and stiffness.

As can be seen in Figure 7-7, the relationship between the coefficient of thermal expansion and healing is not linear. On the contrary, the healing ratio reaches a maximum when the coefficient of thermal expansion becomes close to 0.5mm/ºC. This supports the hypothesis raised

in previous publications (Garcia et al., 2012, Salih et al., 2018), as it might indicate that binders with too low a thermal expansion would result in poor healing performance, as the cracks cannot become completely filled. On the other hand, if the expansion is too high, the flow of bitumen could exceed the flow capacity of the internal pore network (especially in dense mixtures, as is the case in the present study), increasing internal pressure and consequently the interstitial space between aggregate particles. As a result, the samples get damaged and the healing results reduce again.

In addition, viscosity and stiffness are linearly correlated (R^2=0.938), which means that bitumens with high viscosity also present high stiffness. The author believes that when these parameters are too high, the healing cannot be effective as it is very difficult to move the bitumen through the cracks. On the contrary, when they are too low, the flow of bitumen is easier but the strength of the repaired crack is also lower. As a consequence, there is an intermediate point where the healing is optimum. In this case (Figure 7-8), it happens when the viscosity is close to 3Pa.s and the dynamic modulus is close to 5.5MPa.

In Section 7.4.1, and taking into account the overall results presented in Figure 7-1, it was advanced that the most advisable bitumen in terms of healing performance was the Shell 50/70, as it: (1) presented one of the lowest critical energies; (2) obtained the highest healing results for the range of operational healing energies (around 4.3MK.s); and (3) offers practically 100% healing if enough energy is applied. As can be seen now in Figure 7-7 and Figure 7-8, this bitumen is the one whose coefficient of thermal

expansion, stiffness and viscosity are also optimum, reinforcing the previous explanation.

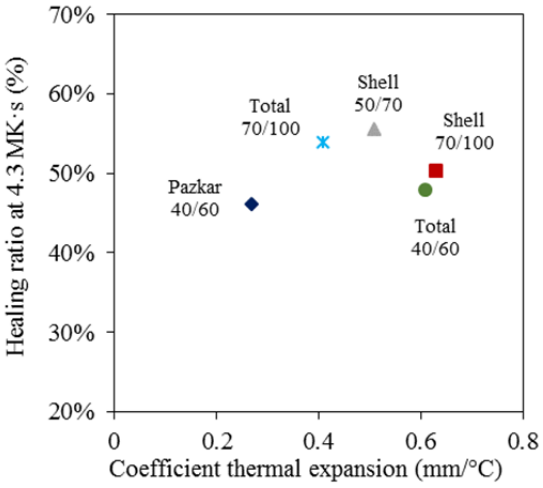

Figure 7-7 Correlation between coefficient of thermal expansion and healing ratio at 4.3MK·s.

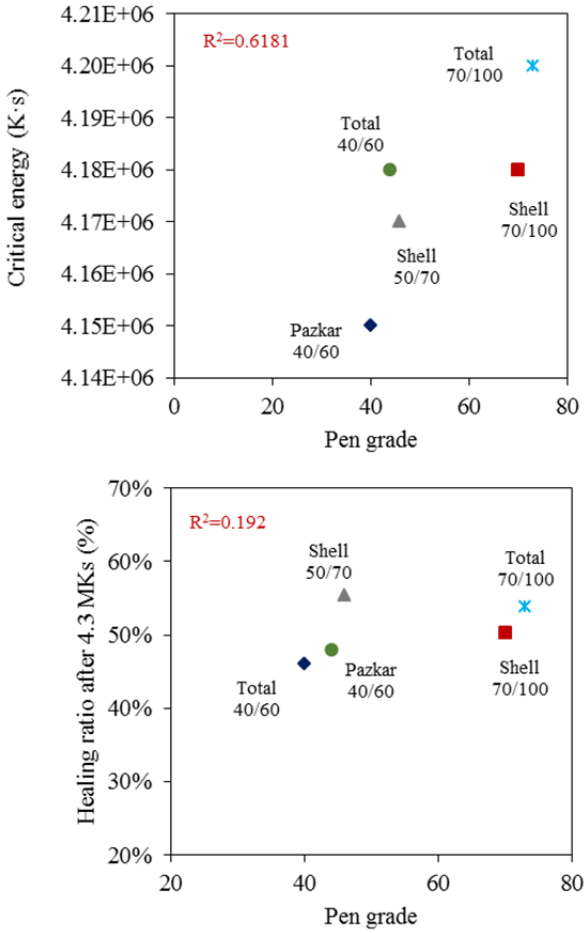

Figure 7-8 Correlation between viscosity (top) and stiffness (bottom) and healing ratio after 4.3MK·s.

7.6 Summary

This chapter has discussed the effect of using 5 types of virgin bitumen on the self-healing from mechanical, rheological and chemical points view. The following chapter will deal with the conclusions and recommendations, as well as with some proposals for future research, which are extracted from the present thesis.

Chapter 8: **Conclusions and Recommendations**

8.1 Introduction

In this project, three self-healing aspect were investigated. First, comparing the effect of heat sources and intensity on the self-healing rate for different air voids HMA. Induction heating was compared against infrared heating which mimics the sun's radiation. Secondly, investigating the mechanical, volumetric, chemical and healing abilities of mixes containing recycled and commercial conductive particles. The evaluation includes the implementation abilities, performance and safety characteristics. Finally, the effect of bitumen properties was studied. The bitumen was investigated by two approaches, bitumen ageing and bitumen grade. The first approach was achieved by evaluating the healing performance of different stages and percentages of aged and RAP mixes. The second was achieved by studying the healing rates and rheological properties of different bitumen grades.

In the following sections, the main findings and conclusions are presented after the investigation and analysis conducted in this study:

8.2 Conclusions related to heat source and air voids

In Chapter 4 a comparison between two different methods to induce self-healing in asphalt mixture, induction and infrared heating, was performed. The materials used were asphalt mixture with 4.5%, 11% and 21% air voids content. Furthermore, in order to compare results between different types of asphalt mixture, temperatures were transformed into

energy. Moreover, results were interpreted in terms of surface tension, pressure, energy dissipation forces due to friction and thermal expansion. From this investigation, the following conclusions could be extracted:

1. The temperature increase rate of asphalt mixture exposed to induction heating was higher than the temperature increase rate of similar mixture exposed to infrared heating.
2. Asphalt mixture exposed to induction energy healed in seconds or minutes, while similar mixtures exposed to infrared heating needed several hours to obtain the same results.
3. The energy needed for healing cracks in asphalt mixture exposed to induction heating was lower than the energy needed in asphalt mixture exposed to infrared heating. The reason for this is that with the induction energy method, heat was directly applied into bitumen, while for the infrared method, aggregates also had to be heated.
4. When asphalt mixture was healed by the infrared method, the maximum healing level and total energy needed to reach that level were independent of the radiation intensity or heating rate, as long as the temperature of the mixture remained above a critical value.
5. The maximum healing level reached by asphalt mixture was always lower for dense asphalt than for asphalt mixtures with higher air voids content. The reason for this is that more aggregates tended to break during crack generation in dense mixtures. Cracks in aggregates can be filled by bitumen (partial healing) but not completely recovered.

6. When the steady state temperature is reached, the internal pressure is dissipated, bitumen tends to flow downwards and cracks re-open. As a consequence, the strength of the material reduces, and the air voids content of asphalt mixture increases in the upper parts of the test specimens.
7. It has been hypothesized that the (1) continuous thermal expansion and (2) viscosity reduction of bitumen during heating play a major role on asphalt self-healing. For this reason, to optimize asphalt self-healing, as important as increasing the temperature of asphalt mixture is considering the thermal expansion of the materials involved.

8.3 Conclusions related to the properties of mixes containing different conductive particles

From the study and discussion detailed through Chapter 5, the following conclusions could be obtained:

1. None of the studied fibres presented problems of homogeneity or segregation inside compacted asphalt mixes. However, shear and bending stress applied during manufacturing produced reductions in shavings and steel wool size.
2. Asphalt density increased with the amount of metal particles, independently of their type. However, the air voids content remained practically constant for the studied contents and types of metal particles.

3. None of the studied fibres produced environmental issues resulting from hazardous leaching.
4. Both indirect tensile strength (ITS) and stiffness tend to slightly improve by adding metal particles to the mix. The addition of steel grit significantly improves ITS but reduces by around 13% the resistance to water damage, compared to control mixes without metal. It is hypothesised that its rounded shape works as a very strong aggregate in dry conditions but in the presence of water, the particle-binder adhesion can get strongly compromised.
5. The skid resistance and the resistance to abrasion met the values required by specifications with all the types of metal particles. However, as long as the size of the particles increase (wool-grit-shavings-tyre), the skid resistance tends to increase, while the resistance to abrasion tends to decrease.
6. For a given heating time, the fibres from old tyres increase the temperature of the samples up to 400% more than the rest of the fibres. This difference was not observed in the healing results due the configuration of healing tests. It is expected that when only microcracks are produced (i.e. real case of road subjected to fatigue damage) this type of fibre will produce healing rates significantly higher than those observed in the present research.
7. For the rest of metal particles, the healing ratio is proportional to their content and to the applied healing energy. Steel grit and wool produced healing results very similar and satisfactory, while the results obtained by the shavings were considerably lower.

8. The results from recycled fibres from old tyres showed them to be especially convenient for use in lower structural layers (base and sub-base), as they can enhance the mechanical performance and heat by induction even at greater distances from the induction coil. In addition, their high content of iron makes them susceptible to corrosion by oxidation in the presence of water, so encouraging their use in lower layers protected from water action. Finally, their use in the thickest road layers maximises their economic and ecological potential.
9. Shavings also produced improvements in mechanical properties of asphalt, such as indirect tensile strength, stiffness, skid resistance and resistance to abrasion. However, their inferior heating potential makes them only suitable for superficial layers (surface and binder layers) where induction maintenance is expected.
10. Finally, it was proved that the use of commercial metal particles did not produce any additional benefit in terms of mechanical performance, compared to the studied waste materials. On the contrary, they involve economic and environmental impacts that can be minimised by using waste particles.

8.4 Conclusions related to aged and RAP mixes

Chapter 6 investigated how the healing capacity of asphalt mixes is progressively affected due to the ageing process occurring over the service life of a road. Also, the effect produced by introducing aged material (RAP)

into new mixtures was investigated. Both procedures led to very similar conclusions that can be summarised as follows:

1. Both ageing and RAP additions produce a higher dynamic modulus at low reduced frequencies, higher R-values and lower crossover frequencies. As a consequence, bitumen is stiffer and its flow through the interior pore network is more difficult.
2. For a given compaction effort, ageing processes and RAP additions reduce the density and increase the air voids content of asphalt mixes.
3. Mixes with lower compaction levels tend to produce better healing results.
4. Ageing of asphalt mixes and RAP additions reduce effectiveness and energy efficiency of induction healing treatments. Thus, the maximum healing level that can be achieved decreased, while the energy needed to reach it increased.
5. Also the critical energy that triggers the healing phenomena was slightly higher when the material was aged, or RAP was added to the mix.
6. Significant decreases in healing performance are produced during the first ageing days in the oven and when low RAP contents are added. However, once the parameters of 9 days of ageing and 60% of RAP content are reached, variations in healing performance became less pronounced. This might indicate that a minimum residual healing (around 20%) is always achievable, independent of the degree of ageing.

7. 80% of RAP content produces similar binder stiffening and air voids content after compaction to mixes aged for 3 days. However, in terms of healing performance with the studied materials and under the considered conditions, the following empirical correlation was found:

$$EA(days) = 0.15\ RC(\%)$$

Considering previous conclusions, it can be deduced that ageing processes and RAP addition produce two contradictory effects that affect healing performance in a positive, and a negative, way. On the one hand, resulting mixes have higher air voids content, predicting improved healing behaviour. On the other hand, the stiffening of bitumen and its lower viscosity make its flow through cracks and air cavities more difficult, predicting poorer results. In view of the final results, it can be concluded that the detrimental effect is stronger and, as a consequence, both ageing phenomena and RAP additions reduce the healing capacity of asphalt mixes.

It must also be added that induction heating is a method, which allows the closing of cracks but does not reduce the ageing level present in the pavement. In order to maintain the rheological properties of the mastic in optimum conditions to carry out the induction healing when this is necessary, the author proposes the addition of metal particles, together with encapsulated rejuvenators that can be progressively released during the service life of the road. This encapsulation technology is feasible and is being already developed by different authors with encouraging results (Su et al., 2013b, Su et al., 2013a, Garcia et al., 2011a, Garcia et al., 2010b). The

combination of both might lead to one of the main steps forward in road durability and extension of service life.

8.5 Conclusions related to bitumen type

Chapter 7 studied how different bitumen properties related to mechanical performance, rheology, composition and thermal expansion, affect the healing capacity of hot mix asphalt when electromagnetic induction is applied. The main conclusions can be listed as follows:

1. The five types of bitumen considered in the present study had very similar properties despite covering the conventional range of bitumens normally used in Europe.
2. Also the healing performance was similar for the five types, which indicates that, within the conventional range of bitumens, the type of bitumen is not a sensitive variable. Hence, the main conclusion of the present investigation is that, if for a given application it is necessary to switch the type of bitumen, the healing capacity of the resulting asphalt mix will not be significantly affected.
3. In general, with the exception of marginal cases, there is no linear correlation between bitumen properties and healing parameters ($R^2 < 0.9$).
4. However, signs were found of possible non-linear correlations between healing and coefficient of thermal expansion, stiffness and viscosity, as follows:

(a) The maximum healing ratio was produced when the coefficient of thermal expansion was close to 0.5mm/ºC, being reduced when the

coefficient was higher and lower. This could support the hypothesis described in the literature, which states that when the expansion capacity of a binder is reduced, cracks cannot be effectively healed. On the other hand, when it is too high, the flow of bitumen can exceed the flow capacity of the pore network, increasing internal pressure and damaging the sample.

(b) Bitumen viscosity and stiffness are strongly correlated and, in both cases, there is an optimum value that produces maximum healing. The author has hypothesised that when both are too high, it is difficult to move the binder through the cracks and, as a consequence, the healing is less effective. On the contrary, when they are too low, the flow of bitumen is easier but the strength of the repaired crack is also lower, due to the poorer mechanical performance of the repairing bitumen.

Although these two trends were observed, it was mentioned that variations in both inputs (bitumen properties) and outputs (healing results) were very small. This means that, in order to fully verify such trends and rule out that they are not simply produced by data scatter, further investigation with a wider range of binders is advisable. This was not included in the present investigation being out of its scope, as to study that, it would be necessary to use binders out of the conventional range normally used for road applications in Europe.

8.6 Future Work

Due to the limited time and resources available for this study, some research areas need more investigation to validate and evaluate the use of self-healing by induction heating. These can be summarized as follows:

1. It is recommended to construct a trial pavement section or large-scale experiment to evaluate the in-situ performance of a flexible pavement structure containing conductive particles in different configurations. Such a study will be useful for evaluating site construction, nature of cracking and healing performance. Moreover, it will allow the effect of real time ageing on the self-healing to be studied.
2. Since the present study was limited to one aggregate type and gradation, it is recommended to study other aggregate types and gradations, as well as a wider range of bitumen types and grades, to better understand the effect of the aggregate type and gradation and the bitumens on the self-healing phenomenon.
3. Conducting an economical investigation is highly recommended for future studies to ensure the feasibility of the induction heating self-healing technique compared to common maintenance practice. This study can include environmental, life cycle and practical assessment for the HMA produced using this method.
4. Combine other self-healing methods like capsules with the conductive fibres and evaluate the self-healing as well as the mix mechanical properties.

References

A. ONGEL, J. H., AND E. KOHLER 2007. State of the Practice in 2006 for Open-Graded Asphalt Mix Design. *Technical Memorandum: UCPRC-TM-2008-07.* California Department of Transportation.

ABO-QUDAIS, S. & SULEIMAN, A. 2005. Monitoring fatigue famage and crack healing by ultrasound wave velocity. *Nondestructive Testing and Evaluation,* 20**,** 125-145.

ABOUFOUL, M. & GARCIA, A. 2017. Influence of air voids characteristics on the hydraulic conductivity of asphalt mixture. *Road Materials and Pavement Design,* 18**,** 39-49.

AIREY, G. 2003. State of the art report on ageing test methods for bituminous pavement materials. *International Journal of Pavement Engineering,* 4**,** 165-176.

AL-MANSOORI, T., MICAELO, R., ARTAMENDI, I., NORAMBUENA-CONTRERAS, J. & GARCIA, A. 2017. Microcapsules for self-healing of asphalt mixture without compromising mechanical performance. *Construction and Building Materials,* 155**,** 1091-1100.

AL-MANSOORI, T., NORAMBUENA-CONTRERAS, J., MICAELO, R. & GARCIA, A. 2018. Self-healing of asphalt mastic by the action of polymeric capsules containing rejuvenators. *Construction and Building Materials,* 161**,** 330-339.

ANDERSSON, H., KELLER, M. W., MOORE, J. S., SOTTOS, N. R. & WHITE, S. 2007. Self healing polymers and composites. *Self Healing Materials.* Springer.

ARPACI, V. S., KAO, S.-H. & SELAMET, A. 1999. *Introduction to heat transfer*, Prentice Hall.

ASPHALT_RESEARCH_CONSORTIUM 2011. Asphalt Research Correspondent. FHAW research program comprising Western Research Institutes, Texas A&M University, University of Wisconsin-Madison, University of Nevada-Reno and Advanced Asphalt Technologies.

AYAR, P., MORENO-NAVARRO, F. & RUBIO-GÁMEZ, M. C. 2016. The healing capability of asphalt pavements: a state of the art review. *Journal of Cleaner Production,* 113**,** 28-40.

BAZIN, P. & SAUNIER, J. Deformability, fatigue and healing properties of asphalt mixes. Proceedings of the 2nd International Conference on the Structural Design of Asphalt Pavements, 1967 Michigan, USA. PP 438-451.

BHASIN, A., LITTLE, D. N., BOMMAVARAM, R. & VASCONCELOS, K. 2008. A framework to quantify the effect of healing in bituminous materials using material properties. *Road Materials and Pavement Design,* 9**,** 219-242.

BHASIN, A. & MOTAMED, A. 2011. Analytical models to characterise crack growth in asphaltic materials and healing in asphalt binders. *International Journal of Pavement Engineering,* 12**,** 371-383.

BHASIN, A., PALVADI, S. & LITTLE, D. 2011. Influence of aging and temperature on intrinsic healing of asphalt binders. *Transportation Research Record: Journal of the Transportation Research Board***,** 70-78.

BOYER, R. E. & ENGINEER, P. S. D. 2000. Asphalt Rejuvenators “Fact, or Fable”. *Transportation systems*.

BSI 2002. BS EN 13043:2002 Aggregates for bituminous mixtures and surface treatments for roads, airfields and other trafficked areas. London, England: British Standard Institute.

BSI 2003a. BS EN 12697-8:2003 Bituminous mixtures. Test methods for hot mix asphalt. Determination of void characteristics of bituminous specimens. London, England: British Standard Institute.

BSI 2003b. BS EN 12697-23:2003 Bituminous mixtures. Test methods for hot mix asphalt. Determination of the indirect tensile strength of bituminous specimens. London, England: British Standard Institute.

BSI 2003c. BS EN 12697-33:2003 Bituminous mixtures. Test methods for hot mix asphalt. Specimen prepared by roller compactor. London, England: British Standard Institute.

BSI 2004. BS EN 12697-17:2004 Bituminous mixtures. Test methods for hot mix asphalt. Particle loss of porous asphalt specimen. London, England: British Standard Institute.

BSI 2008a. BS EN 1436:2007+A1:2008 Road marking materials. Road marking performance for road users. London, England: British Standard Institute.

BSI 2008b. BS EN 12697-12:2008 Bituminous mixtures - Test methods for hot mix asphalt. Determination of the water sensitivity of bituminous specimens. London, England: British Standard Institute.

BSI 2009a. BS EN 12591:2009 Bitumen and bituminous binders. Specifications for paving grade bitumens. London, England: British Standard Institute.

BSI 2009b. BS EN 12697-5:2009 Bituminous mixtures. Test methods for hot mix asphalt. Determination of the maximum density. London, England: British Standard Institute.

BSI 2011. BS EN 13036-4:2011 Road and airfield surface characteristics. Test methods-Method for measurement of slip-skid resistance of a surface. The pendulum test. London, England: British Standard Institute.

BSI 2012a. BS EN 12697-6:2012 Bituminous mixtures. Test methods for hot mix asphalt. Determination of bulk density of bituminous specimens. London, England: British Standard Institute.

BSI 2012b. BS EN 12697-26:2012 Bituminous mixtures. Test methods for hot mix asphalt. Stiffness. London, England: British Standard Institute.

BSI 2012c. BS EN 14770:2012 Bitumen and bituminous binders. Determination of complex shear modulus and phase angle. Dynamic Shear Rheometer (DSR). London, England: British Standard Institute.

BSI 2016a. BS EN 13108-1:2016 Bituminous mixtures. Material specifications. Asphalt Concrete. London, England: British Standard Institute.

BSI 2016b. BS EN 13108-7:2016 Bituminous mixtures. Material specifications. Porous Asphalt. London, England: British Standard Institute.

CASTRO, M. & SÁNCHEZ, J. A. 2006. Fatigue and healing of asphalt mixtures: discriminate analysis of fatigue curves. *Journal of transportation engineering,* 132**,** 168-174.

CHENG, D. 2002. *Surface free energy of asphalt-aggregate system and performance analysis of asphalt concrete based on surface free energy.* Texas A & M University.

CHIU, C.-T., HSU, T.-H. & YANG, W.-F. 2008. Life cycle assessment on using recycled materials for rehabilitating asphalt pavements. *Resources, Conservation and Recycling,* 52**,** 545-556.

CHIU, C. & LEE, M. 2006. Effectiveness of seal rejuvenators for bituminous pavement surfaces. *Journal of Testing and Evaluation,* 34**,** 390.

CRAVEN, J. M. 1969. *Cross-linked thermally reversible polymers produced from condensation polymers with pendant furan groups cross-linked with maleimides*.

DE LIRA, R. R., CORTES, D. D. & PASTEN, C. 2015. Reclaimed asphalt binder aging and its implications in the management of RAP stockpiles. *Construction and Building Materials,* 101**,** 611-616.

DEPARTMENT_OF_TRANSPORT_AND_MAIN_ROADS 2017. Technical Specification-Transport and Main Roads Specifications MRTS30 Asphalt Pavements. *In:* ROADS, D. O. T. A. M. (ed.). Queensland Goverment.

DINH, B. H., PARK, D.-W. & LE, T. H. M. 2018. Effect of rejuvenators on the crack healing performance of recycled asphalt pavement by induction heating. *Construction and Building Materials,* 164**,** 246-254.

DOMONE, P. & ILLSTON, J. 2010. *Construction materials: their nature and behaviour*, CRC Press.

DRY, C. 1994. Matrix cracking repair and filling using active and passive modes for smart timed release of chemicals from fibers into cement matrices. *Smart Materials and Structures,* 3**,** 118.

DUARTE, A. A., STRIER, D. E. & ZANETTE, D. H. 1996. The rise of a liquid in a capillary tube revisited: A hydrodynamical approach. *American Journal of Physics,* 64**,** 413-418.

DURRIEU, F., FARCAS, F. & MOUILLET, V. 2007. The influence of UV aging of a Styrene/Butadiene/Styrene modified bitumen: Comparison between laboratory and on site aging. *Fuel,* 86**,** 1446-1451.

EAPA 1998. *Heavy duty surfaces: the arguments for SMA,* The Netherlands, European Asphalt Pavement Association.

EAPA 2007. Long-Life Asphalt Pavements-Technical version. Belgim: European Asphalt Pavement Association.

ENERGY_INSTITUTE 2006. IP 469/01: Determination of saturated, aromatic and polar compounds in petroleum products by thin layer chromatography and flame ionization detection. Energy Institute.

ETRMA 2011. End of Life Tyres: A Valuable Resource with Growing Potential. European Tyre and Rubber Manufacturers' Association.

EUROPEAN_LIME_ASSOCIATION 2010. Hydrated lime: a proven additive for durable asphalt pavements–critical literature review. *Report to the European Lime Association/Asphalt Task Force*.

FRANCKEN, L. 1979. Fatigue performance of a bituminous road mix under realistic test conditions. *Transportation Research Record*.

FWA, T. F., SINHA, K. C. & RIVERSON, J. D. N. 1990. Influence of Rehabilitation Decisions on Pavement‐Maintenance Planning. *Journal of Transportation Engineering,* 116**,** 197-212.

GALLEGO, J., DEL VAL, M. A., CONTRERAS, V. & PAEZ, A. 2013. Heating asphalt mixtures with microwaves to promote self-healing. *Construction and Building Materials,* 42**,** 1-4.

GARBER, N. & HOEL, L. 2014. *Traffic and highway engineering*, Cengage Learning.

GARCIA, A. 2012. Self-healing of open cracks in asphalt mastic. *Fuel,* 93**,** 264-272.

GARCIA, A., BUENO, M., NORAMBUENA-CONTRERAS, J. & PARTL, M. N. 2013. Induction healing of dense asphalt concrete. *Construction and Building Materials,* 49**,** 1-7.

GARCÍA, A., NORAMBUENA-CONTRERAS, J., BUENO, M. & PARTL, M. N. 2015. Single and multiple healing of porous and dense asphalt concrete. *Journal of Intelligent Material Systems and Structures,* 26**,** 425-433.

GARCIA, A., SCHLANGEN, E. & VAN DE VEN, M. 2010a. Two ways of closing cracks on asphalt concrete pavements: microcapsules and induction heating. *Key Engineering Materials,* 417**,** 573-576.

GARCIA, A., SCHLANGEN, E. & VAN DE VEN, M. 2011a. Properties of capsules containing rejuvenators for their use in asphalt concrete. *Fuel,* 90**,** 583-591.

GARCIA, A., SCHLANGEN, E., VAN DE VEN, M. & LIU, Q. 2012. A simple model to define induction heating in asphalt mastic. *Construction and Building Materials,* 31**,** 38-46.

GARCIA, A., SCHLANGEN, E., VAN DE VEN, M. & SIERRA-BELTRÁN, G. 2010b. Preparation of capsules containing rejuvenators for their use in asphalt concrete. *Journal of Hazardous Materials,* 184**,** 603-611.

GARCIA, A., SCHLANGEN, E., VAN DE VEN, M. & VAN VLIET, D. 2011b. Induction heating of mastic containing conductive fibers and fillers. *Materials and Structures,* 44**,** 499-508.

GARCIA, A., SCHLANGEN, E., VEN, M. V. D. & TNO, D. V. V. 2011c. Crack repair of asphalt concrete with induction energy. *HERON,* 56.

GOMEZ-MEIJIDE, B., AJAM, H., LASTRA-GONZALEZ, P. & GARCIA, A. 2016. Effect of air voids content on asphalt self-healing via induction and infrared heating. *Construction and Building Materials,* 126**,** 957-966.

GOOD, R. J. & VAN OSS, C. J. 1992. The modern theory of contact angles and the hydrogen bond components of surface energies. *Modern Approaches to Wettability.* Springer.

GRANT, T. P. 2001. *Determination of asphalt mixture healing rate using the Superpave indirect tensile test.* University of Florida.

GRIFFIN, R., SIMPSON, W. & MILES, T. 1959. Influence of Composition of Paving Asphalt on Viscosity, Viscosity-Temperature Susceptibility, and Durability. *Journal of Chemical and Engineering Data,* 4**,** 349-354.

HAGER, M. D., GREIL, P., LEYENS, C., VAN DER ZWAAG, S. & SCHUBERT, U. S. 2010. Self-Healing Materials. *Advanced Materials,* 22**,** 5424-5430.

HAGOS, E. T. 2008. *The effect of aging on binder proporties of porous asphalt concrete*, TU Delft, Delft University of Technology.

HAIMBAUGH, R. E. 2001. Practical induction heat treating. ASM international.

HAMRAOUI, A. & NYLANDER, T. 2002. Analytical Approach for the Lucas–Washburn Equation. *Journal of Colloid and Interface Science,* 250**,** 415-421.

HASSN, A., ABOUFOUL, M., WU, Y., DAWSON, A. & GARCIA, A. 2016. Effect of air voids content on thermal properties of asphalt mixtures. *Construction and Building Materials,* 115**,** 327-335.

HEFER, A. W. 2004. *Adhesion in bitumen-aggregate systems and quantification of the effect of water on the adhesive bond.* PhD, Texas A&M University.

HEYES, D., MITCHELL, P. & VISSCHER, P. 1994. Viscoelasticity and near-newtonian behaviour of concentrated dispersions by Brownian dynamics simulations. *Trends in Colloid and Interface Science VIII.* Springer.

HIGHWAYS_ENGLAND 2008a. MANUAL OF CONTRACT DOCUMENTS FOR HIGHWAY WORKS VOLUME 2 NOTES FOR GUIDANCE ON THE SPECIFICATION FOR HIGHWAY WORKS. *SERIES NG 900 road pavements - bituminous bound materials.* Highways England.

HIGHWAYS_ENGLAND 2008b. MANUAL OF CONTRACT DOCUMENTS FOR HIGHWAY WORKS, VOLUME 1 SPECIFICATION FOR HIGHWAY WORKS. *Series 900 Road pavements - bituminous bound materials.* Highways England.

HIGHWAYS_ENGLAND 2011. Interim Advice Note 157/11. *Thin Surface Course Systems. Installation and Maintenance.* Highways England.

HORVATH, A. 2003. Life-Cycle Environmental and Economic Assessment of Using Recycled Materials for Asphalt Pavements.

HORVATH, A. 2004. Construction Materials and the Environment. *Annual Review of Environment and Resources,* 29**,** 181-204.

HUNTER, R. N. 1994. *Bituminous mixtures in road construction*, Thomas Telford.

ISACSSON, U. & LU, X. 1995. Testing and appraisal of polymer modified road bitumens—state of the art. *Materials and Structures,* 28**,** 139-159.

KANDHAL, P. 1993. Waste Materials in Hot Mix Asphalt - An Overview. *In:* WALLER, H. F. (ed.) *Use of Waste Materials in Hot Mix Asphalt.* West Conshohocken, PA: ASTM International.

KANITPONG, K. & BAHIA, H. 2003. Role of adhesion and thin film tackiness of asphalt binders in moisture damage of HMA (with

discussion). *Journal of the Association of Asphalt Paving Technologists,* 72.

KATZ, A. 2004. Environmental Impact of Steel and Fiber-Reinforced Polymer Reinforced Pavements. *Journal of Composites for Construction,* 8**,** 481-488.

KIM, B. & ROQUE, R. 2006. Evaluation of healing property of asphalt mixtures. *Transportation Research Record: Journal of the Transportation Research Board,* 1970**,** 84-91.

KIM, Y. R., CASTORENA, C., RAD, F. Y., ELWARDANY, M., UNDERWOOD, S., FARRAR, M. J. & GLASER, R. R. 2015. Long-Term Aging of Asphalt Mixtures for Performance Testing and Prediction. *Quarterly Report (April-June, 2015), National Cooperative Highway Research Program, No. Project***,** 9-54.

KIM, Y. R. & LITTLE, D. N. 1990. One-dimensional constitutive modeling of asphalt concrete. *Journal of engineering mechanics,* 116**,** 751-772.

KIM, Y. R., LITTLE, D. N. & BURGHARDT, R. 1991. SEM analysis on fracture and healing of sand-asphalt mixtures. *Journal of Materials in Civil Engineering,* 3**,** 140-153.

KRINGOS, N., SCHMETS, A., SCARPAS, A. & PAULI, T. 2011. Towards an understanding of the self- Healing capacity of asphaltic mixtures. *Heron,* 56**,** 49-79.

LE GUERN, M., CHAILLEUX, E., FARCAS, F., DREESSEN, S. & MABILLE, I. 2010. Physico-chemical analysis of five hard

bitumens: Identification of chemical species and molecular organization before and after artificial aging. *Fuel,* 89**,** 3330-3339.

LENNTECH. 1998. *EU's drinking water standards. Council Directive 98/83/EC on the quality of water intented for human consumption. Adopted by the Council, on 3 November 1998* [Online]. Available: https://www.lenntech.com/applications/drinking/standards/eu-s-drinking-water-standards.htm 2018].

LI, V. C. & YANG, E.-H. 2007. Self healing in concrete materials. *Self Healing Materials.* Springer.

LITTLE, D. N. & BHASIN, A. 2007. Exploring Mechanism of Healing in Asphalt Mixtures and Quantifying its Impact. *Self healing materials.* Springer.

LITTLE, D. N., EPPS, J. A. & SEBAALY, P. 2001. The benefits of hydrated lime in hot mix asphalt. *National Lime Association*.

LITTLE, D. N., LYTTON, R. L., WILLIAMS, D. & KIM, Y. R. 1997. *Propagation and healing of microcracks in asphalt concrete and their contributions to fatigue*, Marcel Dekker, New York.

LIU, Q., GARCIA, A., SCHLANGEN, E. & VEN, M. V. D. 2011. Induction healing of asphalt mastic and porous asphalt concrete. *Construction and Building Materials,* 25**,** 3746-3752.

LIU, Q., SCHLANGEN, E. & VAN DE VEN, M. 2012. Induction Healing of Porous Asphalt Concrete Beams on an Elastic Foundation. *Journal of Materials in Civil Engineering,* 25**,** 880-885.

LIU, Q., SCHLANGEN, H. & VAN BOCHOVE, G. The first engineered self-healing asphalt road: How is it performing? ICSHM 2013:

Proceedings of the 4th International Conference on Self-Healing Materials, Ghent, Belgium, 16-20 June 2013, 2013. Magnel Laboratory for Concrete Research.

LUCÍA, O., MAUSSION, P., DEDE, E. J. & BURDÍO, J. M. 2014. Induction Heating Technology and Its Applications: Past Developments, Current Technology, and Future Challenges. *IEEE Transactions on Industrial Electronics,* 61**,** 2509-2520.

LYTTON, R., CHEN, C. & LITTLE, D. 2001. Microdamage healing in asphalt and asphalt concrete, volume IV: A viscoelastic continuum damage fatigue model of asphalt concrete with microdamage healing.

LYTTON, R. L., UZAN, J., FERNANDO, E. G., ROQUE, R., HILTUNEN, D. & STOFFELS, S. M. 1993. *Development and validation of performance prediction models and specifications for asphalt binders and paving mixes*, Strategic Highway Research Program.

MALLICK, R. B. & EL-KORCHI, T. 2013. *Pavement engineering: principles and practice*, CRC Press.

MARTIN, J. R. & WALLACE, H. A. 1958. *Design and construction of asphalt pavements*, McGraw-Hill Book Company.

MCKAY, J. F., AMEND, P. J., COGSWELL, T. E., HARNSBERGER, P. M., ERICKSON, R. B. & LATHAM, D. R. 1978. Petroleum Asphaltenes: Chemistry and Composition. *Analytical Chemistry of Liquid Fuel Sources.* AMERICAN CHEMICAL SOCIETY.

MENOZZI, A., GARCIA, A., PARTL, M. N., TEBALDI, G. & SCHUETZ, P. 2015. Induction healing of fatigue damage in asphalt test samples. *Construction and Building Materials,* 74**,** 162-168.

MILLER, J. S. & BELLINGER, W. Y. 2014. Distress identification manual for the long-term pavement performance program. United States. Federal Highway Administration. Office of Infrastructure Research and Development.

MOBASHER, B., MAMLOUK, M. S. & LIN, H.-M. 1997. Evaluation of Crack Propagation Properties of Asphalt Mixtures. *Journal of Transportation Engineering,* 123**,** 405-413.

MODARRES, A. & RAHMANZADEH, M. 2014. Application of coal waste powder as filler in hot mix asphalt. *Construction and Building Materials,* 66**,** 476-483.

MODARRES, A., RAHMANZADEH, M. & AYAR, P. 2015. Effect of coal waste powder in hot mix asphalt compared to conventional fillers: mix mechanical properties and environmental impacts. *Journal of Cleaner Production,* 91**,** 262-268.

MORENO-NAVARRO, F., AYAR, P., SOL-SÁNCHEZ, M. & RUBIO-GÁMEZ, M. C. 2017. Exploring the recovery of fatigue damage in bituminous mixtures at macro-crack level: the influence of temperature, time, and external loads. *Road Materials and Pavement Design,* 18**,** 293-303.

MORENO-NAVARRO, F. & RUBIO-GÁMEZ, M. C. 2016. A review of fatigue damage in bituminous mixtures: Understanding the

phenomenon from a new perspective. *Construction and Building Materials,* 113**,** 927-938.

MROUEH, U.-M., ESKOLA, P. & LAINE-YLIJOKI, J. 2001. Life-cycle impacts of the use of industrial by-products in road and earth construction. *Waste Management,* 21**,** 271-277.

NUNN, M., BROWN, A., WESTON, D. & NICHOLLS, J. 1997. Design of long-life flexible pavements for heavy traffic. *TRL REPORT 250*.

OFORI-ABEBRESSE, E. K. 2006. *Fatigue resistance of hot-mix asphalt concrete mixtures (HMAC) using the Calibrated Mechanistic with Surface Energy Measurements (CMSE).* Master Of Science, Texas A&M University.

ONGEL, A. & HARVEY, J. 2004. Analysis of 30 years of pavement temperatures using the enhanced integrated climate model (EICM). *Draft report prepared for the California Department of Transportation. Pavement Research Center, Institute of Transportation Studies, University of California Davis,* UCPRC-RR-2004/05.

OSMAN, S. A. 2004. *The role of bitumen and bitumen/filler mortar in bituminous mixture fatigue.* PhD, University of Nottingham.

PALIUKAITE, M., VAITKUS, A. & ZOFKA, A. Evaluation of bitumen fractional composition depending on the crude oil type and production technology. 2014 2014 Vilnius. Vilnius Gediminas Technical University, Department of Construction Economics & Property, 1-7.

PAVEMENT_INTRACTIVE. 2010. *HMA Pavement* [Online]. Available: http://www.pavementinteractive.org/article/hma-pavement/.

PHILLIPS, M. Multi-step models for fatigue and healing, and binder properties involved in healing. Eurobitume workshop on performance related properties for bituminous binders, Luxembourg, 1998.

PONTE, K. D., NATARAJAN, B. M., AHLMAN, A. P., BAKER, A., ELLIOTT, E. & EDIL, T. B. 2017. Life-Cycle Benefits of Recycled Material in Highway Construction. *Transportation Research Record: Journal of the Transportation Research Board,* 2628**,** 1-11.

PRONK, A. 2005. Partial Healing, A New Approach for the Damage Process during Fatigue Testing of Asphalt Specimen. *Asphalt Concrete.* American Society of Civil Engineers.

QIU, J. 2008. Self-healing of asphalt mixes: literature review. *Delft University of Technology*.

QIU, J. 2012. *Self healing of asphalt mixtures: Towards a better understanding of the mechanism.* PhD Thesis, Delft University of Technology.

READ, J. 1996. *Fatigue cracking of bituminous paving mixtures.* University of Nottingham.

READ, J. & WHITEOAK, D. 2003. *The shell bitumen handbook*, Thomas Telford.

REERINK, H. 1973. Size and shape of asphaltene particles in relationship to high-temperature viscosity. *Industrial & Engineering Chemistry Product Research and Development,* 12**,** 82-88.

RMA 2016. Stockpile Cleanup Report. Rubber Manufacturers Association, U.S. Tire Manufactues Association.

ROWE, G., BAUMGARDNER, G. & SHARROCK, M. Functional forms for master curve analysis of bituminous materials. Proceedings of the 7th international RILEM symposium ATCBM09 on advanced testing and characterization of bituminous materials, 2016 Rhodes, Greece. 81-91.

RUDNEV, V., LOVELESS, D., COOK, R. L. & BLACK, M. 2002. *Handbook of induction heating*, CRC Press.

SALIH, S., GÓMEZ-MEIJIDE, B., ABOUFOUL, M. & GARCIA, A. 2018. Effect of porosity on infrared healing of fatigue damage in asphalt. *Submitted to Construction and Building Materials*.

SCHLANGEN, E. 2013. *Self-Healing of Concrete* [Online]. Delft University of Technology. Available: http://www.selfhealingconcrete.blogspot.co.uk/.

SCHLANGEN, H., GARICA, A., VAN DE VEN, M., VAN BOCHOVE, G., VAN MONTFORT, J. & LIU, Q. Highway A58: The first engineered self healing asphalt road. ICSHM 2011: Proceedings of the 3rd International Conference on Self-Healing Materials, Bath, UK, 27-29 June 2011, 2011.

SCHOLZ, T. V. 1995. *Durability of bituminous paving mixtures.* PhD Thesis, University of Nottingham.

SEO, Y. & KIM, Y. R. 2008. Using acoustic emission to monitor fatigue damage and healing in asphalt concrete. *KSCE Journal of Civil Engineering,* 12**,** 237-243.

SES_GMBH-ANALYTICAL_SYSTEMS 2017. IATROSCAN MK-6/6s, TLC-FID / FPD Dual Detection System. SES GmbH - Analytical Systems, Germany.

SHELL, B. 1995. *The shell bitumen industrial handbook*, Thomas Telford.

SHEN, S. & SUTHARSAN, T. 2011. Quantification of Cohesive Healing of Asphalt Binder and its Impact Factors Based on Dissipated Energy Analysis. *Road Materials and Pavement Design,* 12**,** 525-546.

SI, Z., LITTLE, D. & LYTTON, R. 2002. Characterization of microdamage and healing of asphalt concrete mixtures. *Journal of materials in civil engineering,* 14**,** 461-470.

SIENKIEWICZ, M., KUCINSKA-LIPKA, J., JANIK, H. & BALAS, A. 2012. Progress in used tyres management in the European Union: A review. *Waste Management,* 32**,** 1742-1751.

SIMPSON, W., GRIFFIN, R. & MILES, T. 1961. Relationship of asphalt properties to chemical constitution. *Journal of Chemical and Engineering Data,* 6**,** 426-429.

SU, J.-F., QIU, J. & SCHLANGEN, E. 2013a. Stability investigation of self-healing microcapsules containing rejuvenator for bitumen. *Polymer Degradation and Stability,* 98**,** 1205-1215.

SU, J.-F., QIU, J., SCHLANGEN, E. & WANG, Y.-Y. 2015. Investigation the possibility of a new approach of using microcapsules containing waste cooking oil: In situ rejuvenation for aged bitumen. *Construction and Building Materials,* 74**,** 83-92.

SU, J.-F., SCHLANGEN, E. & QIU, J. 2013b. Design and construction of microcapsules containing rejuvenator for asphalt. *Powder Technology,* 235**,** 563-571.

SUN, Y., LIU, Q., WU, S. & SHANG, F. Microwave heating of steel slag asphalt mixture. 2013 Annual Meeting of Chinese Ceramic Society's Building Materials, Professional Committees of Stone and Aggregate and Utilization of Solid Waste, SBM 2013, November 28, 2013 - December 1, 2013, 2014 Wuhan, China. Trans Tech Publications Ltd, 193-197.

SUNG, Y. T., KUM, C. K., LEE, H. S., KIM, J. S., YOON, H. G. & KIM, W. N. 2005. Effects of crystallinity and crosslinking on the thermal and rheological properties of ethylene vinyl acetate copolymer. *Polymer,* 46**,** 11844-11848.

TA-INSTRUMENTS 2006. TMA Thermomechanical Analyzer-Q Series Getting Started Guide. New Castle, USA: TA Instruments.

THEYSE, H., DE BEER, M. & RUST, F. 1996. Overview of South African mechanistic pavement design method. *Transportation Research Record: Journal of the Transportation Research Board,* 1539**,** 6-17.

THOM, N. 2014. *Principles of pavement engineering, 2nd Edition,* London, UK, ICE Publishing (Institute of Civil Engineers).

TRASK, R., WILLIAMS, H. & BOND, I. 2007. Self-healing polymer composites: mimicking nature to enhance performance. *Bioinspiration & Biomimetics,* 2**,** P1.

TRAXLER, R. 1936. The Physical Chemistry of Asphaltic Bitumen. *Chemical reviews,* 19**,** 119-143.

TRAXLER, R. N. Durability of asphalt cements (with discussion). Association of Asphalt Paving Technologists Proceedings, 1963.

VAN DER ZWAAG, S. & BRINKMAN, E. 2015. *Self Healing Materials: Pioneering research in the Netherlands*, IOS Press.

VAN DIJK, W., MOREAUD, H., QUEDEVILLE, A. & UGE, P. The fatigue of bitumen and bituminous mixes. Presented at the Third International Conference on the Structural Design of Asphalt Pavements, Grosvenor House, Park Lane, London, England, Sept. 11-15, 1972., 1972.

VAN GOOSWILLIGEN, G., DE HILSTER, E. & ROBERTUS, C. Changing Needs and Requirements for Bitumen and Asphalts. PROCEEDINGS OF THE 6TH CONFERENCE ON ASPHALT PAVEMENTS FOR SOUTHERN AFRICA, CAPSA'94, HELD CAPE TOWN OCTOBER 1994. VOL 2, 1994.

VAN TITTELBOOM, K., DE BELIE, N., VAN LOO, D. & JACOBS, P. 2011. Self-healing efficiency of cementitious materials containing tubular capsules filled with healing agent. *Cement and Concrete Composites,* 33**,** 497-505.

WANG, L.-B. 2012. Mechanics of asphalt: microstructure and micromechanics. *International Journal of Pavement Research and Technology,* 5.

WASHBURN, E. W. 1921. The Dynamics of Capillary Flow. *Physical Review,* 17**,** 273-283.

WATER_UK. 2018. *Drinking water technical briefings* [Online]. Available: https://www.water.org.uk/publications/water-industry-guidance/drinking-water-technical-briefings 2018].

WHITE, S. R., SOTTOS, N., GEUBELLE, P., MOORE, J., KESSLER, M. R., SRIRAM, S., BROWN, E. & VISWANATHAN, S. 2001. Autonomic healing of polymer composites. *Nature,* 409**,** 794-797.

WOOL, R. P. 2008. Self-healing materials: a review. *Soft Matter,* 4**,** 400-418.

WU, S.-P., PANG, L., MO, L.-T., CHEN, Y.-C. & ZHU, G.-J. 2009. Influence of aging on the evolution of structure, morphology and rheology of base and SBS modified bitumen. *Construction and Building Materials,* 23**,** 1005-1010.

YANG, Y., QIAN, Z. & SONG, X. 2015. A pothole patching material for epoxy asphalt pavement on steel bridges: Fatigue test and numerical analysis. *Construction and Building Materials,* 94**,** 299-305.

YIN, F., ARÁMBULA-MERCADO, E., EPPS MARTIN, A., NEWCOMB, D. & TRAN, N. 2017. Long-term ageing of asphalt mixtures. *Road Materials and Pavement Design,* 18**,** 2-27.

YODER, E. J. & WITCZAK, M. W. 1975. *Principles of pavement design*, John Wiley & Sons.

ZAKAR, P. 1971. *Asphalt*, Chemical Publishing Company.

ZBOROWSKI, A. & KALOUSH, K. E. 2011. A Fracture Energy Approach to Model the Thermal Cracking Performance of Asphalt Rubber Mixtures. *Road Materials and Pavement Design,* 12**,** 377-395.

ZHENG, C., ZHAO, D., CHEN, C., SONG, Z. & ZHENG, S. 2013. Quantitative test technology study on the mesoscopic strength parameters of the mineral aggregate contact surface of bituminous-stabilized macadam. *Construction and Building Materials,* 40**,** 622-631.

ZOLLINGER, C. J. 2005. *Application of surface energy measurements to evaluate moisture susceptibility of asphalt and aggregates.* MSc, Texas A&M University.